ANL/OEPM-78-11

DR.698

DR.698

ANL/OEPM-78-11

315
2/19/80

ANNUAL REPORT FOR 1978 ON RESEARCH, DEVELOPMENT AND DEMONSTRATION OF NICKEL-ZINC BATTERIES FOR ELECTRIC VEHICLE PROPULSION

Contract No. 31-109-38-4200

by

Gould Inc.

ARGONNE NATIONAL LABORATORY, ARGONNE, ILLINOIS

Operated for the U. S. DEPARTMENT OF ENERGY
under Contract W-31-109-Eng-38

DISCLAIMER

Printed in the United States of America
Available from
National Technical Information Service
U. S. Department of Commerce
5285 Port Royal Road
Springfield, VA 22161

NTIS price codes
Printed copy: A07
Microfiche copy: A01

Distribution Category:
Energy Storage--Electrochemical-
Nearterm Batteries (UC-94ca)

ANL/OEPM-78-11

Annual Report for 1978 on

RESEARCH, DEVELOPMENT AND DEMONSTRATION OF NICKEL-ZINC BATTERIES FOR ELECTRIC VEHICLE PROPULSION

Prepared for

The Office for Electrochemical Project Management
Argonne National Laboratory
Under Contract No. 31-109-38-4200

By

Gould Incorporated
Rolling Meadows, Illinois

October 1979

ADDRESS VERIFICATION

In order that we may verify your address on our distribution list, please detach this form, complete the information requested below, fold as indicated, seal with tape or staple, and place in mail.

Name_____

Mailing Address_____

_____

_____

City_____ State_____ Zip_____

☐ I wish to continue to receive ANL/OEPM reports from near-term electric vehicle battery contractors.

Please return this form even if you do not wish future reports.

If you have returned an identical form to this one in the last 90 days, you need not resubmit another.

Thank You.

FOLD HERE

ARGONNE NATIONAL LABORATORY
Office for Electrochemical Project Mgmt.
Building 205
9700 South Cass Avenue
Argonne, IL 60439

Attn: Dawn Landis

TABLE OF CONTENTS

I. FOREWORD

This Progress Report is the first annual report under Contract No. 31-109-38-4200 and covers the period January 9 through July 31, 1978. Access to additional relevant proprietary data is subject to the intellectual property provisions of Appendix D of this contract. In general, Gould has attempted to restrict its proprietary data to component materials and designs or processes to produce specific components. A standardized parts list is utilized to identify all components, materials, and designs.

II. EXECUTIVE SUMMARY

This is the first annual report describing progress in the 33-month cooperative program between Argonne National Laboratory and Gould Inc.'s Nickel-Zinc/Electric Vehicle Project. The purpose of the program is to demonstrate the technical and economic feasibility of the nickel-zinc battery for electric vehicle propulsion. The successful completion of the program will qualify the nickel-zinc battery for use in the Department of Energy's demonstration program under the auspices of Public Law 94-413.

In order to meet the very ambitious objectives of the program in the time frame required, six major tasks have been underway since the beginning of this contract. These tasks are illustrated in EXHIBIT I, the Program Master Schedule. All tasks are currently well underway and the original schedule for all deliverables and milestones does not have to be altered.

The Milestone Schedule and Status Report (Form 535) is included in this report as EXHIBIT II.

Impressive over the last several months has been the performance of the four-cell battery module delivered to Argonne during the month of June. The battery (EXHIBITS III and IV) was subjected to 145 deep discharge cycles (100% depth of discharge (DOD)) before dropping below 70% of theoretical capacity. The theoretical capacity is based on the actual amount of active nickel hydroxide, as opposed to a percentage based on the rated capacity. It is emphasized that the battery was fabricated in the Pilot Plant and that it does not contain "one-of-a-kind" components; therefore, it represents production state of the art for Gould's nickel-zinc electric vehicle battery technology.

Noteworthy also is the fact that, to date, all milestones have been met and that the program is moving ahead in full force.

Over the last several months, Thermal Management has been recognized as being a very significant factor affecting the performance of the nickel-zinc system. The thermodynamic and I^2R contributions to the heat generation are both very significant; and in order to properly attack this problem, a separate task has been established for the duration of the balance of the program.

Following is a discussion of the progress in each of the six major tasks:

1) TASK A: SEPARATOR DEVELOPMENT

The separator system that has been specified for long cycle life application is the Gould ELECTROPOROUS™ separator. Heretofore, the function of the separator in a nickel-zinc cell had been defined as a barrier to zinc dendrites which grow on the electrode surface and eventually bridge the negative and positive electrodes, therefore, small pore size and high degree of tortuosity were the parameters to be optimized. Assumed, of course, was the chemical and dimensional stability.

These requirements are not in themselves sufficient. The metallic zinc will either eventually penetrate through the separator thereby leading to a catastrophic loss in cell capacity via short circuit, or zinc will deposit within the pores of the separator and eventually accumulate in sufficiently large quantity to render the separator a bulk electronic conductor leading to the formation of a leakage path between the electrodes, hence to a gradual loss in capacity. Additionally, with this deposition, the pores of the separator will be plugged and the resistance to electrolyte transport will rise.

With these considerations in mind, the bulk of the separator development effort has been directed at the ELECTROPOROUS™ systems, where the dense polymeric films facilitate electrolyte transport and block the admission of dissolved zinc specie so that neither dendrites can penetrate through nor leakage paths be established. While the emphasis has been on the ELECTROPOROUS™ systems, the microporous separators have not been abandoned because they do work reasonably well in shorter cycle life or lower depth of discharge applications.

2) TASK B: ZINC ELECTRODE DEVELOPMENT

The zinc electrode development effort has been aimed at generating and quantifying an understanding of the basic problems associated with the development of a zinc electrode capable of long cycle life operation. In view of the fact that the generic problem with the zinc electrode is its inherent solubility in the electrolyte, the development effort is being redirected. Basically, the short-term effort is aimed at bringing about incremental improvements in cell/battery performance via improved separators, better charging procedures, modification of current density distribution, improved heat removal, dendrite growth suppression, etc., while the longer range, more profound effort is aimed at immobilizing the discharged zinc. The immobilization of zinc would result in highly improved gravimetric and volumetric energy densities because the required amount of zinc could be close to 1:1 theoretical ampere-hour ratio of the active materials. Additionally, the requirements on the separator would be tremendously reduced. Several approaches are under consideration. While the longer range effort is ambitious, untried, and is a total departure from conventional battery development approaches, success in immobilizing zinc without significant sacrifice in cell voltage and charge/discharge characteristics should result in quantum jump improvements in nickel-zinc technology.

Initial efforts to reduce shape change and densification which are major contributors to loss in capacity with cycle life, are being aimed at optimizing electrode dimensions and bulk density, cell free space, current collector

---

™Gould Trademark

materials and design, heat removal, charging techniques, gassing rates, electrolyte additives, electrode additives, and zinc oxide raw materials. Some experiments have been performed, some are in progress, and others are being designed to study all these parameters. To date, our research effort has yielded significant progress in our understanding of the modes of cell failure.

1) Cell geometry control significantly reduces shape change in 5 and 50 AH cells and has allowed better retention of capacities in 5 AH cells compared with controls.

2) The incorporation of better current collectors and tab designs into zinc electrodes has apparently alleviated some of the heat problems encountered in recent cell tests. Cells with electrodes containing improved grids have shown significantly better cycle life because of better heat removal and reduced shape change.

3) Charging studies indicate the degree of overcharge previously used in cell tests was unnecessary to achieve good cell capacities. Previous testing regimes were placing undue stress on the cells. A modified recharge has been adopted for component testing with improved life.

4) Incorporation of surface active additives in the electrolyte has given better cycle life without the shorting failures observed in control cells. These additives, however, reduced the cell capacities to values lower than the controls. More work is needed in this area.

5) Incorporation of additives in the electrodes used in 5 AH cells significantly reduces the degree of densification.

6) Higher density electrodes promote improved cycle life.

7) Constant potential charging appears to provide improved cell life and capacity retention. Additional work is needed with large cells.

Additionally, work is in progress to better characterize the operating cell environment such as the quantification of the spatial distribution of dissolved zinc and the distribution of the electrolyte both at constant temperature and as a function of temperature. The work that is being done on thermal management is being accelerated.

3) TASK C: PRODUCT DESIGN AND ANALYSIS

The analysis of the commuter vehicle mission has been completed. The factors that have been considered are the cell voltage and configuration and their impact on vehicle performance. Meetings with DOE/TEC, Jet Propulsion Laboratory, General Research Corporation, and major automotive companies have been held. On the basis of all the information gathered, an interactive computer analysis of mission requirements, vehicle space constraints, and battery configuration options was carried out. A high profile (15 inch), 400 AH cell to be used in a

48-volt system has been selected to minimize manufacturing costs while maximizing cycle life, volumetric energy density, and peak power. The projected performance for this design, which is scheduled for October 15, 1978, delivery to Argonne, is 140 WH/L volumetric energy density, 132 W/Kg peak power, 60 WH/Kg gravimetric energy density, and 74 W/Kg sustained power. A deliberate tradeoff of gravimetric energy density for cycle life has been made in order to insure minimum life cycle costs.

Additionally, the smooth transition from the conceptual Phase I designs to the materialization of deliverable hardware was affected. Software has been developed for algorithms that are used to generate production costs at the current level of activity. The algorithms can and will be modified as required to eventually generate production costs for 10,000 electric vehicle batteries per year.

The 400 AH four-cell module that was delivered to Argonne in June, 1978, was subjected to formation cycling with a demonstrated charge/discharge efficiency of 89%. The module was delivered on schedule to meet the hardware delivery milestone.

4) TASK D: CELL/MODULE/BATTERY TESTING

The testing of Gould's first full-size Preliminary Design battery (33 cells, 54 volts) was carried out during the course of this program. It delivered twice the energy density of Gould's lead-acid electric vehicle battery in steady state chassis dynamometer tests. Unfortunately, the battery failed prematurely due to excessive positive electrode growth and cracking.

The Preliminary Design 400 AH components with separator system #800 attained 300 cycles while still retaining 80% of the theoretical capacity of the nickel electrode. All cycles were at 100% DOD.

Extensive testing of nickel electrodes has been carried out while trying to resolve some of the processing problems encountered over the first few months of this program. Recent tests indicate that the problems have been essentially overcome.

Several peak power tests as a function of depth of discharge and sustained power at various depths of discharge on 400 AH cells have demonstrated the superiority of nickel-zinc over lead-acid golf cart batteries which have been designed for peak power. This work has significantly aided the Generation I Design selection which must achieve a 110 W/Kg peak power at 80% DOD

An extensive testing facility has been established. This facility which is minicomputer based real-time sharing system consists of 13 cyclers and CAMAC interface is totally dedicated to the nickel-zinc battery development effort. Additionally, it includes environmental testing, vibrating testing, and power testing capabilities.

5) TASK E: PROCESS DEVELOPMENT

Most of the effort in this area has been directed at resolving the nickel electrode problem of disintegration in the cell operating environment.

Encompassing investigations have been carried out both of the plaque sintering process and of the chemical impregnation process. Both processes have been well characterized and plaque sintering and impregnation conditions have been optimized. The problems have essentially been resolved and processing was returned to the pilot plant level with improved process controls. A multiple plaque molding process and an improved mold filling process have been developed and implemented in the Pilot Plant. The multiple molding process has increased plaque production by a factor of four, and the mold filling process now insures uniform powder distribution in the mold.

Considerable progress has been made in the development of a process for continuous separator production. Several thousands square feet of the Gould microprooous separator has been produced with excellent reproducibility of physical characteristics.

Separator bag production rates have been significantly improved developing and implementing a machine that will facilitate multiple layer bag fabrication. The machine provides for simultaneous quality inspection and bag slitting.

The preform/marrying fabrication technique has been sufficiently developed and is currently in the production mode in the Pilot Plant. Problems associated with the pressing of electrodes with the desired binder were resolved after extensive studies of the related parameters: agglomerate size distribution, binder content distribution, spray drying conditions, and pressing conditions. The optimization of these variables have resulted in a process whereby zinc oxide electrodes can be manufactured continuously and reproducibly.

Processes for the fabrication and incorporation of improved design grid/tab into electrodes have been developed and implemented.

Because of previous design deficiencies, extensive modifications have been made on the new impregnation equipment to render it operational. Additionally, a new waste handling system was designed and implemented to meet the required standards.

6) TASK F: PILOT PLANT

The most significant achievement in this area of endeavor is the actual mobilization of the Pilot Plant with the success being evidenced by the actual production of full-size cells and modules for this program and other applications of nickel-zinc technology. An important milestone was the production of three four-cell (400 AH) modules, with the delivery of one module to Argonne. The module performed satisfactorily while being cycled under fairly severe conditions.

Although many problems and bottlenecks have plagued the start-up and the operation of the Pilot Plant, they have systematically been resolved or brought under control. In spite of the problems and hurdles that have been encountered, several thousands of components have been fabricated and these have resulted in several hundreds of full-size and tri-electrode cells to meet the testing needs of the entire Project.

An extensive materials study was carried out and submitted in report form to Argonne on June 19, 1978. The study includes a manufacturing flow design, the projected materials usage in kilograms per kilowatt-hour, and projected market size through 1980.

A cost accounting system has been implemented to generate realistic and reliable manufacturing economics.

A manufacturing economics analysis which is a milestone and is discussed in more detail in Task F of this report was generated. This analysis indicates that the current costs which represent the first stage pilot production far exceed the estimated selling target price of $75/KwH. To achieve the target selling price, the following items are essential:

1) Heavy investment in mechanization to reduce the labor cost.

2) Improve process yield to reduce scrap rate thereby reducing materials cost.

3) Recycle process scrap and used batteries to reduce materials cost.

4) Improve materials utilization in both negative and positive electrodes to reduce materials cost.

Gould believes that the target selling price can be achieved but it will take heavy investment in plant and equipment, and process development beyond the scope of the current contract. There is no market pull to encourage Gould to make the necessary investment at this time, so a projection of the time table to achieve the costs, in a free market scenario, is impossible. On the other hand, if the federal government decides to stimulate the electric vehicle marketplace through the 1980's by virtue of significant funding for product and process development beyond the present contract and guaranteed battery purchases, the $75/KwH selling price can be achieved by 1986. This goal would be achieved by going through three stages of plant expansion requiring millions of dollars in capital.

TECHNICAL PERFORMANCE SUMMARY

In compliance with the contract, the technical performance as of July 31, 1978, is summarized in graphical form in EXHIBIT V. With the program tasks well underway and the timely meeting of the milestones to date, the forecasts for the end of the program will coincide with the target program goals.

While the promise of component technology is being demonstrated on a laboratory-scale, the state of the art must be established on a cost effective, reproducible, continuous production basis. With the intensive efforts aimed at resolving the problems associated with the nickel electrode and the development of processes to translate laboratory-proven component technology into full-size components, the cycle life and volumetric and gravimetric energy performance of full-size 400 AH cells has improved and should continue to improve during the coming months.

With the ongoing generation of manufacturing economics, specific high cost bottleneck areas are being identified, and the paths towards cost reduction without sacrifice in overall performance are being pursued with vigor.

EXHIBIT I: PROGRAM MASTER SCHEDULE

1. Contract Identification: RESEARCH, DEVELOPMENT, AND DEMONSTRATION OF A NICKEL-ZINC BATTERY FOR ELECTRIC VEHICLE PROPULSION		2. Reporting Period: January 9 thru July 31, 1978	3. Contract Number: 31-109-38-4200
4. Contractor (Name, address): GOULD INC. NICKEL-ZINC BATTERY PROJECT 30 GOULD CENTER ROLLING MEADOWS, ILLINOIS 60008			5. Contract Start Date: JANUARY 9, 1978 6. Contract Completion Date: SEPTEMBER 30, 1980

7. Identification Number	8. Reporting Category (e.g., contract line item or work breakdown structure element)	9. Fiscal Years and Months: FY '78 (J F M A M J J A S) · FY '79 (Q1 Q2 Q3 Q4) · FY '80 (Q1 Q2 Q3 Q4)	10. Percent Complete: a) Planned	b) Actual
1.1	SEPARATOR DEVELOPMENT	▼A ▽B ▽C ▽D	16.3	20.6
1.2	ZINC ELECTRODE DEVELOPMENT		16.3	13.4
2.1	PRODUCT DESIGN & ANALYSIS	▼A ▽B	16.1	11.7
2.2	CELL/BATTERY TESTING	▼A ▼B ▼C ▽D ▽E	16.2	9.6
2.3	PROCESS DEVELOPMENT	▼A, B ▼C ▼D ▽E, F ▽G ▽H ▽I	16.2	17.6
2.4	PILOT MANUFACTURING	▼A ▼B ▽C ▽D ▽E ▽F ▽G	16.2	19.6
3.1	QUALITY ASSURANCE	▼A	13.9	6.1
4.1	CONTRACT ADMINISTRATION		15.6	11.6

11. Remarks

12. Signature of Contractor's Project Manager and Date: Robert J. Stefan, August 31, 1978

13. Signature of Government Technical Representative and Date

EXHIBIT Ia: IDENTIFICATION OF INTERMEDIATE EVENTS ILLUSTRATED IN EXHIBIT I

IDENTIFICATION NUMBER	CATEGORY	EVENTS
1.1	Separator Development	A - Identify 300 Cycle Separator B - Identify 500 Cycle Separator C - Identify 750 Cycle Separator D - Identify 1,000 Cycle Separator
2.1	Product Design & Analysis	A - Generation I Battery Design Established B - Generation II Battery Design Established
2.2	Cell/Battery Testing	A - Initiate Generation I Prototype Cell Tests for Design Verification B - Initiate Generation I Prototype Module Tests for Design Verification C - Complete Preliminary Design Evaluation D - Initiate Exhaustive Generation I Module Testing E - Initiate Exhaustive Generation I Battery Testing
2.3	Process Development	A - Microporous Separator Continuously Manufactured B - Multiple Positive Molding Implemented C - Sintering Process Established D - Preform/Marry Process Implemented with Alternate Binder E - Positive Impregnation Process Established F - Mechanized Assembly Process G - Recycling Feasibility Study H - Nickel Recycling Process Optimized I - Negative Electrode Process Mechanized
2.4	Pilot Manufacturing	A - Materials Availability Study B - One Experimental Module Delivered C - Manufacturing Economics Study D - Two Baseline Modules Delivered E - Update of Manufacturing Economics Study F - Five Full-Scale Batteries Delivered G - Fifteen Prototype Batteries Delivered
3.1	Quality Assurance	A - Program Quality Assurance Plan Delivered

EXHIBIT II

FORM DOE 535
(10/77)

U.S. DEPARTMENT OF ENERGY

PAGE OF

MILESTONE SCHEDULE AND STATUS REPORT

1. Contract Identification: RESEARCH, DEVELOPMENT AND DEMONSTRATION OF A NICKEL-ZINC BATTERY FOR ELECTRIC VEHICLE PROPULSION	2. Reporting Period: 10-31-78 through 9-30-79	3. Contract Number: 31-109-38-4200
4. Contractor (name, address): GOULD INC. NICKEL-ZINC/ELECTRIC VEHICLE PROJECT 30 GOULD CENTER ROLLING MEADOWS, ILLINOIS 60008		5. Contract Start Date: JANUARY 9, 1978 6. Contract Completion Date: SEPTEMBER 30, 1978

7. Identification Number	8. Reporting Category (e.g., contract line item or work breakdown structure element)	9. Fiscal Years and Months: FY '79 O N D J F M A M J J A S; FY '80 Q1 Q2 Q3 Q4	10. Percent Complete a) Planned	b) Actual
1.1	SEPARATOR DEVELOPMENT	▽B ▽C Δ	59.0	
1.2	ELECTRODE DEVELOPMENT	Δ	66.9	
2.1	PRODUCT DESIGN & TESTING	▽B Δ	58.8	
2.2	CELL/MODULE/BATTERY TESTING	▽D ▽E Δ	60.6	
2.3	PROCESS DEVELOPMENT	▽E&F ▽G ▽H ▽F Δ	58.8	
2.4	PILOT PLANT	▽D ▽E ▽F Ⓐ	58.8	
2.5	THERMAL MANAGEMENT	Δ	38.0	
3.1	QUALITY ASSURANCE	Δ	58.4	
4.1	CONTRACT ADMINISTRATION	Δ	57.6	

11. Remarks

12. Signature of Contractor's Project Manager and Date	13. Signature of Government Technical Representative and Date
August 31, 1978	

EXHIBIT III: FOUR-CELL BATTERY MODULE DELIVERED TO ARGONNE

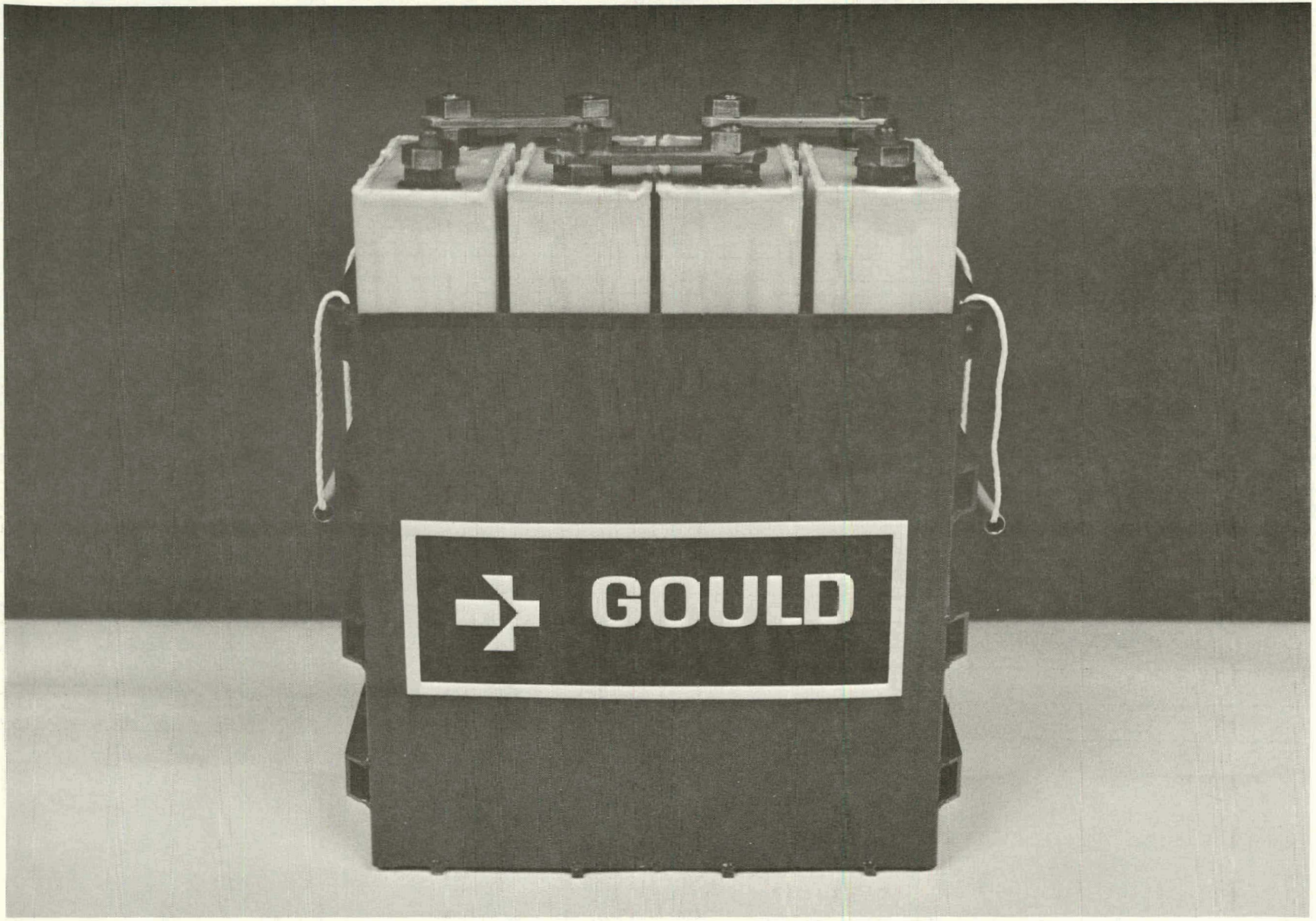

EXHIBIT IV: FOUR-CELL BATTERY MODULE WITH POWER SUPPLY DELIVERED TO ARGONNE

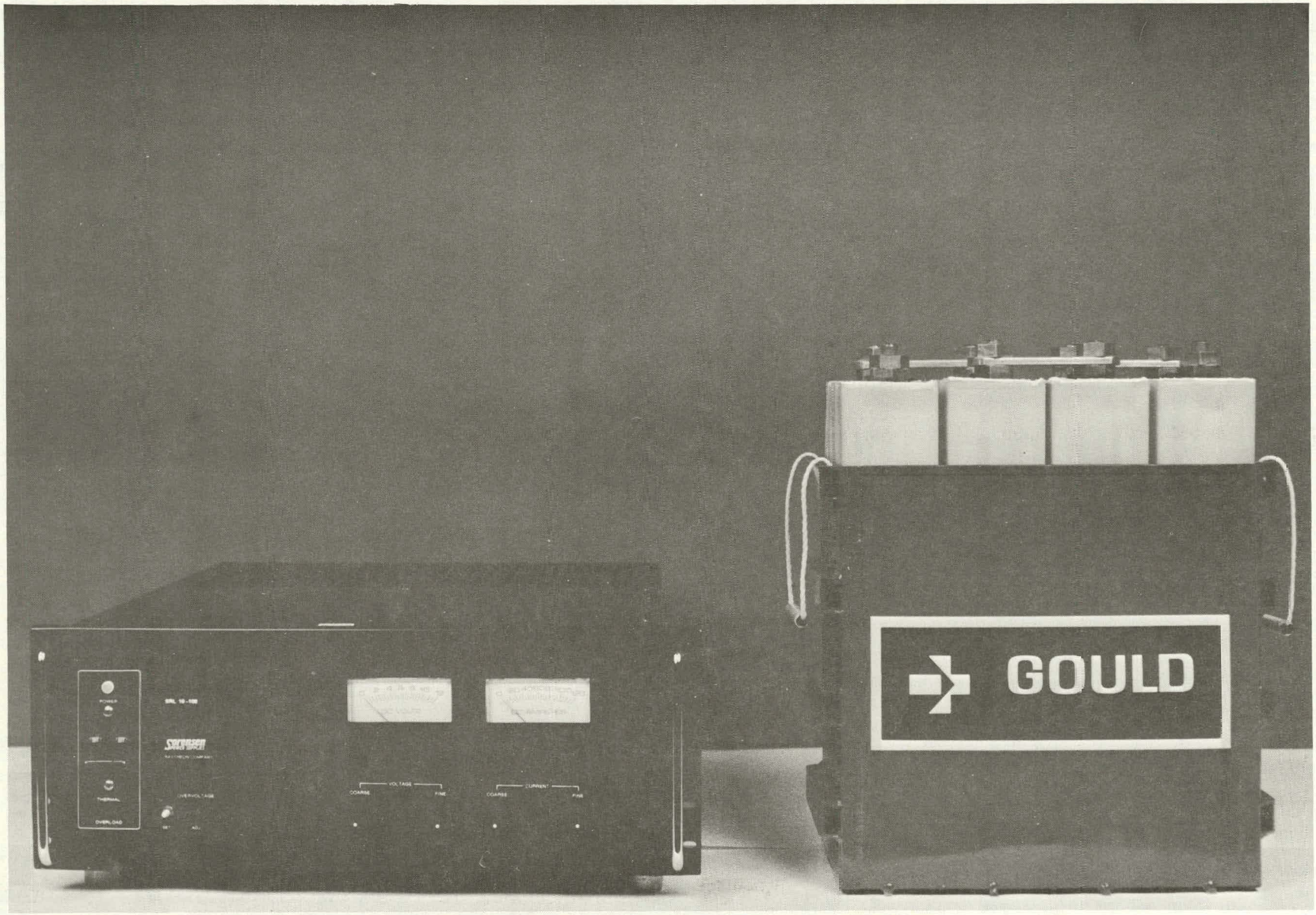

EXHIBIT V: TECHNICAL PERFORMANCE AS OF JULY 31, 1978

CHARACTERISTICS	CONTRACT GOALS (SET JAN, 1978)	PRESENT DEMONSTRATION			CONTRACTOR FORECAST (FOR JAN, 1979) PERFORMANCE
		LAB CELLS	FULL CELLS* OR MODULE	FULL BATTERY*	
1. Battery Capacity[1] (KWH)	20-30	0.064	0.64	21.120	20-30
2. Battery Dimension					
Height (cm)	To Be Determined	N/A	38.9	50.0	To Be Determined
Width (cm)	" " "	N/A	17.0	53.6	" " "
Length (cm)	" " "	N/A	7.5	91.5	" " "
3. Volume (L)	To Be Determined	N/A	5.0	245	To Be Determined
4. Weight (Kg)	-	N/A	10	360	-
5. Volumetric Energy[1] (WHR/L)	>120	N/A	128	86.2	>120
6. Specific Energy[1] (WHR/Kg)	>70	N/A	64	58.7	>70
7. Specific Power (W/Kg)					
Peak Battery[2] - 5/sec. avg.	125	N/A	75**	60.5***	125
Sustained @ C/3 @ 50% DOD	45	N/A	>45**	>45.0***	45
8. Duty Cycle					
Charge (Hours)	4-8	C/16	C/8 (Varied)	C/16	4-8
Discharge (Hours)	2-4	C/3 (100% DOD)	C/5 (Varied) (80% DOD)	~C/2 (80% DOD)	2-4
9. Lifetime					
Deep Discharges[3]	>400	>300	>80+	20	>400
Wet Life (Years)	>2	-	>1.5	-	>2
10. Price/Energy[4] ($/KWH)	<75	N/A	215	240	<75
11. Energy Efficiency (%)	>60	>60	>60	>60	>60

[1] C/3 rate discharge; 8-hour charge; rated at 100% discharge
[2] At 80% discharged state
[3] 80% depth of discharge based on rated capacity
[4] Price delivered to auto manufacturer for production for 10,000 units per year
*Refer to data on cells or batteries made in Pilot Plant. Previous data generated on full-size cells but made in laboratory are not considered relevant
**Equipment limited at present, extrapolated results
***Electric vehicle controller limit at 550 Amps
+Four-cell module being tested by Argonne

III. TECHNICAL PROGRESS

TASK A: SEPARATOR DEVELOPMENT

Methodology and Objectives

The separator development program consists of a fundamental, multidisciplinary, integrated approach directed to: 1) generating an understanding of the functional mechanisms operative in a realistic battery system environment and developing materials based on this understanding; 2) testing 5 and 50 AH cells constructed with newly developed separator materials; 3) performing extensive physico-chemical testing which is fed back to the fundamental research efforts; and 4) developing processes for continuous separator production. This effort is reiterative and evolutionary. The following summarizes the technical milestones for this Task:

Identify separator system with the potential of 300 deep discharge cycles	April, 1978 Specified on time
Identify separator system with the potential of 500 deep discharge cycles	December, 1978
Identify separator system with the potential of 750 deep discharge cycles	October, 1979
Identify separator system with the potential of 1,000 deep discharge cycles	September, 1980

Generic Concepts

Gould's separator development effort is directed at two different concepts. The first is an ELECTROPOROUS™ separator. An electroporous separator combines size discrimination with membrane ion transport characteristics. In accordance with the first milestone of this Task, this concept has been chosen as the prime candidate for achieving 300+ deep discharge cycle performance. However, work also continues on the second approach, the microporous concept, as long as further performance improvements can be envisioned. This concept utilized a film whose functionality is based upon size discrimination. There are commercially available materials which fit this classification, e.g., Celanese's Celgard. In addition, Gould has proprietary versions based upon various combinations of inorganic and organic materials.

Additionally, Gould is maintaining a continued awareness of the state of the art of separator technology by continuous monitoring of separator developments both in the commercial and government sectors. Any new materials that are developed are screened by Gould as they become available; and if they have any promise of success, they are extensively tested in 5 and 50 AH cells.

Consistent with the foregoing discussion, the separator function and failure modes are briefly discussed. Heretofore, the function of the separator in a nickel-zinc cell had been defined as a barrier to zinc dendrites which grow on the electrode surface and eventually bridge the negative and positive electrodes; therefore, small pore size and high degree of tortuosity were the

parameters to be optimized. Assumed, of course, was the chemical and dimensional stability.

These requirements are not in themselves sufficient, for as seen in EXHIBITS A-I and A-II, the metallic zinc will either eventually penetrate through the separator, thereby leading to a catastrophic loss in cell capacity via short circuit, or zinc will deposit within the pores of the separator and eventually accumulate in sufficiently large quantity to render the separator a bulk electronic conductor, leading to the formation of a leakage path between the electrodes or block the pores of the separator, hence causing a gradual loss in cell capacity as seen in EXHIBIT A-III.

With these considerations in mind, the bulk of the separator development effort has been directed at the ELECTROPOROUS™ systems, where the dense polymeric films facilitate electrolyte transport and block the admission of dissolved zinc specie so that neither dendrites can penetrate through nor leakage paths be established. While the emphasis has been on the ELECTROPOROUS™ systems, the microporous separators have not been abandoned because they do work reasonably well in shorter cycle life or lower depth of discharge applications.

ELECTROPOROUS™ Separators

Although generically these separators are the separators of choice for eventual electric vehicle usage, tests to date in 5 and 50 AH cells have exhibited low cycle life. The failures have been attributed to processing flaws in laboratory-made films and first run large-scale materials, defective nickel electrodes, and a too low separator temperature threshold to withstand local hot spot activity.

The nickel electrode problem has been vigorously attacked over the past several months so that its contribution to cell failure is minimized. The thermal generation and management problem is currently under investigation, and studies have already been made toward its control. Both of these major areas will be discussed under separate headings.

In spite of the fact that the cell data has not been very impressive on the ELECTROPOROUS™ systems, a good deal of knowledge has been generated about the functional mechanisms operative in the cell environment and the functionalities and physical structure that the separator system must possess in order for it to perform adequately in a cell. Additionally, methods and processes have been developed to permit full-scale continuous production of films. Among these continuous fabrication techniques are: 1) continuous film casting of water-based dispersions on a strippable substrate; 2) blown film extrusion; 3) substrate coating; and 4) coextrusion between two strippable polymeric films. Although solvent casting has been considered, it has been intentionally avoided because of safety considerations; however, non-aqueous solvent systems will be investigated if necessary. With the above processes that have developed internally or in collaboration with external vendors, separators can be continuously produced from solid or liquid raw materials.

Most impressive about these systems is the improved zinc stopping power of one to three orders of magnitude higher than the state of the art microporous materials and the retention of the required chemical stability and electrolyte transport characteristics. An updated summary of the zinc penetration rate (ZPR) for several separator systems is found in EXHIBIT A-IV.

The best performance to date in 5 AH cells that incorporate one type of ELECTROPOROUS separator has been about 80 cycles with reasonable capacity retention and 260 cycles with fairly low capacity retention. A series of nine 5 AH cells that have been on test to determine the effect of depth of discharge have all been removed from testing. Although the behavior of the cells is somewhat erratic, there seems to be a relationship between depth of discharge and cycle life. Additional work will be done in this area to quantify this effect further.

All the above cells failed prematurely by shorting. They have all been autopsied and a recurring feature is the presence of visible holes in the separator. Careful examination using Scanning Electron Microscopy (SEM) revealed that the flaws are induced by hot spots on the electrode surface, followed by the growth of zinc through the holes and by shorting. The zinc electrodes from these cells have a higher degree of shape change than is normally observed.

In order to modify the chemical and physical structure of the separator system, work has been going on over the past several months to balance the functional components so as to minimize resistance to electrolyte transport and maximize zinc stopping power without compromising chemical stability. Several promising polymer systems were reported during this reporting period. For films of 0.002" in thickness, resistance to electrolyte transport is 3 ohm-cm (0.015 ohm-cm^2). In order to attain these resistance values, the film is first subjected to a proprietary process. In order to fully stabilize these systems, it will probably be necessary to crosslink them.

Several other polymer systems have recently come under investigation where the solvents are non-aqueous. Good, flexible, tough films with good resistance characteristics can be obtained. Several of these materials may be amenable to melt extrusion processing, obviating the need for solvents completely.

A new material that is being extensively evaluated in cell tests and by post autopsy analysis is an electroporous-type film that is available commercially, albeit in limited quantities and at a fairly high price. The first 5 AH cell that was built with this separator is showing reasonably good performance with 90% theoretical cell capacity retention (EXHIBIT A-V) at about 80 cycles. More of this material has been received, and four new cells have been built and placed on test. The performance of these new cells is not as good as the one discussed above. The reason for this discrepancy is not yet known.

In summary, the ELECTROPOROUS^{TM} separator concept remains the system of choice for ultimate electric vehicle nickel-zinc battery applications. This reaffirmation is based on basic scientific principles and experimental data generated over the last several months. The fact that the performance of these separators in actual cell tests is not impressive yet indicates that a good amount of basic research must be done to better understand the separator functions and characteristics in the operating environment before a sound concept may, through proper engineering, be translated to a reliable operational level.

Microporous Separators

The activity in this area of separator development has not been as extensive, although a considerable amount of testing has been carried out with both the Gould inorganic/organic and the commercially available polypropylene based microporous separators. The process development work done with the Gould microporous system is discussed in Task E.

The major problem in this development has been the unavailability of adequately stable substrates that simultaneously possess uniform fiber density and porosity, good wet strength characteristics, and good wettability by the coating material. Consequently, a program was established with a vendor to develop substrates that have the desired physical and chemical characteristics that facilitate coating on a reasonably large scale. Although an exhaustive evaluation of commercially available systems was carried out, all were found to be inadequate, principally on a technical basis. A concerted and collaborative effort over the last several months has resulted in the development of a substrate that has the required characteristics for the coating operations. Initial coating trials have been carried out successfully on the continuous coating line at Gould, and large quantities of substrate are being produced by the vendor so that the large-scale continuous production trials may be resumed. These coating trials are part of another collaborative effort with a major coating vendor.

Although the microporous approach is not deemed to be the concept of choice for long life, deep discharge applications, it may be adequate for milder applications. Additionally, in cell tests, it has been found to improve the performance in terms of delaying or preventing catastrophic shorts. The inorganic/organic composite acts as a thermal barrier against hot shorts, thereby promoting longer life when used in conjunction with the commercial microporous separator.

EXHIBIT A-I: ZINC DENDRITE MIGRATION THROUGH SEPARATOR LEADING TO CATASTROPHIC FAILURE

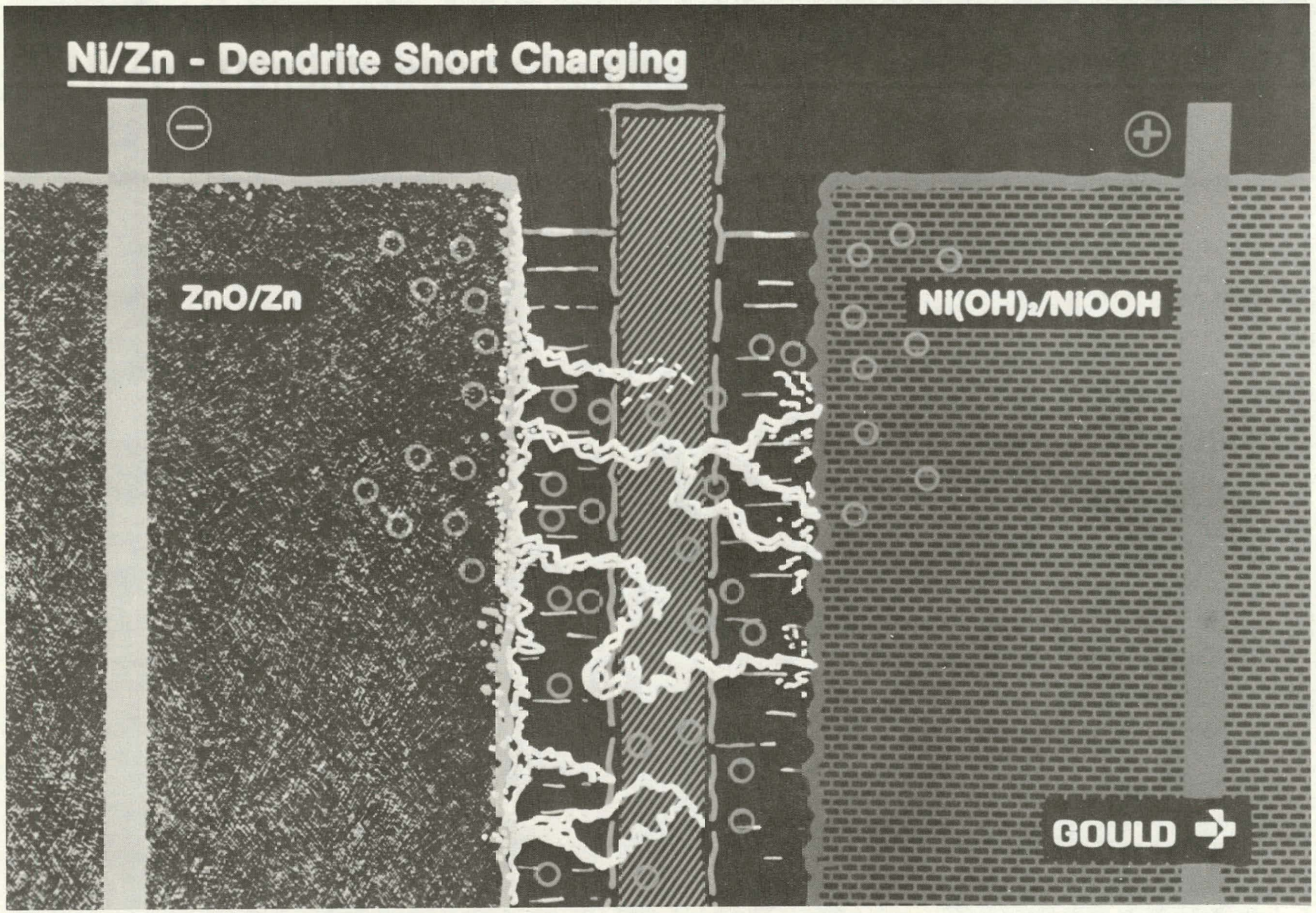

EXHIBIT A-II: ZINCATE DIFFUSION THROUGH SEPARATOR, LEADING TO ZINC DEPOSITION AND GENERATION OF AN ELECTRONIC LEAKAGE PATH BETWEEN THE ELECTRODES

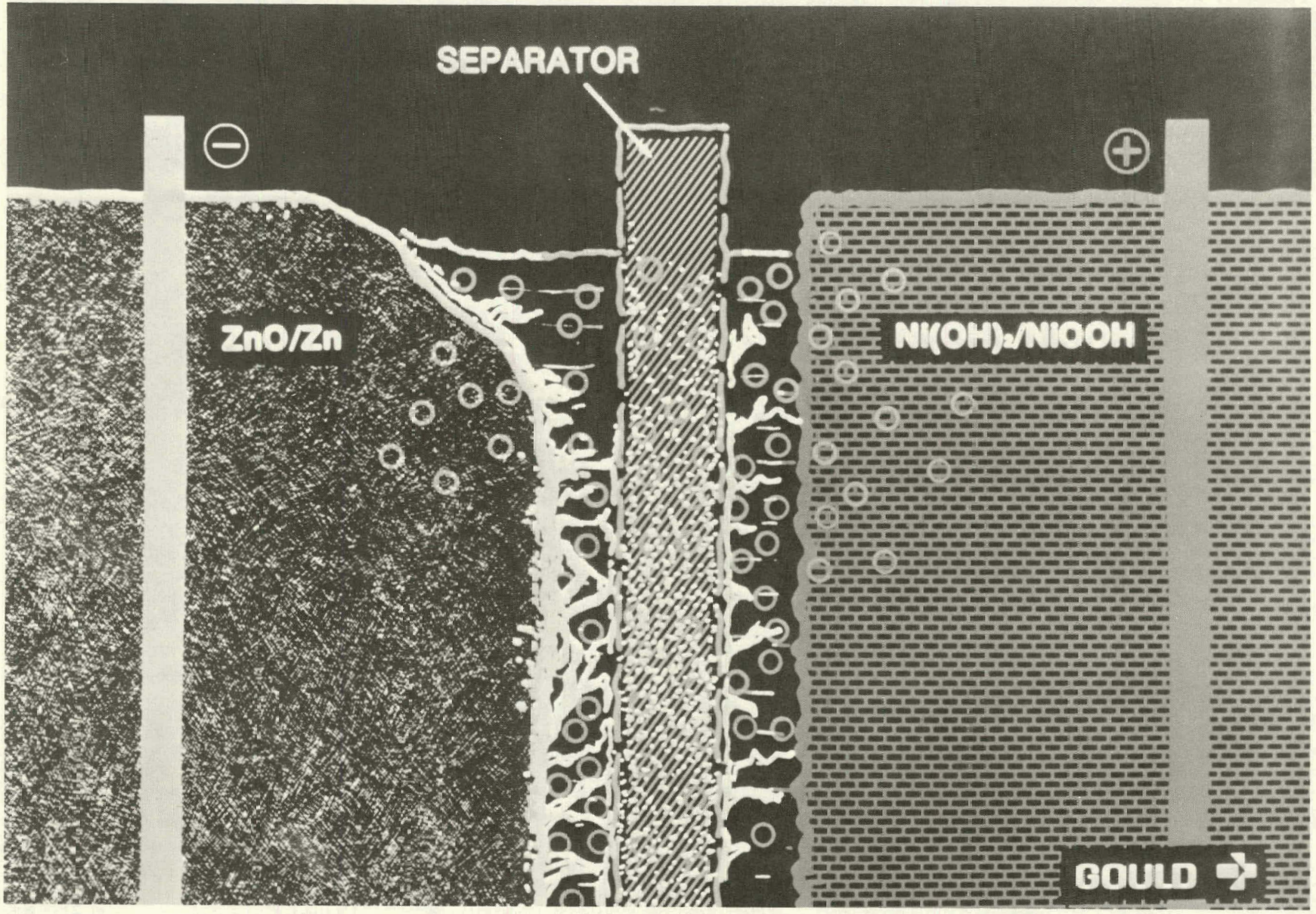

EXHIBIT A-III: TYPICAL CELL LIFE PERFORMANCE EXHIBITING GRADUAL LOSS OF CAPACITY

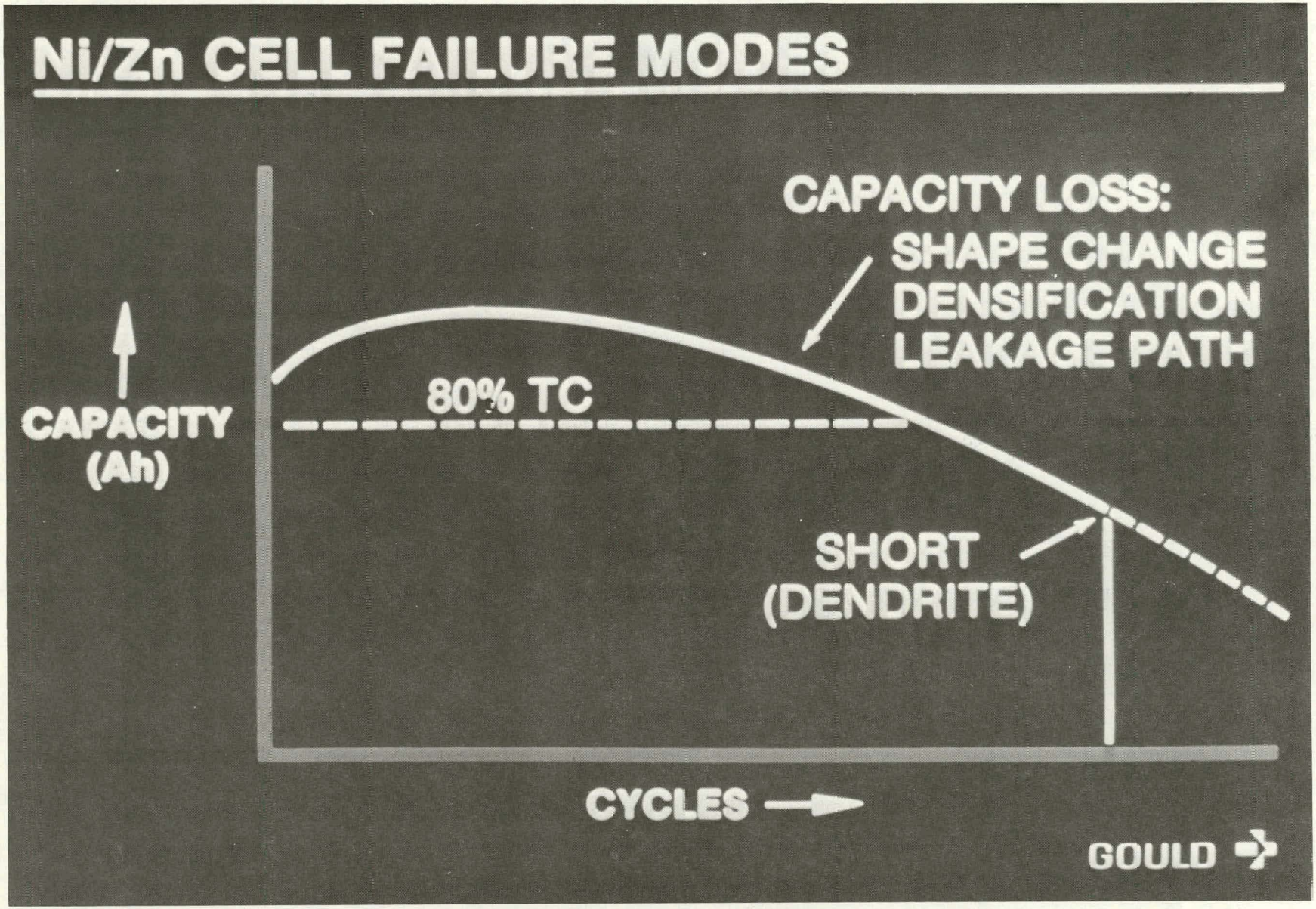

EXHIBIT A-IV: UPDATED SUMMARY OF ZINC PENETRATION RATE DATA FOR SEVERAL SEVERAL SYSTEMS; SEPARATOR PART NUMBERS ARE LISTED ON THE FIGURE

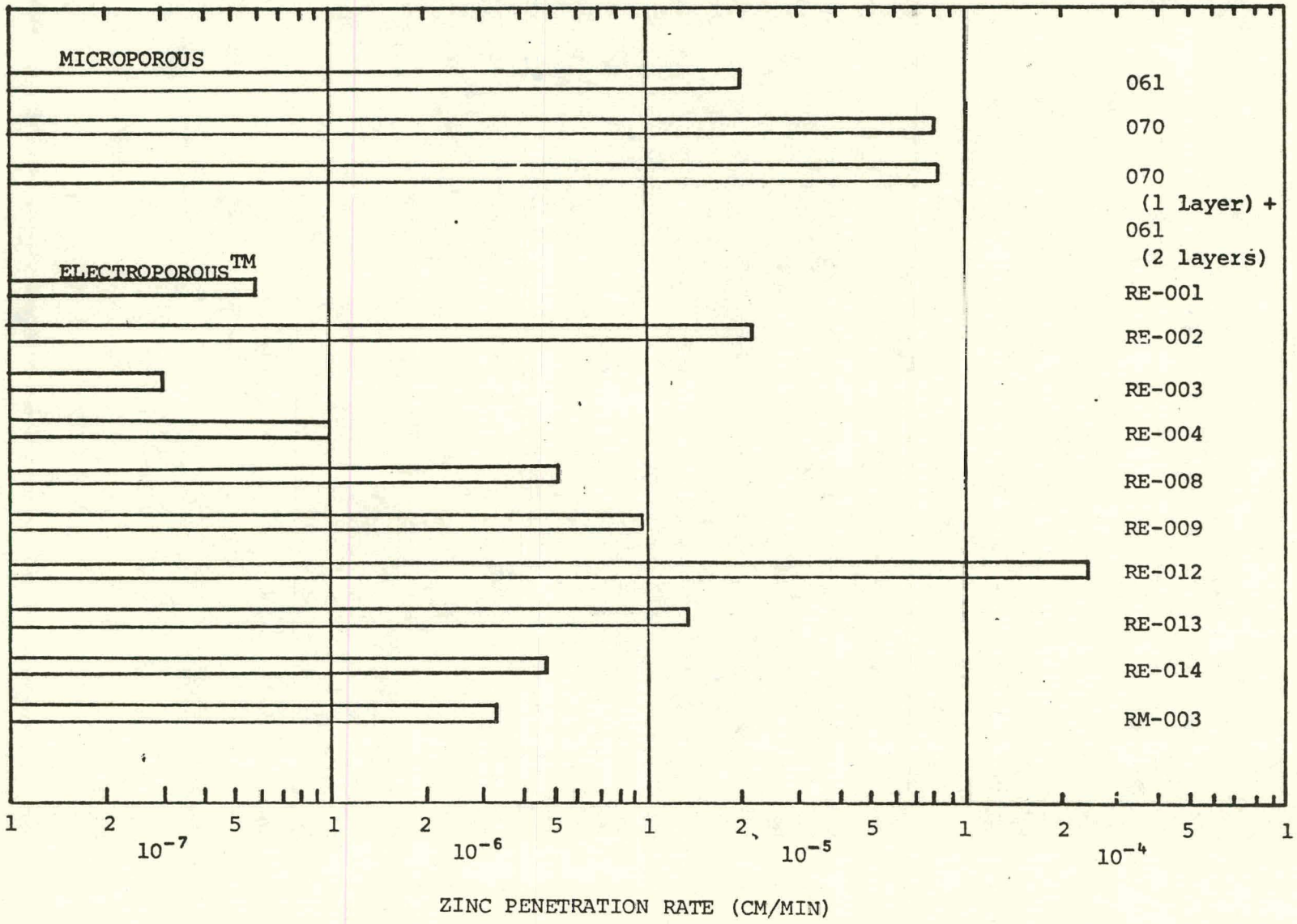

EXHIBIT A-V: CYCLE LIFE CURVE FOR CELL BUILT WITH COMMERCIAL ELECTROPOROUS SEPARATOR

PURPOSE OF TEST: Initial Evaluation of Commercial Electroporous Separator
CELL MODIFICATION: Two Layers Separator
CELL NUMBER: NZ5.78.828.91.1
CYCLE REGIME: Component Testing (1.2C/9 Charge; C/3 Discharge, 100% DOD)

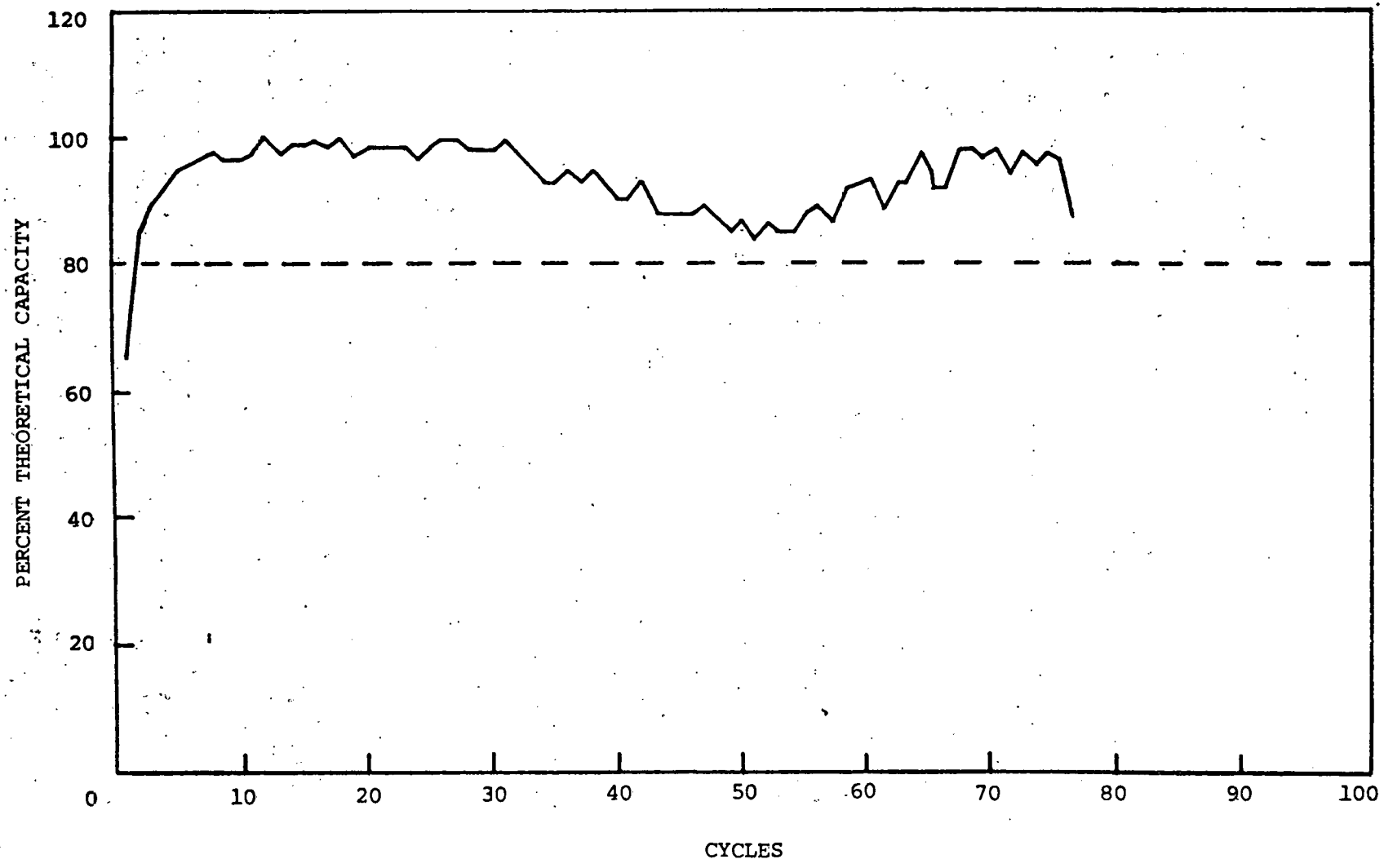

TASK B: ZINC ELECTRODE DEVELOPMENT

Methodology

Although the separator system has, to date, been the life-limiting component of the nickel-zinc system, the contribution to the loss in capacity from the shape change of the zinc electrode, the densification of zinc, the topography of the electrodeposit, passivation, and dendrite growth is significant.

The shape change problem has been subjected to a great deal of study by many investigators. However, the results of these investigations have been either inconclusive or at least not applied in a practical manner. Most of the investigations have been aimed at a particular aspect such as membrane pumping and "washing" effects, gravity effects, effect of additives, etc. The overall task of quantifying the entire system in terms of all the interactive components and the dynamic processes that are simultaneously operative has not been thoroughly confronted.

The principal aim of this effort is to develop electrodes that are capable of long life applications by understanding the mechanisms operative in the system, quantifying them, generating mathematical models and representations of the empirical findings, and developing an empirical mathematical model which will represent the electrodes in their true environment. The mathematical model will then enable Gould to perform computer experiments in order to optimize the zinc electrode in the operating environment.

This effort is divided into two subtasks, namely electrode shape change and dendrite growth, and zinc densification.

The generic problem with the nickel-zinc system is the inherent solubility of zinc in the electrolyte. Any cell that has electrodes of finite dimensions will have associated with it certain inhomogenities, the most basic of which is evidenced in the distribution of the current density. This inhomogeneity in turn causes other problems such as gradients in concentrations of both electrolyte and dissolved zinc, nonuniformity of temperature distribution, convective flow across the surface of the electrode, etc. These factors are mechanistic symptoms of the more basic problem of inhomogeneous current density distribution, which can influence the system because of the generic source of the problem, namely the solubility of the electrode.

The resulting effects of this overall autocatalytic problem as a function of cycling the electrodes are the redistribution of the active material and accelerated dendrite formation. These lead respectively to gradual loss and catastrophic loss in capacity (EXHIBIT B-I, B-II, and B-III). Both of these phenomena can be at least partially overcome by engineering considerations and improved separator systems.

A more elusive problem is that of bulk or surface densification which results in a loss in available surface area of the electrode; hence, a loss in utilizable capacity. As with the previous phenomena, densification is another mechanistic symptom of the generic problem.

If the zinc in the discharged state were not soluble as is the case with cadmium or mercury, the cycle life that could be expected from a nickel-zinc cell would be of the order of that of nickel-cadmium.

In view of the foregoing discussion, the component development effort is being redirected. The short-term effort is aimed at bringing about incremental improvements in cell/battery performance via improved separators, better charging procedures, modification of current density distribution, improved heat removal, dendrite growth suppression, etc., while the longer range, more profound effort is aimed at immobilizing the discharged zinc. The immobilization of zinc would result in highly improved gravimetric and volumetric energy densities because the required amount of zinc could be close to 1:1 theoretical ampere-hour ratio of the active materials. Additional, the requirements on the separator would be tremendously reduced. While the longer range effort is ambitious, untried, and is a total departure from conventional battery development approaches, success in immobilizing zinc without significant sacrifice in cell voltage and charge/discharge characteristics should result in quantum jump improvements in nickel-zinc technology.

Following is a discussion of the results of efforts aimed at realizing shorter range incremental improvements in the state of the art of nickel-zinc technology.

Initial efforts to reduce shape change and densification, which are major contributors to loss in capacity with cycle life, are aimed at optimizing electrode dimensions and bulk density, cell free space, current collector materials and design, heat removal, charging techniques, gassing rates, electrolyte additives, electrode additives, and zinc oxide raw materials. Some experiments have been performed, some are in progress, and others are being designed to study all these parameters. To date, our research effort has yielded significant progress in our understanding of the modes of cell failure. Developments that contribute to improved cycle life are summarized below.

1) Shielding of electrodes significantly reduced shape change in 5 and 50 AH cells and has allowed better retention of capacities in 5 AH cells compared with controls.

2) The incorporation of better current collectors and tab designs into zinc electrodes has apparently alleviated some of the heat problems encountered in recent cell tests. Cells with electrodes containing improved grids have shown significantly better cycle life because of better heat removal and reduced shape change.

3) Charging studies indicate the degree of overcharge previously used in cell tests was unnecessary to achieve good cell capacities. Previous testing regimes were placing undue stress on the cells. A modified recharge has been adopted for component testing to improve life.

4) Incorporation of surface active additives in the electrolyte has given better cycle life without the shorting failures observed in control cells. These additives, however, reduced the cell capacities to values lower than the controls. More work is needed in this area.

5) Incorporation of organic additives in the electrodes used in 5 AH cells significantly reduces the degree of densification.

6) Higher density electrodes promote improved cycle life.

7) Constant potential charging appears to provide improved cell life and capacity retention. Additional work is needed with large cells.

A more detailed discussion of each of the above improvement areas is presented. Additionally, the work that is being done to better characterize the operating cell environment such as the quantification of the spatial distribution of dissolved zinc and the distribution of the electrolyte both at constant temperature and as a function of temperature will be described. The work that is being done on thermal management will be discussed under its own heading since it concerns the entire cell and its components.

Electrode Shielding

The purpose of shielding the electrode pack is twofold. First, it is desirable to reduce the high current density which normally prevails at the edge of finite electrodes; and second, to minimize the amount of electrolyte. By using this configuration, shape change has been reduced dramatically as evidenced by the retention of the electrode dimensions (EXHIBITS B-IV and B-V). Cycle life performance in 5 AH cells has been improved by 60%. Concurrent with reduction in shape change, there is an increase in gravimetric energy density by 4 to 5% because of the replacement of electrolyte with the much less dense material.

Additional work in this area involves the use of thermally conductive foams, improved current collectors/tabs, heat pipes, etc. These are discussed in more detail in the thermal management section.

Current Collector/Tab Designs

The purpose of incorporating the current collectors with the new designs into the zinc electrode initially was to modify the current density distribution thereby promoting longer cycle life.

The cells that contain the new designs all performed better than the standards (EXHIBITS B-VI, B-VII, B-VIII, and B-IX). The utilization of the electrodes with the improved collector/tab designs was superior to the standard. Although close scrutiny reveals some structural differences among the electrodes using the three different collector designs, it is not unambiguously obvious because with the high solid area, the electronic cross-section is probably sufficiently large to obviate any electrical differences at the current densities imposed on these cells. One of the obvious benefits derived is better heat dissipation to the cell terminal. The improved heat dissipation results in better utilization of the electrode, hence, a reduction in degree of shape change and a delay in densification. It is to be emphasized that these 50 AH five-electrode cells were made in the Pilot Plant and that they represent a product made under realistic production conditions.

Charging

Extensive studies combining charging and analyses of gases evolved during the charging operation have been carried out to determine the gassing mechanisms, current, and ampere-hour efficiencies. Gas evolution rates and volumes were measured with a gas chromatograph. Typical gas evolution rates as a function of charging time are shown in EXHIBITS B-X, B-XI, and B-XII for constant current, constant potential, and pulsed charging imposed on a constant background current. The results of these studies indicate that:

1) Lower recharge at either constant current or constant potential is sufficient to charge the cells without loss in efficiency and increased cycle life.

2) Constant potential charging promotes improved cycle life by 140%.

3) Pulsed charging does not contribute beneficially to cycle life performance.

4) Reduction in degree of overcharge reduces the heat generation at the end of charge; therefore, it is less severe on the components.

Electrolyte Additives

Several electrode surface active electrolyte additives have been investigated to date in cells using standard components. The purpose of these additives is to promote uniform as opposed to sporadic nucleation within the pores of the electrodes to promote a smoother electrodeposit which should delay the densification process and maintain the porosity and available surface area. Additionally, because the electrodeposit is smooth, electrode homogeneity is maintained and dendrite formation is retarded. These advantages should lead to prolonged cycle life by minimizing dendrite formation.

Several cells that contained additives were subjected to cycle life testing. While a reasonable increase in cycle life was observed, there was a fairly drastic loss in capacity. It should be pointed out that while all the cells were built with similar components, all the control cells failed via massive shorting caused by hot spots and dendrite formation, while the cells that contained the additives only gradually lost the capacity.

New additives are continuously being screened in Hull cell tests and examined by scanning electron microscopy. What is examined is the morphology and structure of the electrodeposit as a function of current density and cycling. The promising additives are then tested in 5 or 50 AH cells.

Work has continued on the development of a procedure for rinsing potassium hydroxide from the electrode without degradation of the electrode. Improvements have been made using alcohols for rinsing instead of water but the process is not yet adequate to permit good characterization of the electrode.

Tests of 50 AH cells have been conducted to determine the effect of low potassium hydroxide concentrations on shape change and cell performance. Data from

a previous tri-electrode electric vehicle cell indicated that low electrolyte concentrations may reduce shape change. Concentrations of 10% (2.0 M) and 20% (4.2 M) were selected for investigation. Cells with 10% potassium hydroxide had short cycle life and did not accept charge well enough to reach full capacity. These cells failed to reach 20% capacity after 15 cycles. The internal resistance of these cells remained high with cycling.

Electrode Additives and Binders

Because of the nature of the process for the fabrication of the negative electrodes, a binder system is required. The binder should lend itself to ceramic processing techniques yet not hamper the basic electrochemical behavior of the electrode. Simultaneously, proper choice of binder system can enhance electrode performance by retarding shape change and/or densification.

Our studies have been aimed at developing a system that will facilitate processing and enhance electrode performance. To this end, several polymeric materials have been evaluated in the manufacturing process and subsequently in actual cells. The binder should promote better performance because of the driving force for electrolyte absorption into the electrode body.

About ten different systems have been evaluated in actual 5 AH cell tests. One system has been found to work adequately well and is the binder system in the electric vehicle electrodes that are currently being manufactured in the Pilot Plant. Comparative testing with a conventionally used binder (Teflon) system indicates that longer cycle life can be obtained.

High Density Electrodes

Some initial experiments with electrodes that have been pressed to a higher green density than conventional have indicated that better capacity retention is maintained (EXHIBITS B-XIII and B-XIV). Although the cell tests demonstrated favorable results, pressing to densities greater than 3 g/cm^3 is not a viable alternative since the type of equipment required for such an operation for electrodes that are larger than 8 in^2 is impractical in a high rate battery operation where thousands of components per hour must be produced.

Electrode Raw Materials

Several zinc oxide raw materials have been used in conjunction with a binder and evaluated in 5 AH cell tests to determine suitability and to optimize electrode performance. All the materials are in the micrometer or submicrometer particle size range and are in the surface area range of $\sim$3 to 11 m^2/g. The best performance has been obtained with the currently used zinc oxide. No attempts have been made at blending combinations of powders to modify surface area particle size distribution.

During the course of the present program, some "binderless" electrodes were fabricated and tested. These 5 AH electrodes were fabricated in collaboration with an external vendor using the vendor's proprietary process. Although charge acceptance of the 5 AH cells that contained these electrodes was superior to any corresponding cell containing electrodes fabricated with a binder, they all

failed by catastrophic shorting in less than 60 cycles. Three different groups of electrodes, hence cells, were constructed.

By the nature of the process that is used to make the electrode parts, the final surface area of the powder in the electrode is higher than the starting powder surface area. No significant differences were observed in the cycle life performance of cells from the three groups. A significant feature to note is the excellent capacity retention up to the point of shorting as compared to the gradual loss observed with the binder containing electrode cells. Autopsy of these cells revealed that the geometric area of the electrodes was reduced by about 50% and that the current collector was totally bare in that region, yet the cell was still delivering 100% of the theoretical capacity of the nickel electrode. It must be borne in mind that the theoretical capacity of the nickel electrode is the maximum attainable capacity on the basis of the one electron reaction of the total available $Ni(OH)_2$ and not theoretical capacity based on rated which can sometimes be a much lower value that has been arbitrarily assigned to enhance the apparent performance of the cells or components.

The reason for this exceptional performance with 50% of the geometric area on the zinc electrode is not known at this time, and additional work is required to understand this phenomenon so that it may be beneficially utilized.

Electrode Geometry

Electrode size may have an influence on cycle life. To determine the events of this influence, three sizes of cells were designed based on available electrode sizes and materials. Electrode sizes 8" x 14", 4" x 7", and 2" x 3.5" were selected because of their identical symmetry. Eight of ten 2" x 3.5" electrode cells, which have 10 AH capacity, have approximately 95 to 100% capacity. Two other cells show signs of shorting.

Spatial Distribution of Dissolved Zinc

Since there is a redistribution of zinc on the electrode during cycling and because the nickel-zinc system is a dynamic system, the need to know the movement and concentrations of the species involved in this redistribution is important in order to characterize the operative mechanisms and devise a solution to the problem. Most of the effort during this first part of the program has been devoted to devising the experimental methods, techniques, and components in order to dynamically measure the variables as a function of cycle life.

In order for the dissolved zinc concentration measurements to have any significance, associated parameters such as electrolyte concentration and temperature must also be measured. Also, carbonation of the solution must be minimized. The development of a suitable system to measure the dissolved zinc has been discussed in previous reports. These electrodes are embedded in a 5 AH tri-electrode cell for measurements. The experiments are carried out in a constant temperature bath with the top of the cell being purged with argon to minimize carbonation.

The calibration of the standard electrode potential for a known change in hydroxyl ion concentration has been well characterized. The potential obeys a Nernstian relationship for the hydroxyl ion concentrations tested (.25 Molar to 15 Molar).

The effect of zincate in solution and its possible effect on the standard electrode potential was also examined. On monitoring the potential in saturated zincate solutions of known hydroxyl ion concentrations, it was found that it is insensitive to zincate.

Also tested was the temperature stability of the standard electrode potential for different hydroxyl ion concentrations. Known solutions of hydroxyl ion concentrations were heated to ∿90° C and the electrode potential was monitored as a function of temperature. Results show that the electrode potential changes 50 to 10 μV.

Tests were also conducted to measure the equilibrium response time of the electrode potential to a known change in hydroxyl ion concentration. Tests conducted consisted of injecting known volumes of either 45% potassium hydroxide or water into a known volume of hydroxyl ion concentration. The electrode potential was monitored with time until equilibrium was established. Results from these tests for both increasing and decreasing hydroxyl ion concentration show that the electrode responds at a rate of ∿.1 Molar (OH^-) per second.

The standard electrodes have been cycles at an approximate C/10 rate with the voltage being stable for greater than 100 hours in 45% potassium hydroxide.

The conclusion from the tests conducted show the electrode to be sensitive to the hydroxyl ion concentration and adequate for incorporation into a test cell for the hydroxide measurement.

Actual simultaneous spatial measurement of dissolved zinc and electrolyte concentration in 5 AH cells will be started in the near future. These measurements which should provide good insight into the dynamic behavior of the present and shape change mechanisms will be made during charging, discharging, rest, and a function of temperature.

Thermal Management

Although this area has been generally discussed in Task B of the Program, it will henceforth be treated as a separate area because of its encompassing nature. In view of the importance of thermal management, it should probably be spelled out as a separate major task for the remainder of the Program.

A good deal of the work in this area has gone into generating the appropriate computer programs to be able to model the cells and batteries under dynamic conditions. In addition to internal software development, two programs have been procured and are operational on a time-sharing system. The first program uses a finite element approach for conducting heat transfer or structure analyses. The second program, which is a revised version of CINDA-3G, uses a finite difference approach. Also, in order to measure the heat generation in cells, a TRONAC calorimeter along with a data acquisition system have been purchased and are currently operational.

A one-dimensional analysis of the temperature distribution in a 400 AH electric vehicle cell has been carried out. The actual measured data is reported in EXHIBIT B-XV.

Since cell thickness is relatively thin compared with cell height and width, the heat transfer process involved is essentially one dimensional. Our analysis gives the temperature profile in the cell as

$$T(x,t) = T_\infty + (\delta^2 \dot{q}'''/\kappa)[0.5(1 - x/\delta) + \kappa/h\delta + 2\sum_{n=1}^{\infty} A_n \cos(\lambda_n x/\delta)\exp(-\lambda_n^2 \alpha t/\delta^2)] \quad (1)$$

where T_∞ is the surrounding temperature, δ is the half thickness of the cell, $\dot{q}'''$ is the heat generation rate per unit volume, κ is thermal conductivity, α is thermal diffusivity, h is the heat transfer coefficient, and the λ_n are the positive roots of the equation

$$\lambda_n \tan \lambda_n = h\delta/\kappa \quad (2)$$

and

$$A_n = (T_0 - T_\infty)/\dot{q}'''\delta^2/\kappa) - (1/\lambda_n)]\sin\lambda_n(\lambda_n + \sin\lambda_n\cos\lambda_n)^{-1} \quad (3)$$

Based on the dimensions and materials of the cell, the mean thermophysical properties of the cell were calculated. With the assumption that the heat transfer from the cell surface was by natural convection and radiation, the value of heat transfer coefficient was then determined. With the above information, only the dimensionless temperature profile can be calculated because the heat generation rate is still unknown. To compare the analysis with the measurements, it is assumed that at the end of discharge, the predicted temperature is equal to the measured one. With this assumption, the temperatures at the center (x = 0) and at an edge (x = δ) were calculated; the results are shown in EXHIBIT B-XVI.

The predicted temperature is a few degrees higher than the measured curve. This is because the heat generation rate is not constant near the end of discharge. If the predicted temperature is matched with the measured temperature at about time $\simeq$ 2.5 h, the agreement between the theory and the measurement would be even better. The comparison indicates: 1) the one-dimensional mathematical model closely approximates the actual system; 2) the thermophysical properties that we used for calculations are correct and can be used for heat transfer analysis of other nickel-zinc batteries; and 3) the heat generation rate of the cell is about 1,440 BTU/h·ft^3 at three hour discharge rate. This number can be used as a check for that from thermodynamic calculations.

The heat generation rate in a cell can also be calculated by using the cell voltage, discharge current, and the thermal efficiency if available. Recent work done at Gould has shown that the heat generation rate can be calculated using the following equation:

$$\dot{Q} = I\left[-\frac{T}{nF}\left(\frac{\partial S}{\partial \xi}\right)_{p,t} + E - Vi\right]$$

Excluding the top and bottom electrolyte reservoirs, the volume of the cell is about 0.103 ft^3. The heat generation rate per unit volume in the cell is

$$\dot{q}''' = 152.5/0.103 = 1481 \text{ BTU/Hr Ft}^3$$

As shown by calculations, the value of $\dot{q}'''$ predicted by one-dimensional heat transfer analysis is

$$\dot{q}''' = 1460 \text{ BTU/Hr Ft}^3$$

If the cell temperature is about 80° F at the beginning of discharge, the cell temperature at the end of three hour discharge is

$$T = 80 + 19.4 \times 3 = 138.2° \text{ F}$$

As shown in EXHIBIT B-XVII, the cell temperature increases linearly with time if the cell is perfectly insulated. The temperature difference between an insulated cell and a natural-convection cell increases with time, this is because natural-convection becomes more significant as the temperature difference between the cell and its surroundings increases. During three hour discharge, the total heat generation is

$$Q = 457.4 \text{ BTU}$$

The heat transferred by natural-convection from the cell to room air is about

$$Q_{N.C.} = 95.4 \text{ BTU}$$

This means that about 21% of the total heat generated is transferred from the cell to room air and 79% remains in the cell.

The first computer program has been chosen to perform further heat transfer analysis for nickel-zinc cells. The program uses a finite element approach to solve three-dimensional heat conduction problems. The input data, heat generation rate, transport properties, and boundary conditions can be space dependent. The first test example is a two-dimensional system with the size and properties of a five-electrode, 50 AH cell. The program is prepared for batch jobs. The input data are supposed to be prepared following the read-formats of the program. Thus, it is somewhat difficult to set up an input data file through our terminal.

The empirically determined thermal distribution and distribution of heat generation rates in actual cells must be measured in order to fully utilize the modeling programs to better characterize the problems. In order to make these measurements, 26 thermistor probes have been calibrated for a temperature range from 0° C to 100° C. With one calibration curve for each probe, the absolute error in temperature measurements is expected to be within ±0.1° C. To protect probes and their lead wires from corrosion in potassium hydroxide, insulation is necessary.

During cell cycling, high terminal temperature and "hot spots" on electrodes have been observed. These two phenomena may relate to the thermal behavior in cells but cannot be explained with a usual heat transfer model for battery systems because they are probably caused by high local heat generation. The high terminal temperature is probably due to high I^2R heat generated at terminals. The temperature can be reduced effectively if the electrical resistance can be reduced. The existence of hot spots is more complicated. It seems that a spot is initiated on the nickel or zinc electrode and then propagates through the other electrode, then to the next electrode, up to the end electrode. The initiation of a short spot is probably due to nonuniformity of electrode material in composition or geometry, which caused a local high electrochemical reaction rate, and in turn, high heat generation rate at that particular spot. It has been observed that hot spots propagate in a direction

consistent with the current direction. Therefore, the spot formed on the next zinc electrode is probably caused by high chemical reaction rate due to the existence of the first spot. This local effect becomes more significant after each cycle. Eventually, the temperature at hot spots increases to the melting temperature of separator materials.

An analysis has been carried out to see the effect of tab width on heat transfer from a nickel-zinc cell. Since heat generated in the cell will be transferred through the cell case to environments in all directions, to find the exact amount of heat transferred through tabs in an actual system is a three-dimensional analysis which is quite complicated. For a qualitative study, we assume that, except for the top, the other surfaces of a cell are perfectly insulated. In other words, the heat generated in the cell will be transferred only through electrode tabs. If the tabs are surrounded by air, heat will then be transferred to the surrounding air by natural convection, then from air to top case wall, and from case wall to room air at room temperature. If heat is uniformly generated in the cell, the highest temperature in the plate will be at the bottom. Assuming that the temperature at the top of the plate is uniform, the heat transfer rate at the top surface is

$$Q = A_o H_o (T_t - T_{air}) + \left[\frac{2\, h_t\, A_t\, \kappa_t}{W_t}\right]^{1/2} W_t \tanh\left[\frac{2 h_t}{\kappa_t \delta_t}\, \ell_t^2\right]^{1/2} (T_t - T_{air})$$

Where $A_o H_o (T_t - T_{air})$ is the heat transferred with no tab and the balance of the expression is the heat transferred through the tab.

$$A_o = A_p - A_t = \delta_p W_p - \delta_t W_t$$

A_p = Cross-sectional area of the plate
A_t = Cross-sectional area of the tab

The temperature distribution in the plate is given by

$$T_p - T_t = \frac{\dot{q}'''}{2 \kappa_p} (\ell_p^2 - y^2) \qquad (5)$$

and

$$T_m - T_t = \frac{\dot{q}'''}{2 \kappa_p}\, \ell_p^2 \qquad (6)$$

where T_m is the maximum temperature within the electrode.

The subscripts o, p, and t indicate

o = Open area at the top of the plate
p = Plate
t = Tab

From equations (4), (5), and (6), we then have

$$T_m - T_{air} = \frac{C_2}{C_1} \dot{q}''' \qquad (7)$$

where

$$C_1 = [2\, h_t\, A_t\, \kappa_t\, W_t]^{1/2} \left\{\tanh\left[\left(\frac{2 h_t}{k_t \delta_t}\right)^{1/2} \ell_t\right]\right\} + (\delta_p W_p - \delta_t W_t) h_o$$

$$C_2 = \delta_p W_p \ell_p + C_1 \ell_p^2 / 2 \kappa_p$$

If the open area at the top of the plate is insulated, $h_o = 0$ and all heat, Q, is transferred through the tab. For this case, we assume $h_o = 0$

$\delta_p = 0.100$ in $K_p = 0.62$ BTU/Hr Ft F
$W_p = 5.000$ in $h_t = 1.50$ BTU/Hr Ft^2 F
$\ell_p = 12.000$ in $K_p = 52.00$ BTU/Hr Ft F (Ni)
$\ell_t = 0.750$ in $= 223.00$ BTU/Hr Ft F (Cu)
$\delta_t = 0.005$ in

then for metal ($\rho 1$)

$$C_1 = 0.159\ W_t$$
$$C_2 = 0.00347 + 0.00152\ W_t$$
$$\frac{T_m - T_{air}}{\dot{q}'''} = 0.0095 + \frac{0.0218}{W_t}$$

and for metal ($\rho 2$)

$$C_1 = 0.180\ W_t$$
$$C_2 = 0.00347 + 0.000404\ W_t$$
$$\frac{T_m - T_{air}}{\dot{q}'''} = 0.00224 + \frac{0.0192}{W_t}$$

T_m (F), T_{air} (F), W_t (ft), $\dot{q}'''$ (BTU/Hr Ft^3)

For the case where heat escapes through the cell case top, and $h_o = h_t = 1.5$ BTU/Hr Ft^2 F, the parameters for metal ($\rho 1$) are

$$C_1 = 0.1589\ W_t + 0.00521$$
$$C_2 = 0.00347 + 0.00961\ (0.1589\ W_t + 0.00521)$$
$$= 0.003471 + 0.00153\ W_t$$
$$\frac{T_m - T_{air}}{\dot{q}'''} = \frac{0.003471 + 0.00153\ W_t}{0.00521 + 0.1589\ W_t}$$

The calculations were carried out for $h_o = 0$ and $h_o = 1.5 \frac{BTU}{Hr\ Ft}$ and the results are shown in EXHIBIT B-XVIII for tab width from 1 to 5 inches. The temperature difference, $(T_m - T_{air})$, for $\dot{q}''' = 750$, 1500 and 3000 $\frac{BTU}{Hr\ Ft}$, is plotted in EXHIBIT B-XIX. If the electrode is in a cell case, the temperature, T_{air}, is not the room temperature, T_{room}. Consider a single electrode and assume that the temperature of case wall is equal to T_{air}, the heat transfer rate through the case wall is

$$Q = A_p\ h\ (T_{air} - T_{room})$$
$$A_p = \delta_p\ W_p = (\frac{0.1}{12})(\frac{5}{12}) = 0.00347\ ft^2$$
$$h \approx 0.54 \frac{K}{W} (\frac{g\beta W_p}{12})^{\frac{1}{4}} (T_{air} - T_{room})^{\frac{1}{4}}$$

for $\dot{q}''' \approx 1500$ BTU Hr Ft^2, we have

$$Q \approx 5.2 \text{ BTU/Hr}$$

$$T_{air} - T_{room} = 583 \text{ F}$$

$$T_m - T_{room} = (T_{air} - T_{room}) + (T_m - T_{air})$$

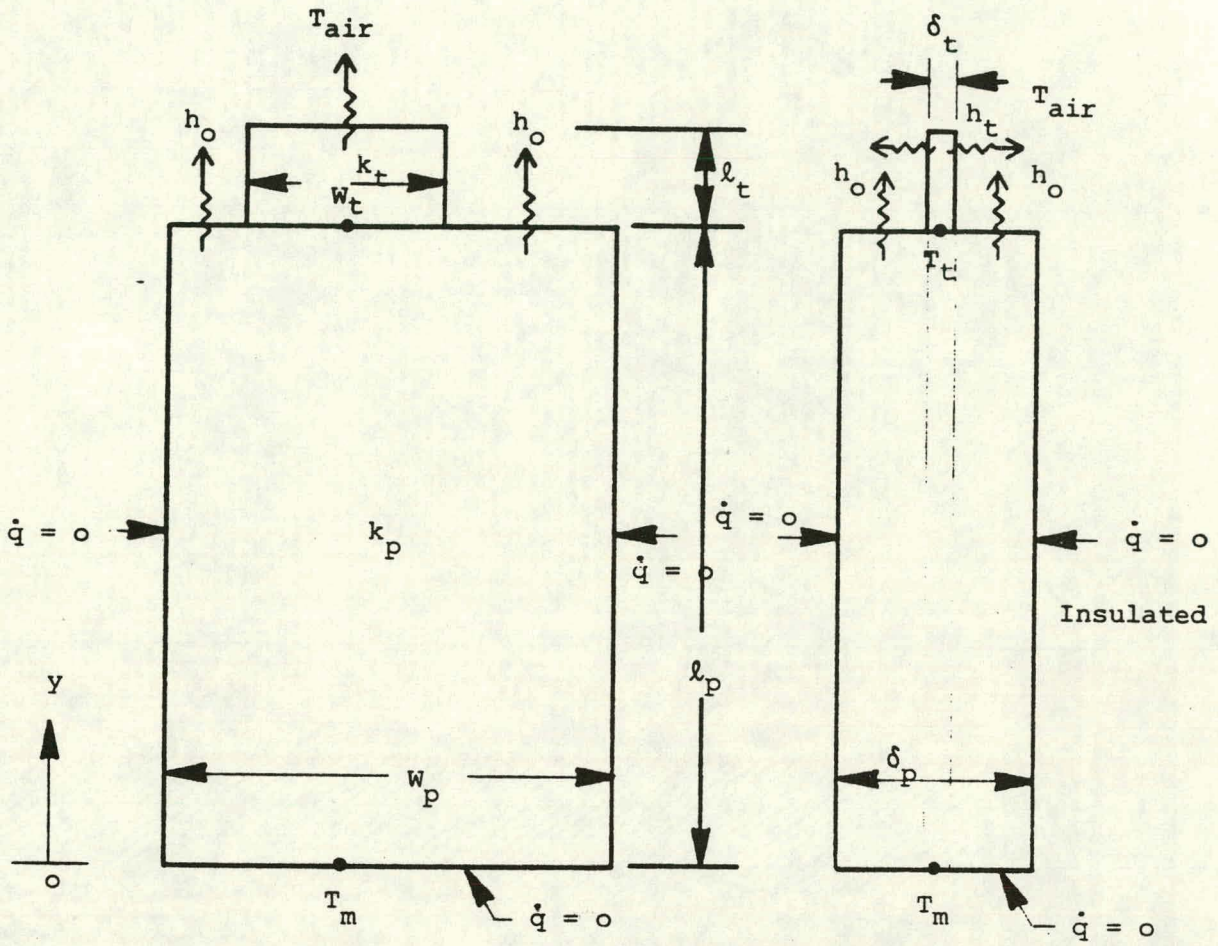
T_{air}
h_o
k_t
W_t
h_o
ℓ_t
$\dot{q} = o$
k_p
$\dot{q} = o$
ℓ_p
y
o
W_p
T_m
$\dot{q} = o$
δ_t
T_{air}
h_t
h_o
h_o
T_t
$\dot{q} = o$
$\dot{q} = o$
Insulated
δ_p
T_m
$\dot{q} = o$

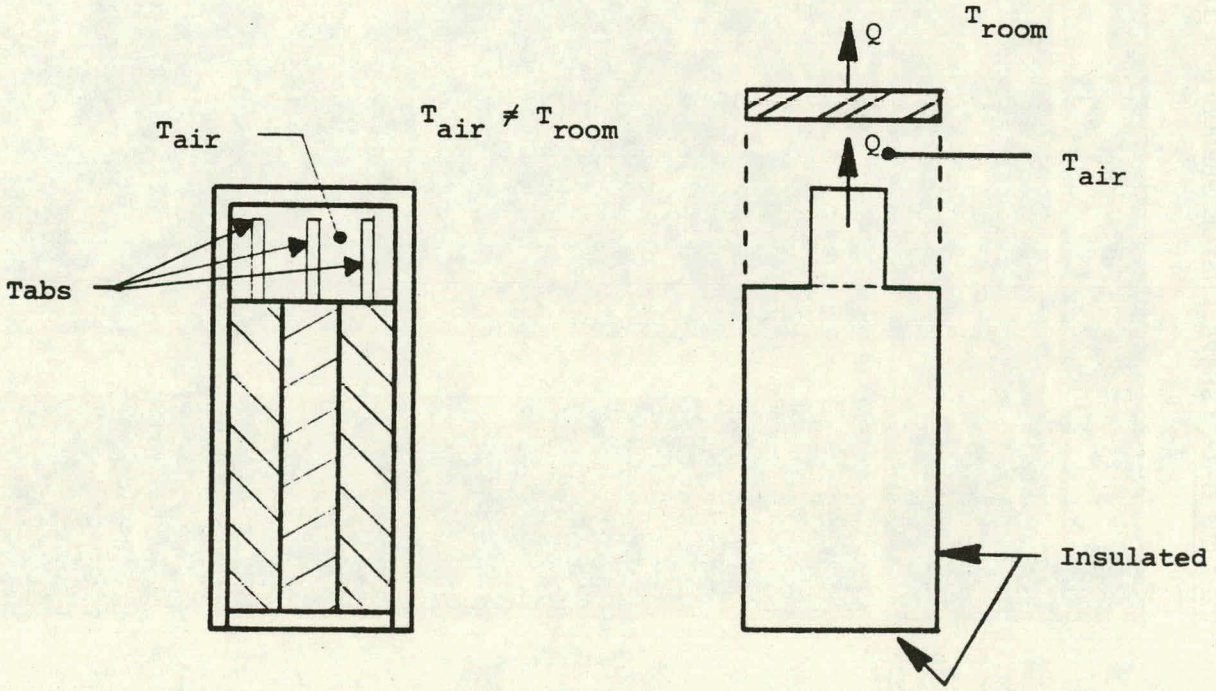
T_{air}
$T_{air} \neq T_{room}$
Tabs
Q
T_{room}
Q
T_{air}
Insulated

EXHIBIT B-I: SHAPE CHANGE PHENOMENON IN THE ZINC ELECTRODE

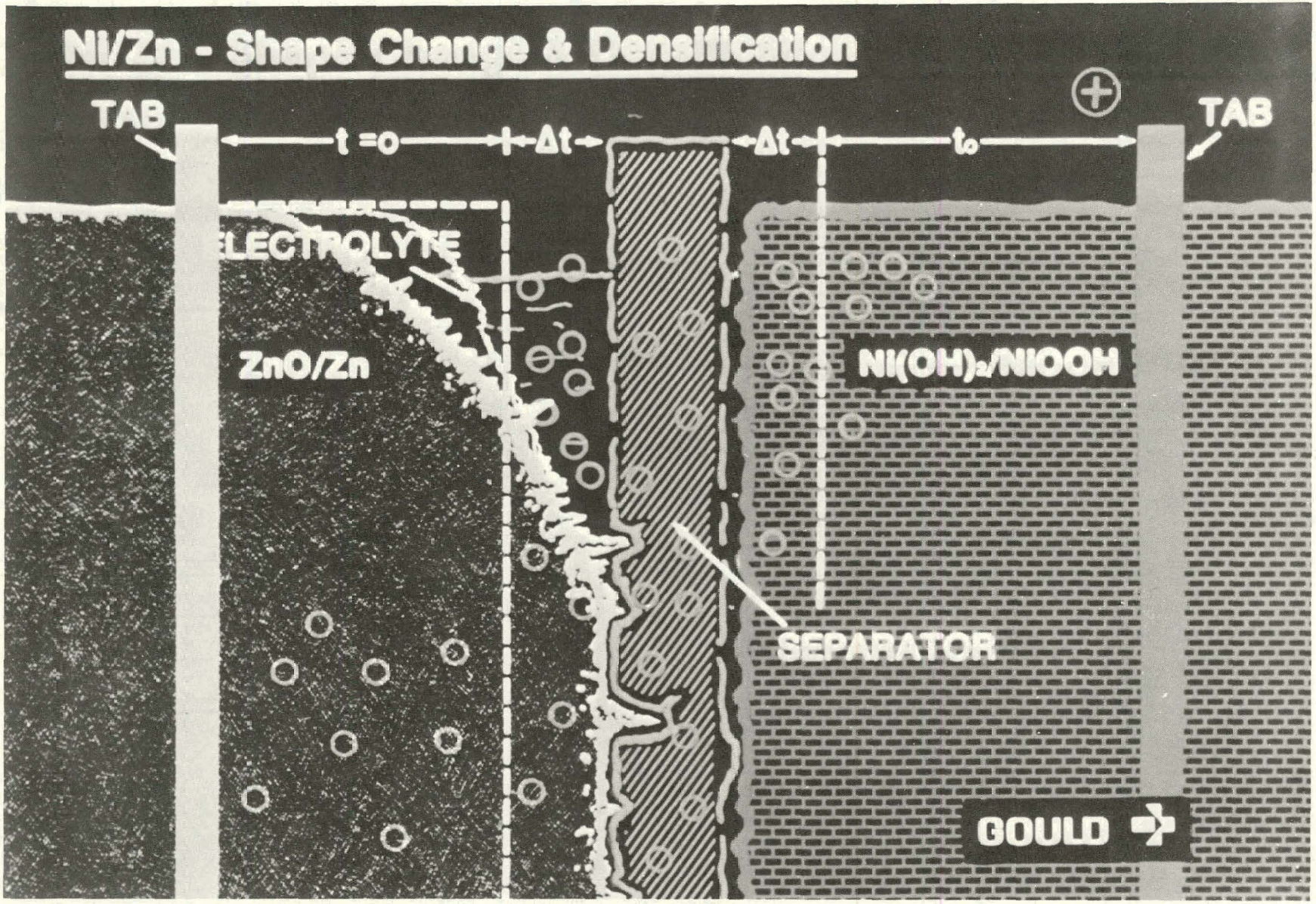

EXHIBIT B-II: TYPICAL CELL LIFE PERFORMANCE EXHIBITING GRADUAL LOSS IN CAPACITY

SEE EXHIBIT A-III

EXHIBIT B-III: ZINC DENDRITE MIGRATION THROUGH SEPARATOR LEADING TO CATASTRIPHIC FAILURE

SEE EXHIBIT A-I

EXHIBIT B-IV: RADIOGRAPH OF CYCLED MIDDLE NEGATIVE ELECTRODE FROM CELL WITH MODIFICATION

CELL NUMBER: NZ50.78.855.4.61
CYCLE NUMBER: 97

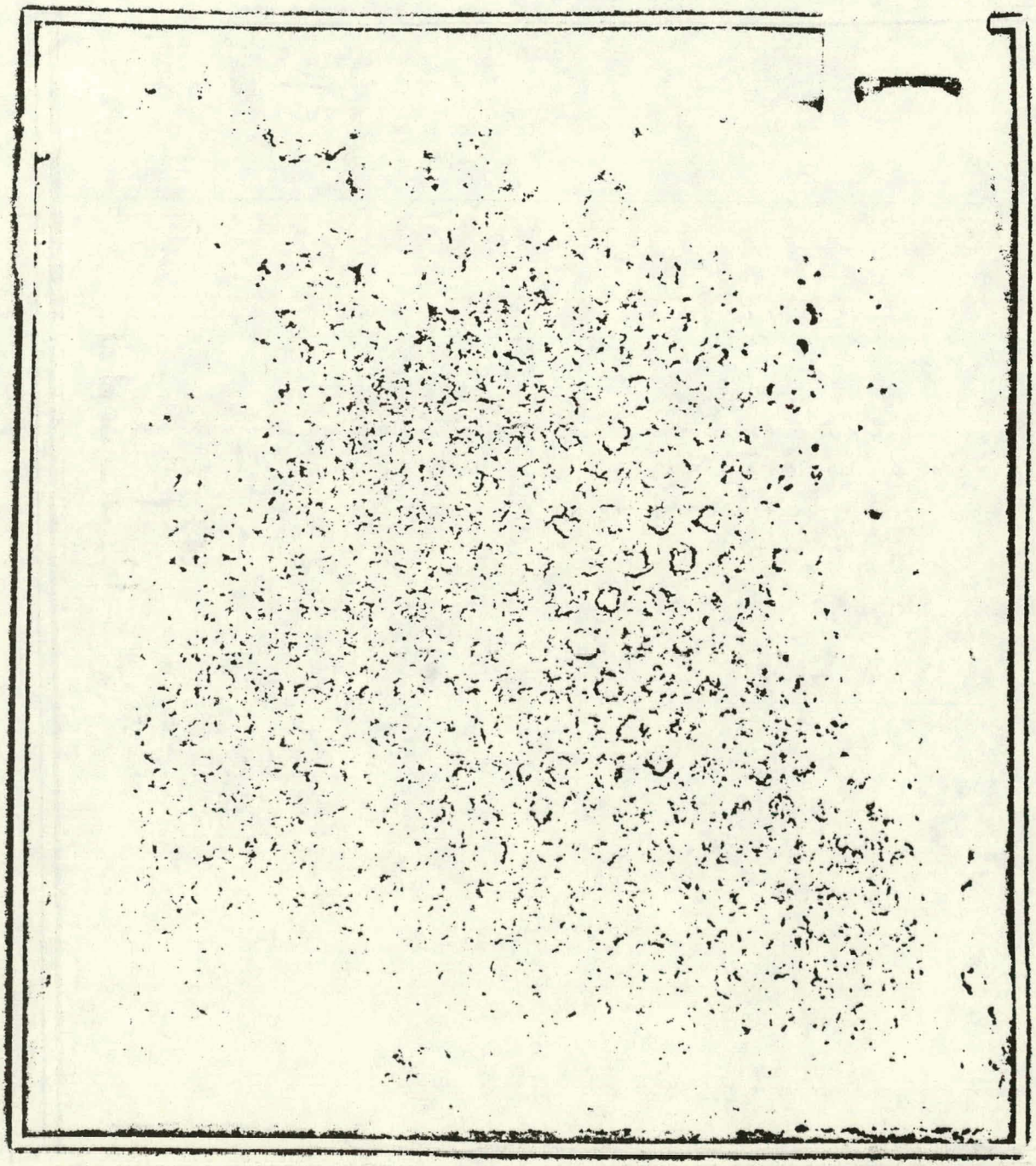

EXHIBIT B-V: RADIOGRAPH OF CYCLED MIDDLE NEGATIVE -- CONTROL

CELL NUMBER: NZ50.78.855.4.66
CYCLE NUMBER; 97

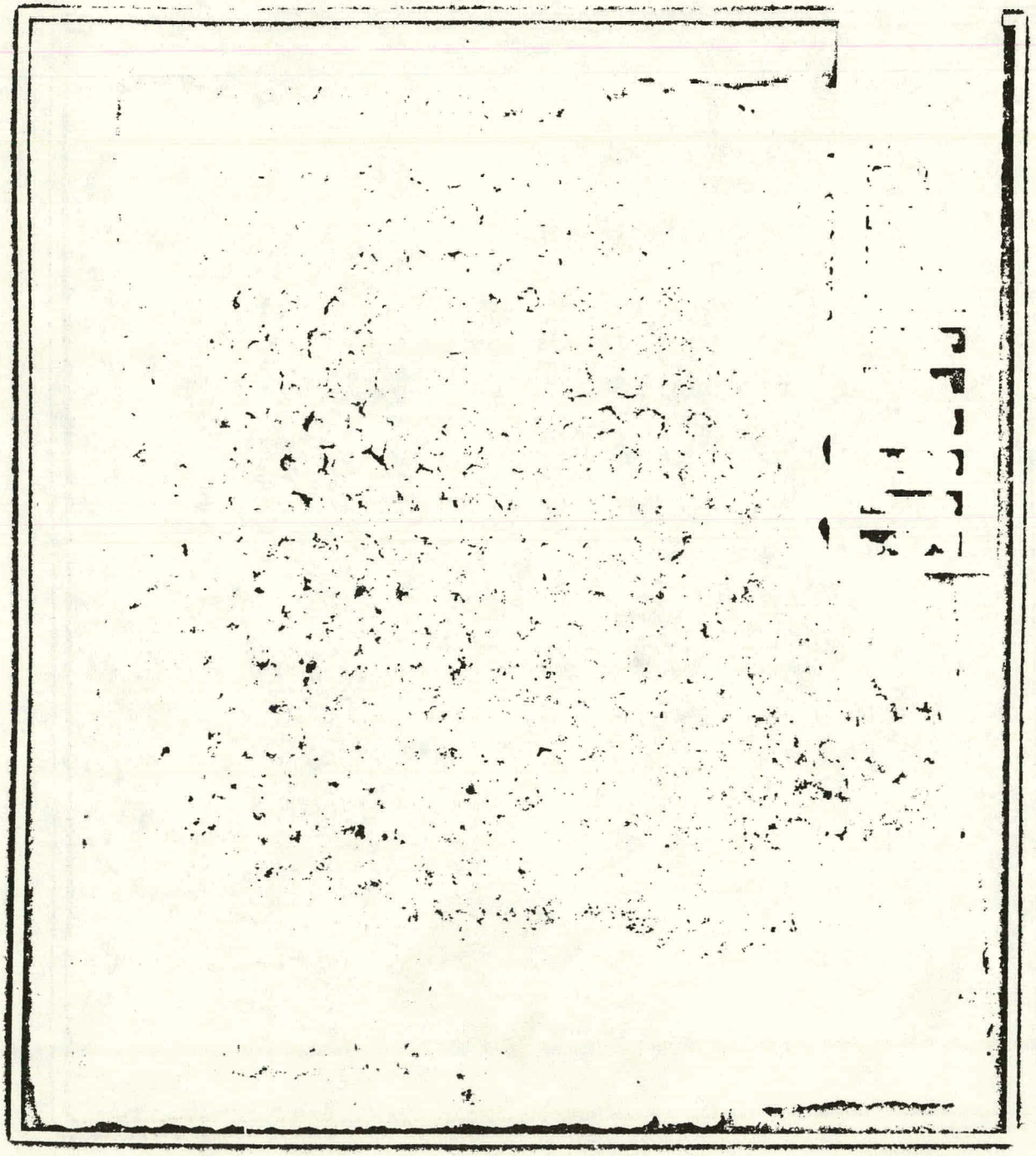

EXHIBIT B-VI: PERFORMANCE OF 50 AH CELLS WITH NEGATIVE COLLECTOR B

CELL NUMBERS: NZ50.77.802.62.37 to 39
CAPACITY: 50 AH
CYCLE REGIME: Component

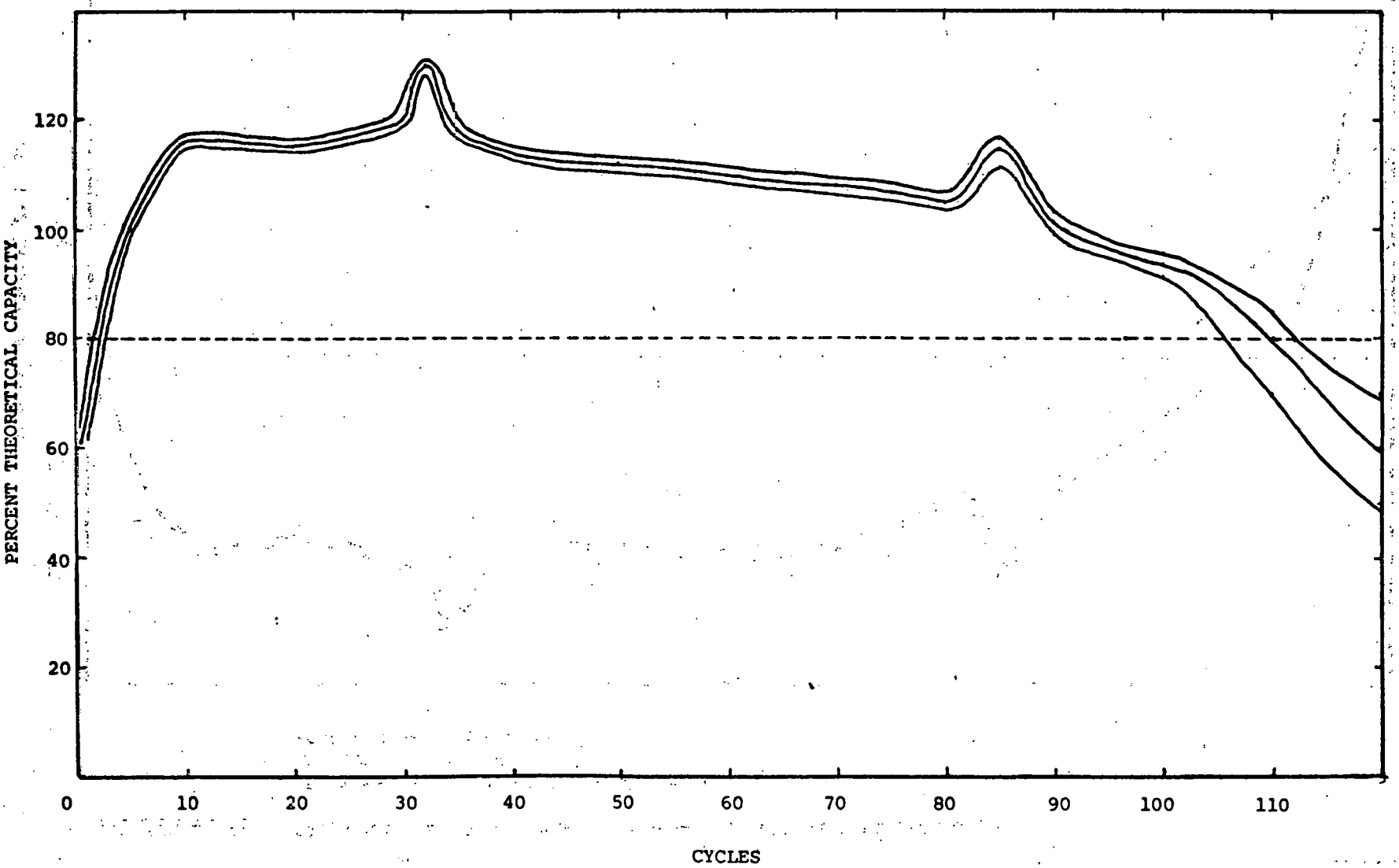

EXHIBIT B-VII: PERFORMANCE OF 50 AH CELLS WITH NEGATIVE CURRENT COLLECTOR C

CELL NUMBERS: MZ50.77.802,62,40 and 41
CAPACITY: 50 AH
CYCLE REGIME: Component

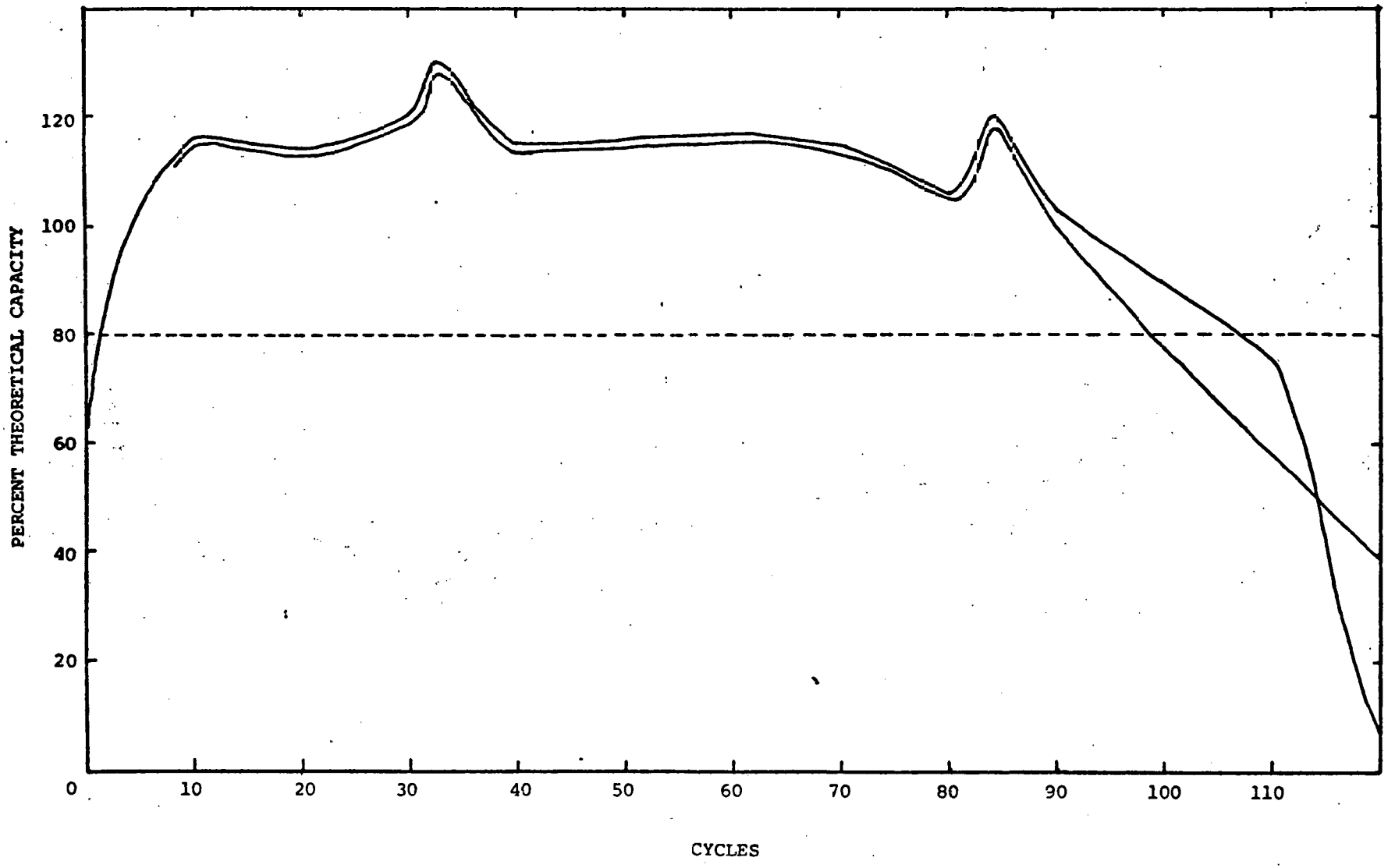

EXHIBIT B-VIII: PERFORMANCE OF 50 AH CELLS WITH NEGATIVE CURRENT COLLECTOR A

CELL NUMBERS: NZ50.77.802.62.34 to 36
CAPACITY: 50 AH
CYCLE REGIME: Component

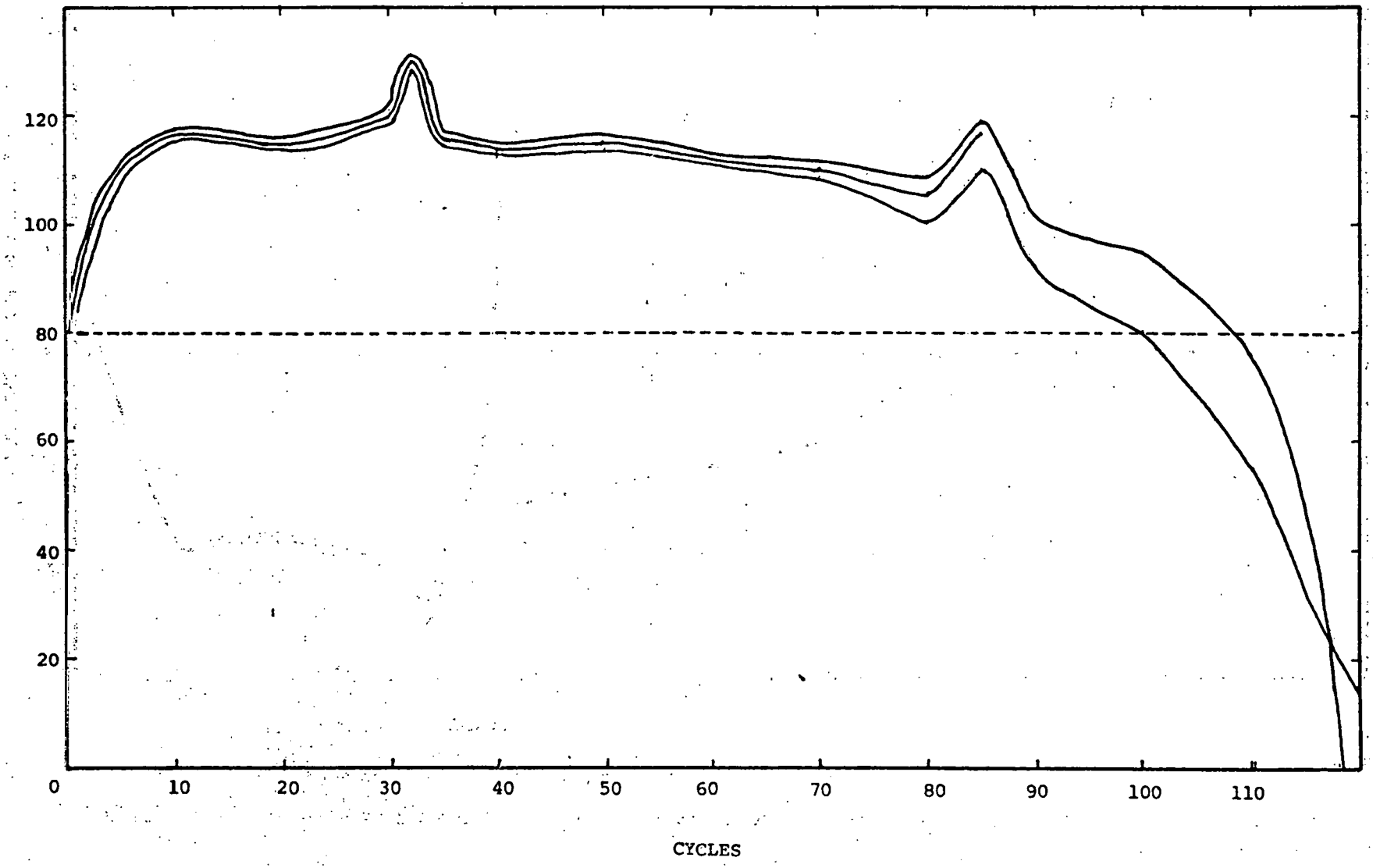

EXHIBIT B-IX: PERFORMANCE OF CONTROL CELLS FOR CURRENT COLLECTOR DESIGN STUDY

CELL NUMBERS: NZ50.77.802.62.50 and 51
CAPACITY: 50 AH
CYCLE REGIME: Component

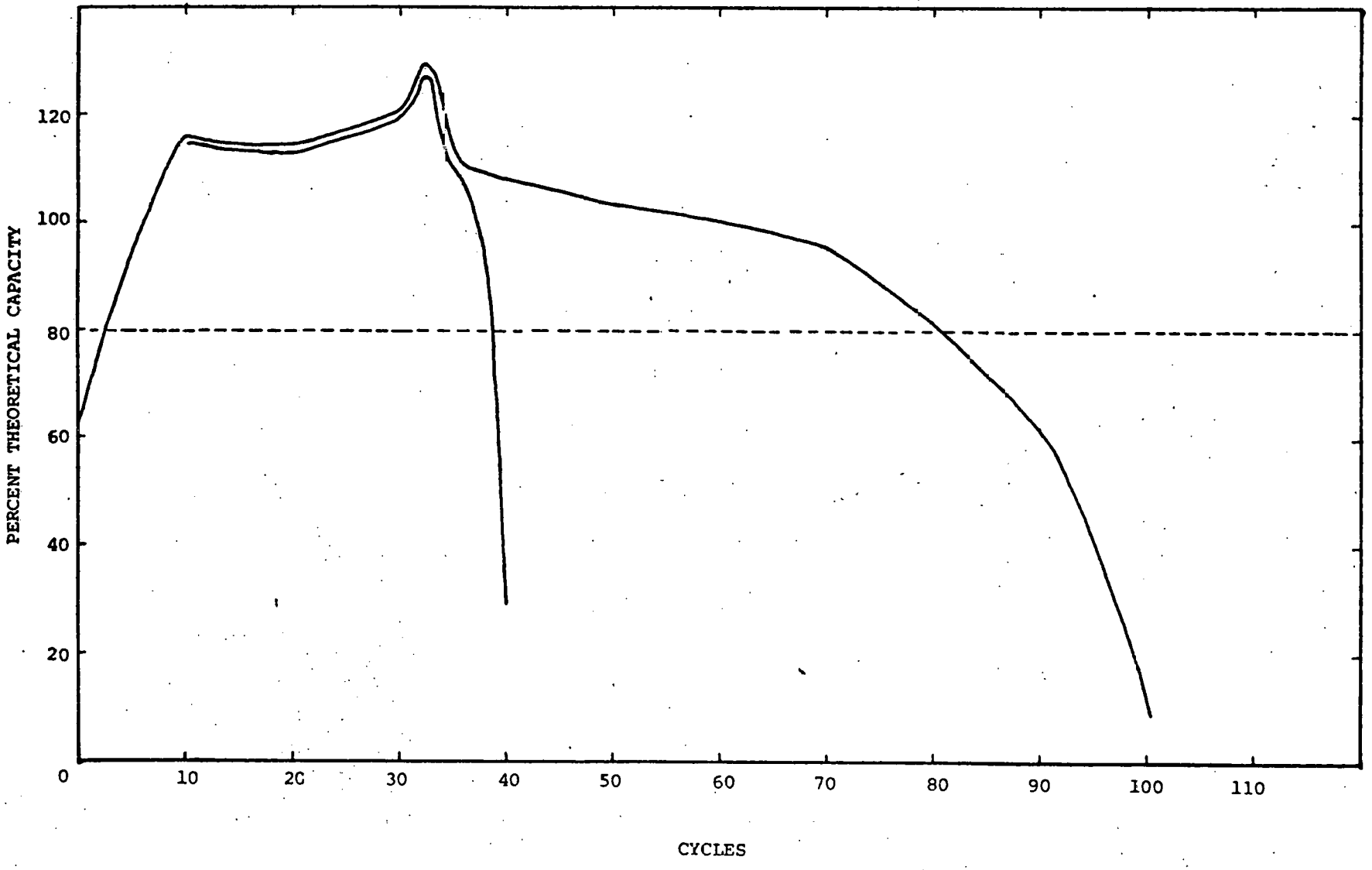

EXHIBIT B-X: CURRENT EFFICIENCY OF CONSTANT CURRENT CHARGE

CELL NUMBER: NZ5.78.850.51.1
CAPACITY: 5 AH
CHARGE: 1.2C/9
CURRENT EFFICIENCY: 89.2% (Nickel)

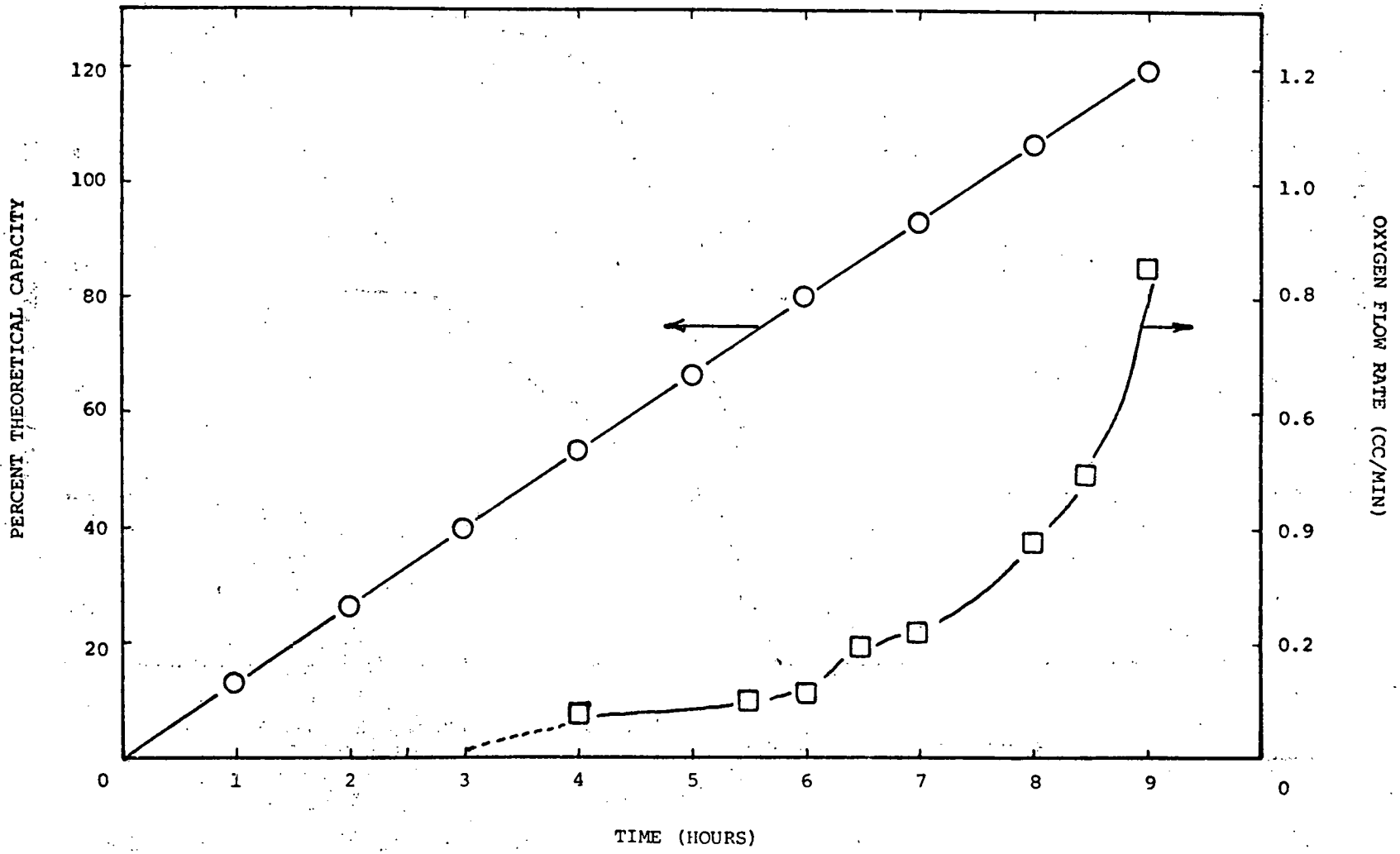

EXHIBIT B-XI: CURRENT EFFICIENCY OF CONSTANT POTENTIAL CHARGES

CELL NUMBER: NZ5,78,850.56.4
CAPACITY: 5 AH
CHARGE: 1.90 Constant Cell Voltage 1.5A Current Limit
CURRENT EFFICIENCY: 94.1% (Nickel)

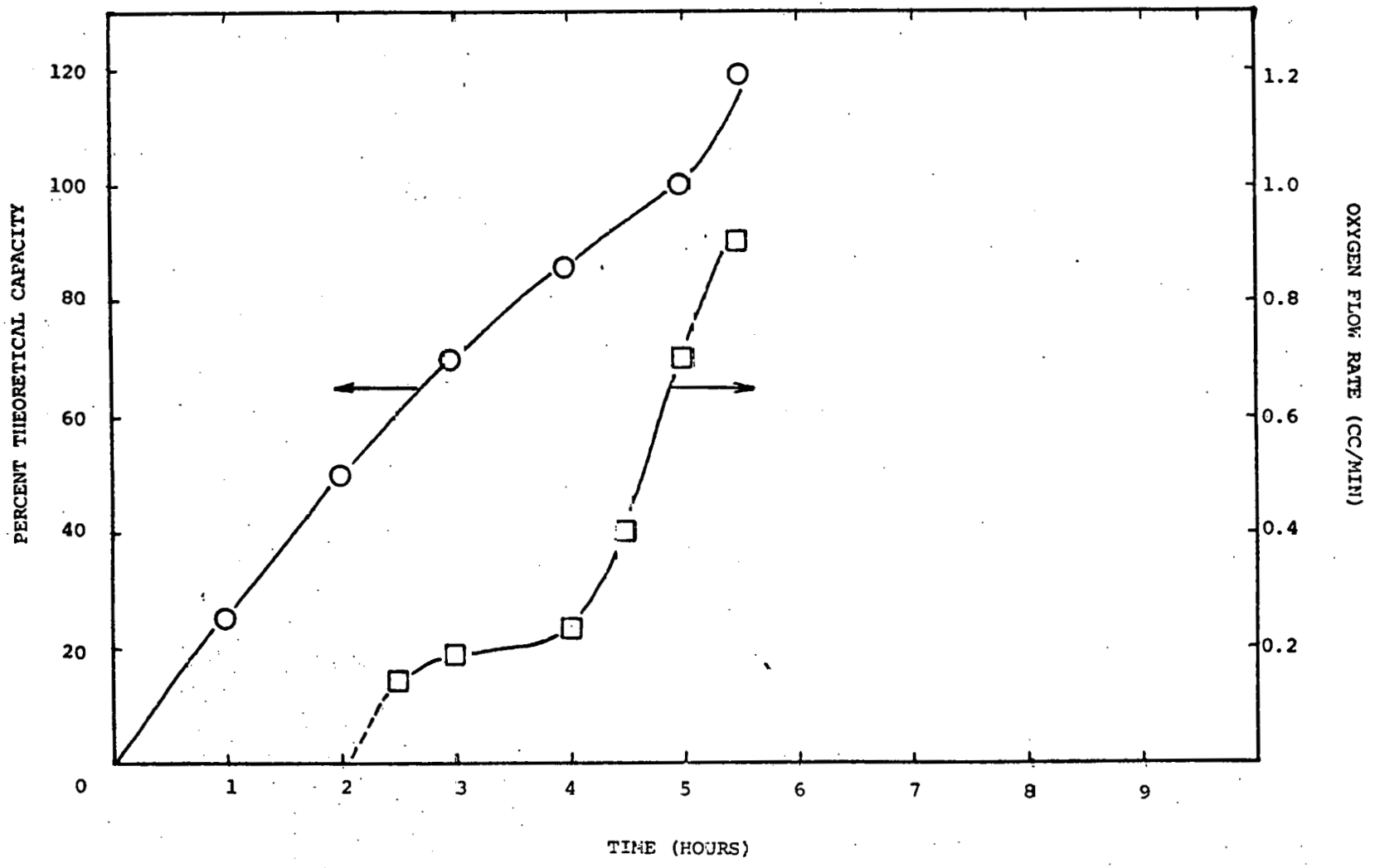

EXHIBIT B-XII: CURRENT EFFICIENCY OF PULSED CURRENT CHARGING

CELL NUMBER: NZ5.78.855.15.1
CAPACITY: 5 AH
CHARGE: 2,7 Amp Amtitude; 1.67 Hz, 16.7% Duty, Background Current 0.3 Amps
CURRENT EFFICIENCY; 91.7% (Nickel)

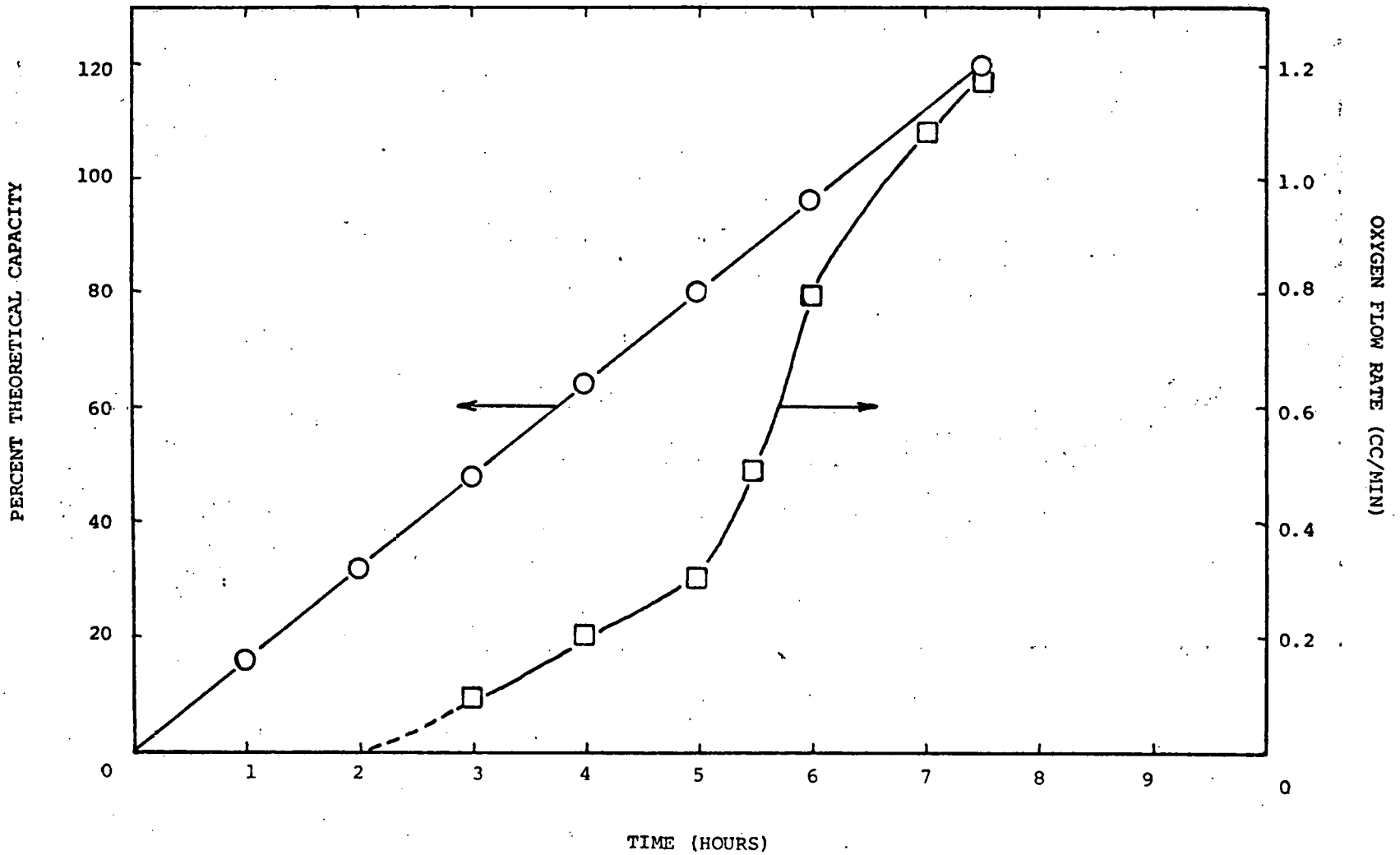

EXHIBIT B-XIII: PERFORMANCE OF HIGH DENSITY NEGATIVES

CELL NUMBERS: NZ5,78,802.128.1 to 3
CAPACITY: 5 AH
CYCLE REGIME: Component

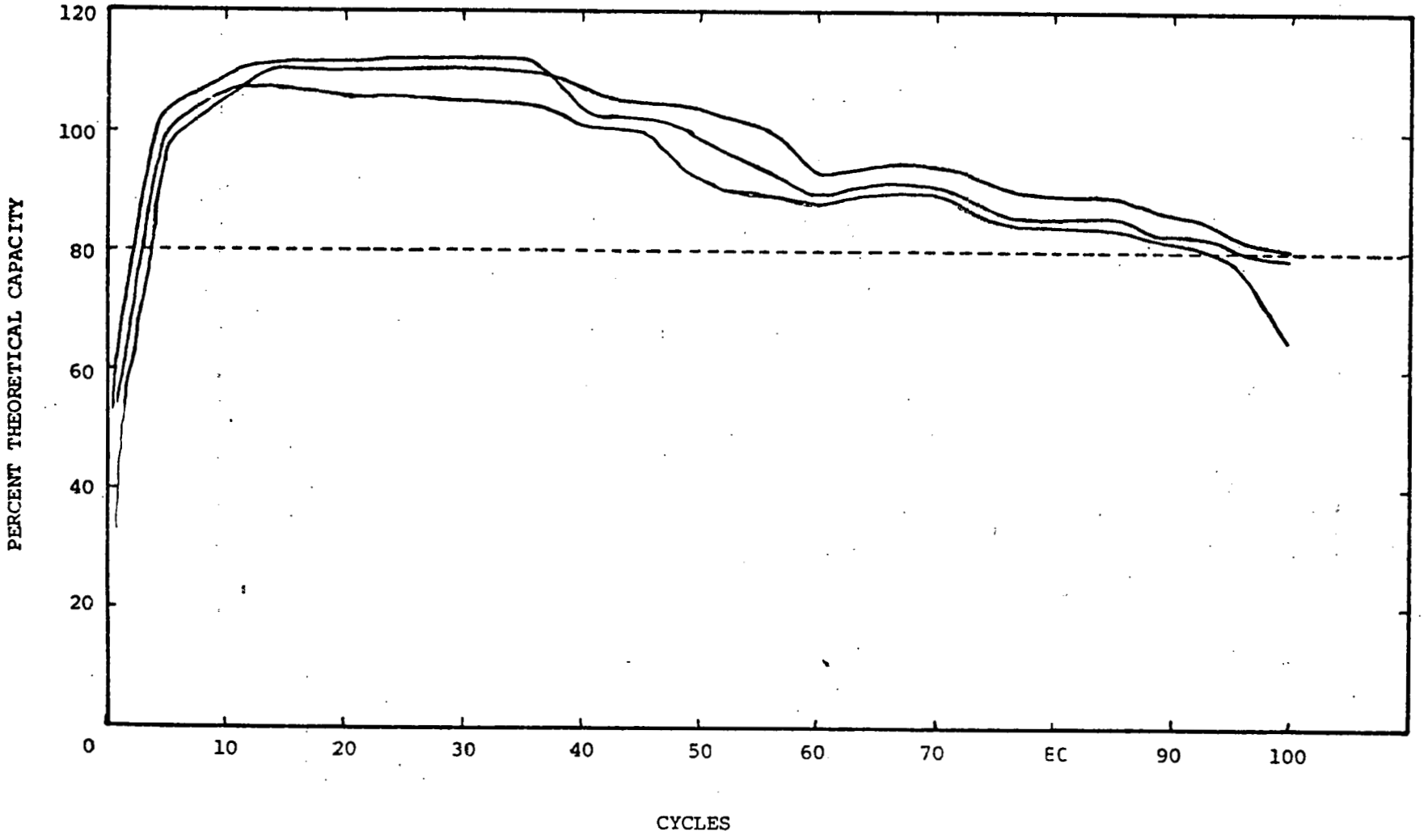

EXHIBIT B-XIV: PERFORMANCE OF CONTROL CELLS

CELL NUMBERS: NZ5.78.855.5.1 to 3
CAPACITY: 5 AH
CYCLE REGIME: Component

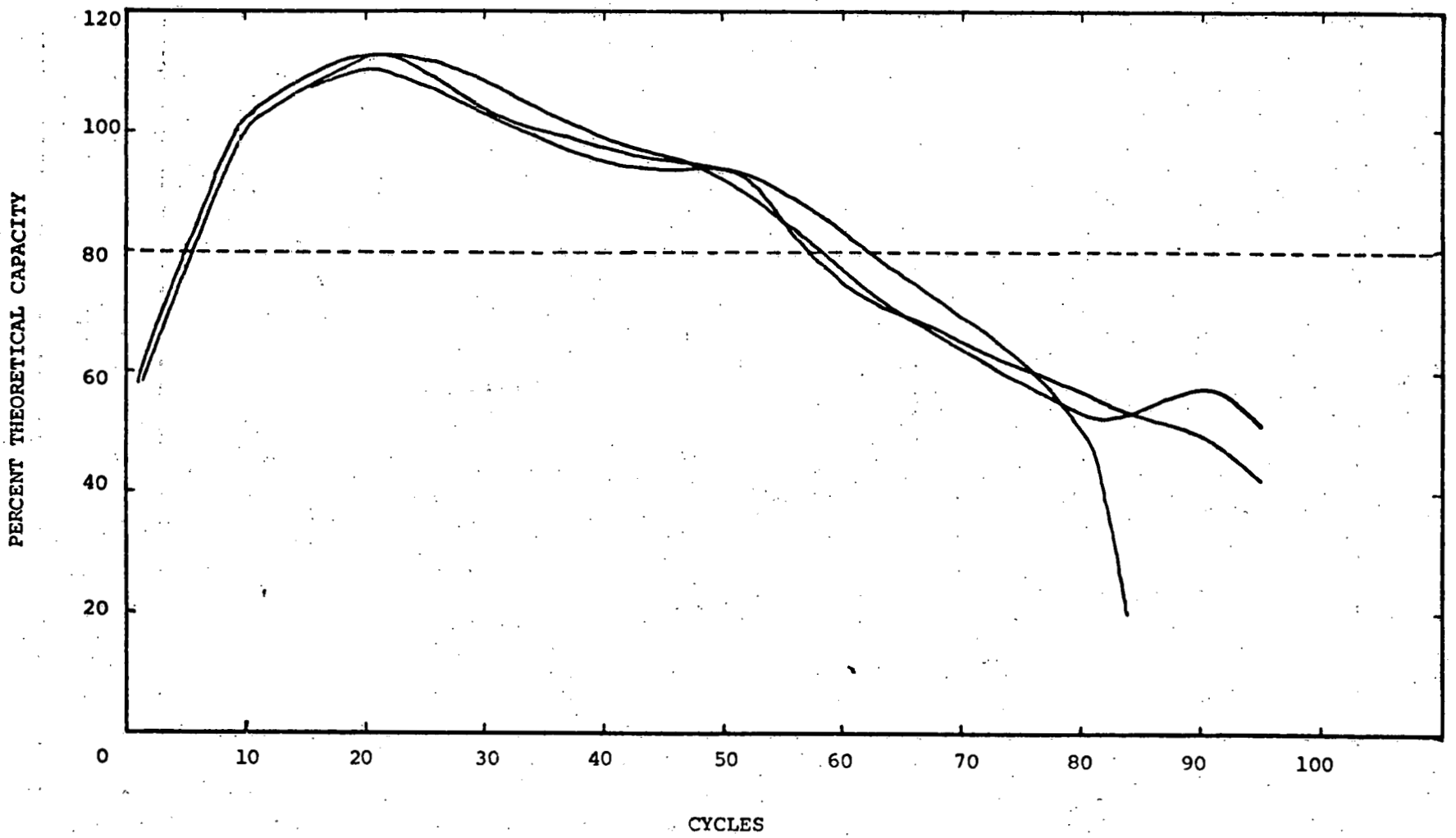

EXHIBIT B-XV: VARIATION OF TEMPERATURE IN A 400 AH CELL WITH CYCLING

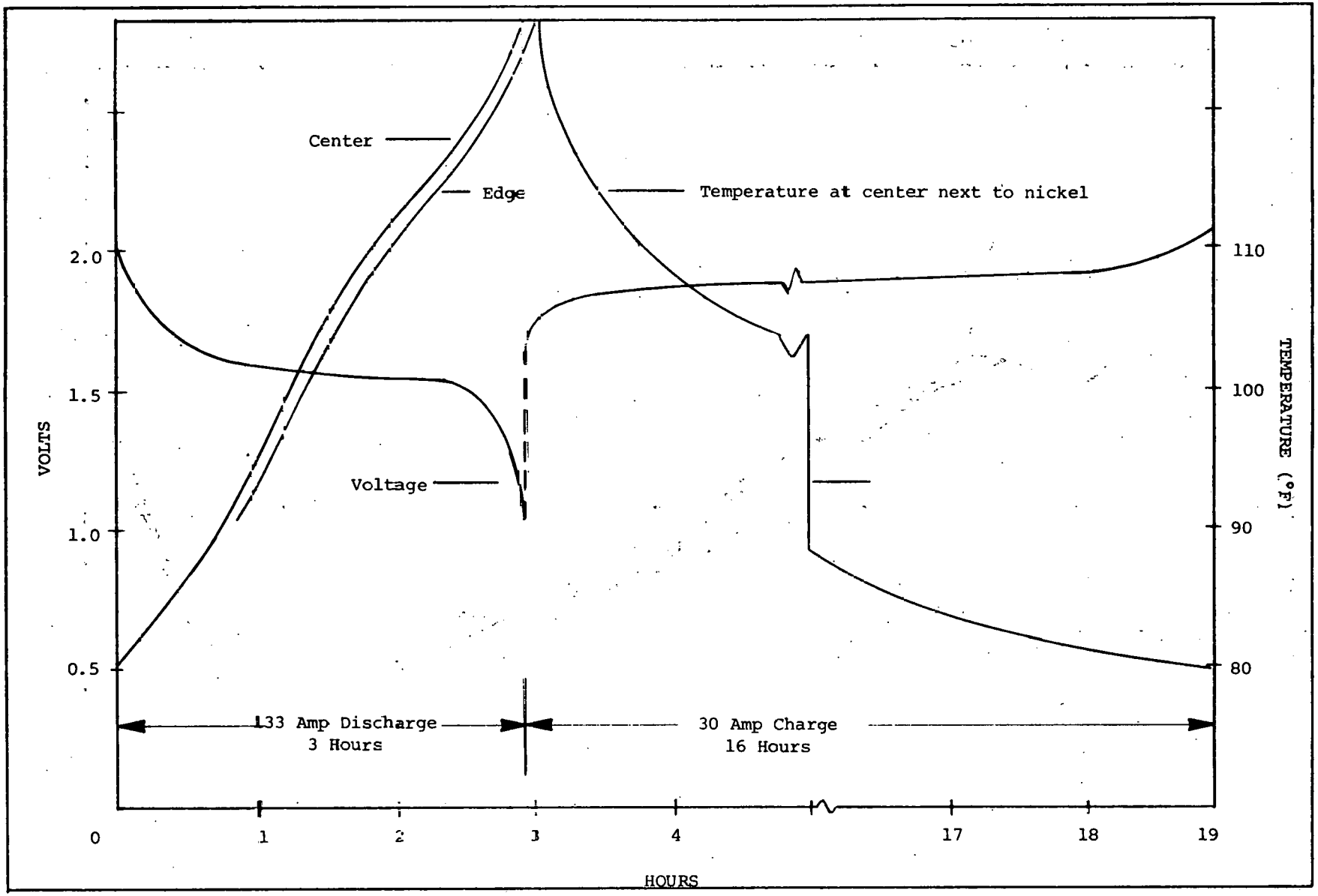

EOD Temperature at 200A 166° F and at 400A 179° F. EOC Temperature at 55A 86° F

EXHIBIT B-XVI: VARIATION OF TEMPERATURE AT CENTER AND THE EDGE IN NICKEL-ZINC CENTER CELL

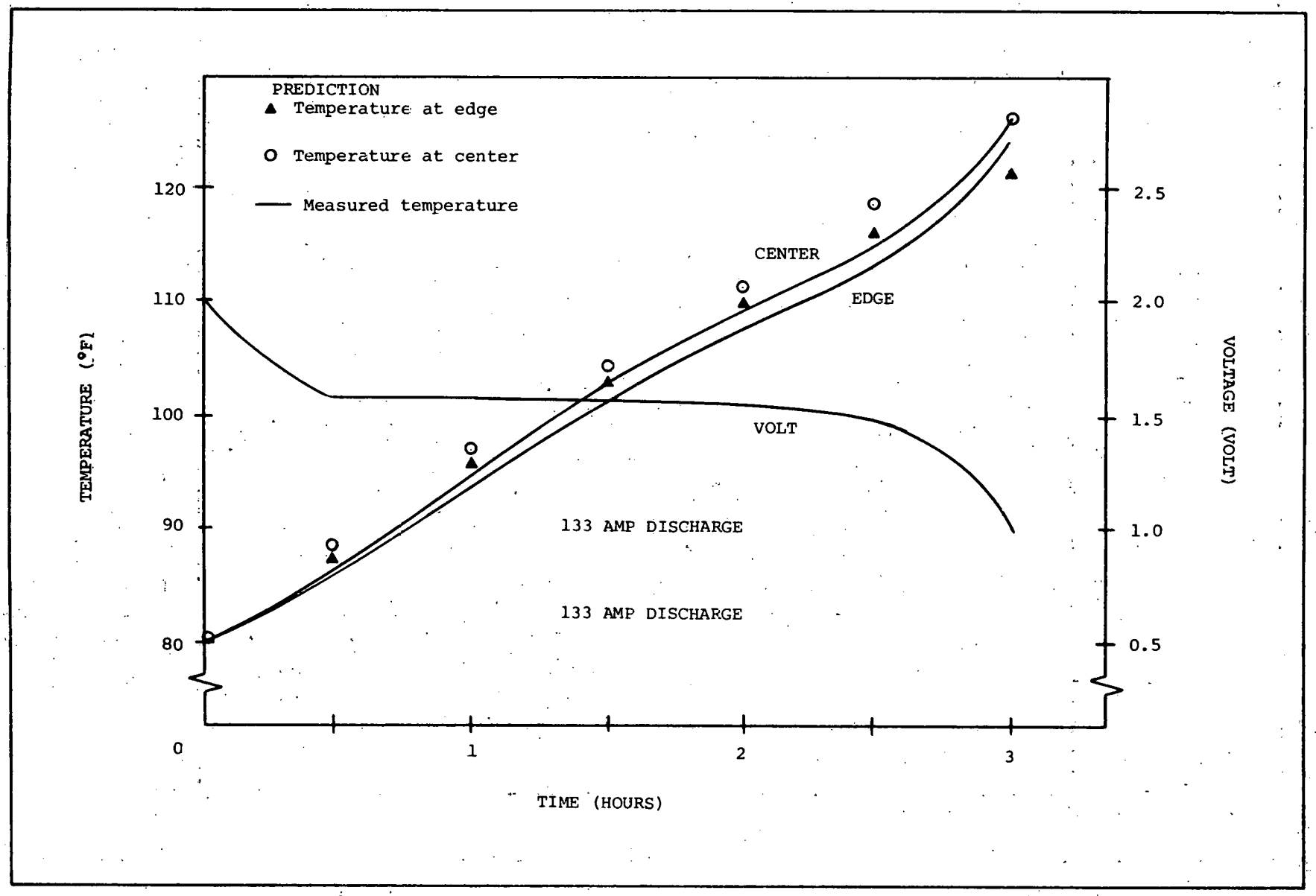

EXHIBIT B-XVII: TEMPERATURE VARIATIONS IN A 400 AH ELECTRIC CELL

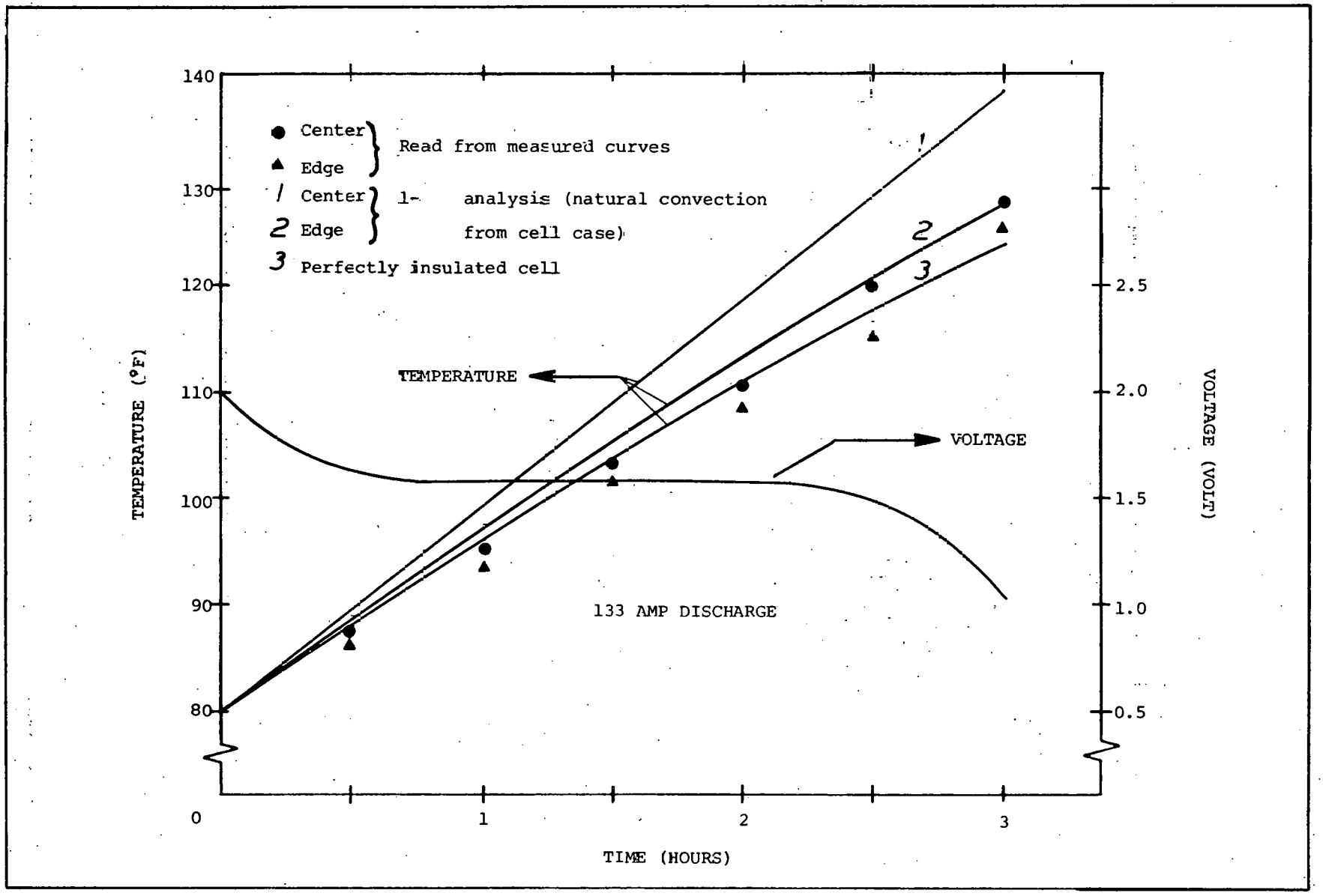

EXHIBIT B-XVIII: HEAT DISSIPATION RATE AS A FUNCTION OF TAB WIDTH

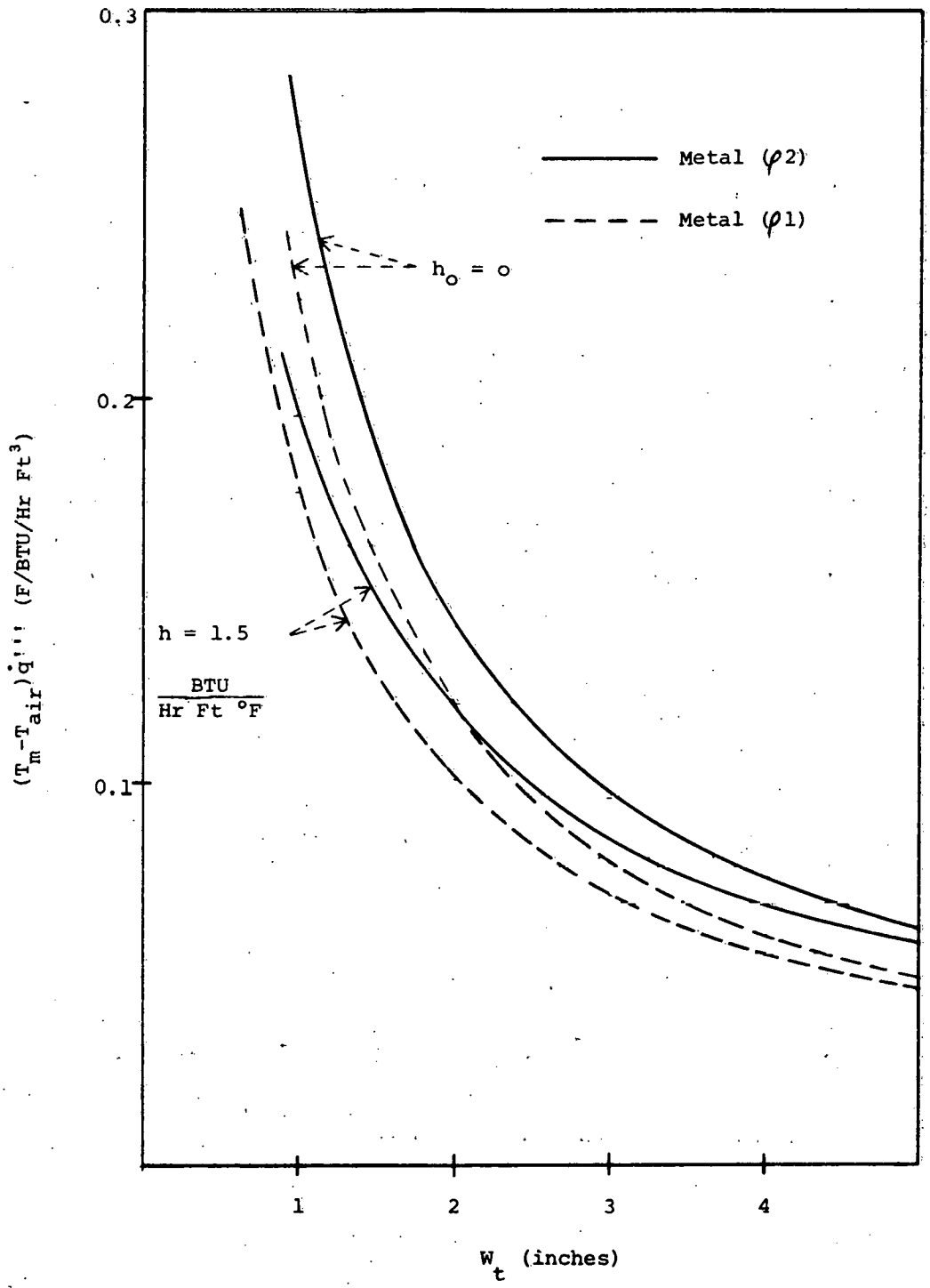

EXHIBIT B-XVIX: HEAT DISSIPATION RATE AS A FUNCTION OF TAB WIDTH

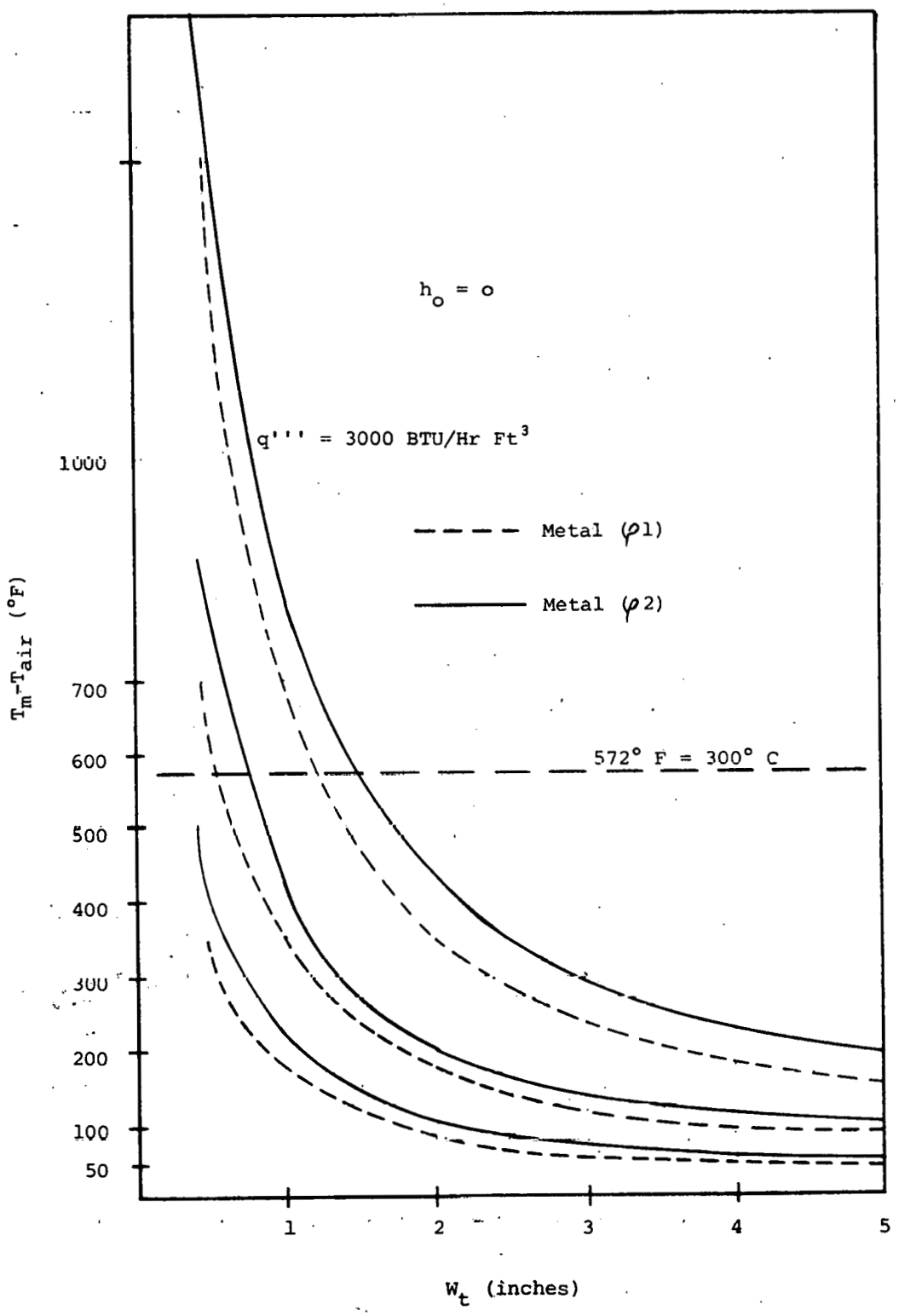

TASK C: PRODUCT DESIGN AND ANALYSIS

Objective

This Task consists of incorporating the major battery components into a battery optimally designed for a commuter vehicle application. This entails the specification of components such as separator and electrode materials along with the establishment of the design configuration such as the number of electrodes per cell, capacity and geometry of the electrodes, intercell connectors, terminals, vents, case, cover, etc. In addition, this Task includes the analysis of cell/module/battery failures in order to assist in the development of improved components and to generate new designs to overcome battery system failure.

Mission Analysis

The successful completion of this Task depends on, first, an analysis of what the battery must do in the commuter application; and secondly, the design of the battery to achieve the targets. To accomplish these objectives, a methodology was generated to aid in the engineering process and establish the design priorities for the Generation I battery (EXHIBIT C-I). In general, working from defined vehicle capabilities and constraints, the battery requirements for the mission were determined and prioritized. Various battery designs were then configured and performance projections were made so that the impacts on vehicle performance could be determined. As a result of the subsequent tradeoff analysis, a design for the Generation I battery was accomplished by the May 15 milestone target.

General impacts of the mission requirements on the battery design are summarized in EXHIBIT C-II and were used as general guidelines in determining minimum performance levels for propulsion batteries.

Meetings that were conducted with DOE/TEC, Jet Propulsion Laboratory, General Research Corporation, and major auto companies resulted in detailed information that was used throughout the analysis. In addition, discussions with Gould Electric Vehicle Power Systems Project were held to benefit from their field experience.

The results of a statistical analysis conducted by the General Research Corporation on a survey of driving habits in Los Angeles, Washington, and St. Louis were obtained to aid in the definition of vehicle capability. These results representing 1% of the population in the respective cities, are partly shown in EXHIBIT C-III. A major conclusion of the study was that a one hundred mile range on a realistic urban driving schedule would be sufficient to capture the 99th percentile of secondary drivers in Los Angeles and Washington while significantly less range was required for the 95th percentile driver. Of greater importance, however, is the fact that the average mission length is significantly less than that of the 99th percentile. The impact of the low average mission length and, therefore, the lack of deep discharge use of the propulsion battery has not been fully characterized in terms of cycle life to date. This relationship is currently being defined with Pilot Plant hardware so that the effects on battery life cycle costs can be determined. Preliminary results indicate that a favorable impact on life cycle costs will be realized.

Acceleration targets for both of these lightweight vehicles are such as to require 50 to 60 watts per pound peak power densities. Since it has been well documented that loss of acceleration is usually the range-limiting factor, the peak power density must be available at 80% DOD. These values have recently been verified by design exercises utilizing computer simulations to determine the peak power requirements for a wide variety of battery powered vehicles when exercised on realistic driving schedules. The schedule required by the Environmental Protection Agency to determine fuel economy and gaseous emissions for new motor vehicles is considered to be the most realistic driving schedule.

As the performance requirements of the battery were determined, data regarding available volumes for propulsion batteries in typical vehicles were examined. The data indicate that volumetric energy densities for the battery must be at least 2 WH/In^3 to achieve vehicle ranges consistent with those previously described as required by auto companies and the general driving population. The present downsizing of the U. S. automotive companies is expected to further restrict available battery volume and is indicative of the importance of this criterion.

This analysis of the mission requirements and imposed physical constraints resulted in a prioritization of the Generation I design targets; they are:

1) Life Cycle Costs
2) Volumetric Energy Density
3) Peak Power
4) Gravimetric Energy Density
5) Sustained Power

Additional GRC data indicated that to reach the 95th percentile of any driver category, accommodations for at least three passengers are necessary. A significant portion of all driver classes also required vehicles capable of freeway operation. These data are shown in EXHIBITS C-IV and C-V.

In support of these data, preliminary commuter car performance specifications were received from two major auto companies. These specifications were examined so that additional battery characteristics could be specified and compared to other published data. The data, shown in EXHIBIT C-VI, indicate that both companies are pursuing a two passenger "city car" with acceptable performance. Although the GRC analysis indicates that a reduction in driver percentile from 95 to 89 will result from this action, the automible manufacturers may feel that the degree of difficulty in commercializing a four passenger electric vehicle is of such a magnitude as to significantly lower the probability of success.

Range targets for one of the auto companies (approximately 75 miles urban; 100 miles cruising) are lower than the targets set by the other and, again, appear to be justified on the basis of GRC's data that the 95th percentile of secondary drivers would be satisfied with 50 mile range in urban driving. However, it is evident that a range safety factor is desired by the auto manufacturers to allow for such variables as climate, driving conditions, terrain, etc. which will effectively reduce vehicle range when conditions are less than optimum.

Life cycle costs, which consists of the manufacturing cost and cycle life targets, are the highest priority so that a cost-effective system can be

offered to the consumer as an incentive for electric vehicle use. Volumetric energy density is the next highest priority due to the difficulty of packaging a sufficient quantity of batteries necessary for the commuter car application. In this application, a 100 mile range is required for consumer acceptance. Peak power requirements are the next priority as it is well documented in the literature that vehicle acceleration is usually the range-limiting factor. Gravimetric energy density is next in priority as vehicle designs can accommodate a range in battery weights and, thus, does not appear to be a limiting factor in reaching a 100 mile range. The analysis further indicated that the target levels, although ambitious, are required based on consumer acceptance, vehicle performance, and operating costs.

Tradeoff Analysis

Computer studies were conducted on three distinct battery designs to determine the effects of battery voltage, capacity, and height on the cost and performance of equal energy configurations. These studies were conducted with an internally developed computer program.

As seen in EXHIBIT C-VII, the use of the current Preliminary Design size electrodes in a 500 AH monoblock configuration achieve a 10% higher gravimetric energy density than the 250 AH monoblock. Similarly, EXHIBIT C-VIII shown that the volumetric energy density of the 500 AH monoblock is 20% greater than the lower capacity 250 AH monoblock. These improvements, due to more efficient utilization of the container space and weight, represent a significant advantage for the high capacity, low voltage battery when compared to the low capacity, high voltage battery. The data are tabulated in EXHIBIT C-IX.

Comparing the 500 AH monoblock with a standard golf cart configuration of 250 AH shows that the 500 AH monoblock has greater volumetric and gravimetric energy densities and far outperforms the shorter golf cart configuration. This difference in performance is also caused by more efficient utilization of the cell container space and weight.

Utilizing these data with the projected performance levels of high and low voltage DC propulsion systems found in EXHIBIT C-X readily shows that the marked improvements in energy densities of the low voltage battery far outweigh the low efficiencies associated with low voltage propulsion systems; and when compared to the high voltage system, offer a superior package. Therefore, the Generation I Design will be derived from the present Preliminary Design dimensions and will be upgraded to provide the peak power requirement of 60 W/Lb. This design should meet all the design targets except for gravimetric energy density. A comparison of projected versus target performance is shown in EXHIBIT C-XI.

Further support for this design choice is found in preliminary data which indicated that lower manufacturing costs and improved cycle life (Priority 1) can be obtained through this design. To verify these data, lab experiments are underway by the Applied Research Group to characterize the electrode size effect on cycle life.

Cells with various internal configurations, all projected to yield the peak power target of 60 W/Lb at 80% DOD with current height electrodes, have been designed. They include the use of various grids and tabs, negative electrode

binders, and separator systems. Cell quantities and specifications have been provided to the Pilot Plant. Since these designs have required the use of thinner electrodes to meet the power demands, some effort has been required in process development. These efforts are detailed in the respective Tasks in this report.

Three prototype Generation I cells are undergoing formation cycling at this time.

The results of a preliminary sensitivity analysis with regard to volumetric and gravimetric energy densities are shown in EXHIBITS C-XII and C-XIII in decending order of impact. These will be examined for optimization in the Generation II Design.

Argonne Hardware Delivery - June 15, 1978

Cell specifications were provided to the Pilot Plant and considerable effort was expended to incorporate some design changes into the cells.

Intercell connections were made through a 0.25" connector as computer projections indicated this to be an optimum thickness. Several module trays have been built and were used for the delivery. A Sorenson charger was delivered with the module to Argonne. The lower amount of recharge may be a result of the use of the latest nickel electrodes. Data generated during the formation of these cells is shown in EXHIBIT C-XIV. Duplicate cells intended to undergo concurrent module testing are now on test at Gould.

EXHIBIT C-I: METHODOLOGY FOR GENERATION I BATTERY DESIGN

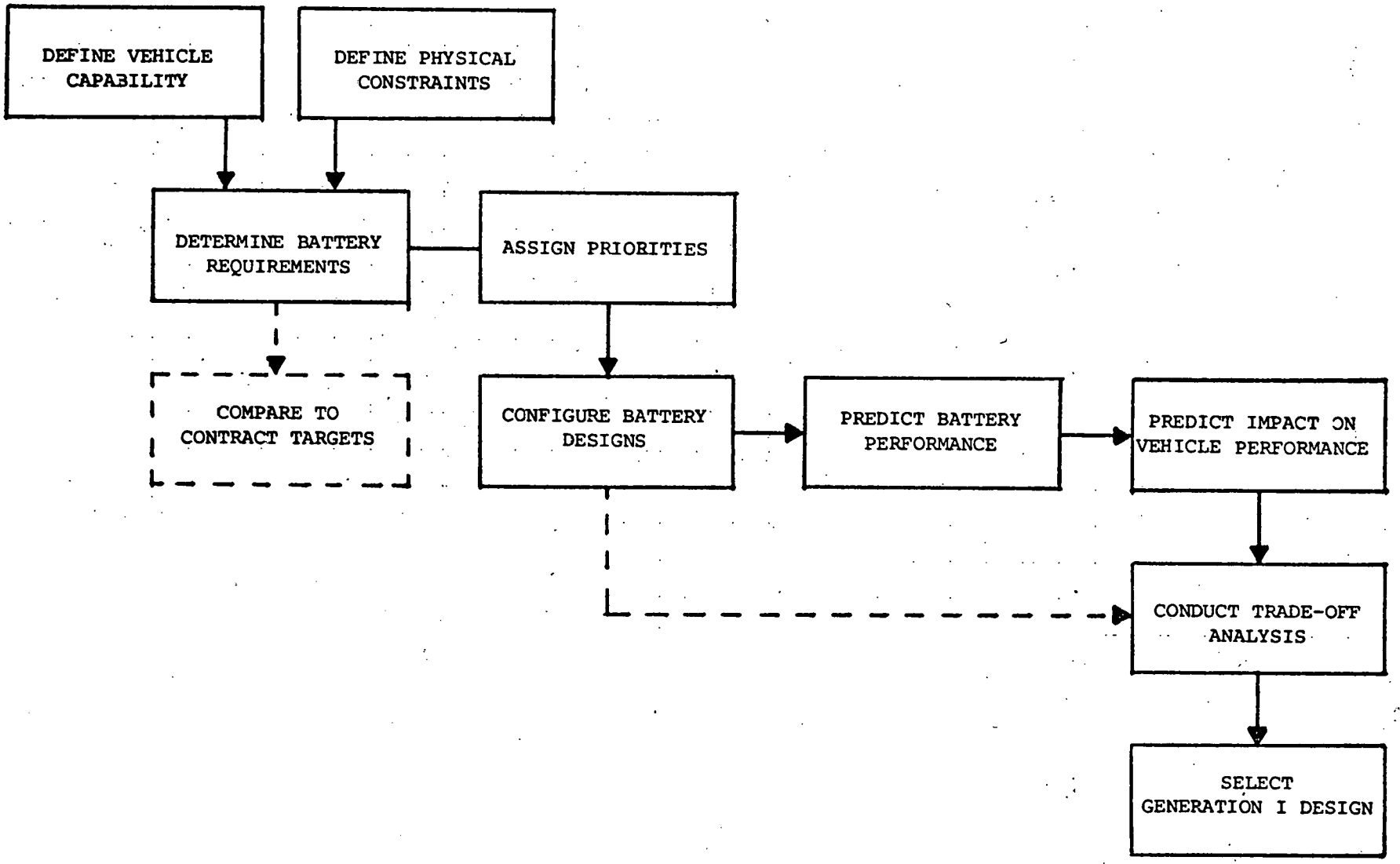

EXHIBIT C-II: IMPACTS OF MISSION REQUIREMENTS ON BATTERY DESIGN

- PASSENGER AND PAYLOAD ACCOMMODATIONS

  Defines nominal weight and size of vehicle and indicates available battery volume

- VEHICLE USE PATTERNS

  Determine energy storage for a given percentile of driver class

- ACCELERATION CHARACTERISTICS OF LOW PERFORMANCE ICE SUBCOMPACTS AND TEST SCHEDULE REQUIREMENTS

  Determines power requirements for minimum performance

EXHIBIT C-III: MAJOR CONCLUSIONS OF GENERAL RESEARCH CORPORATION ANALYSIS

- 2 + 2 OR 4 PASSENGER VEHICLE
- FREEWAY CAPABILITY
- TO CAPTURE THE 95TH PERCENTILE, THESE RANGES ARE REQUIRED:

DRIVER GROUP	LOS ANGELES	WASHINGTON
Primary	135	68
Only	93	53
Secondary	48	34

- WITH A 100 MILE RANGE ON A REALISTIC DRIVING CYCLE, THE FOLLOWING PERCENTILES CAN BE CAPTURED:

DRIVER GROUP	LOS ANGELES	WASHINGTON
Primary	85TH	98TH
Only	94TH	99TH
Secondary	99TH	99TH

- AVERAGE DRIVER TRAVEL, HOWEVER, IS SIGNIFICANTLY LESS THAN 95TH PERCENTILE:

	MEDIAN	AVERAGE	95TH PERCENTILE
LOS ANGELES			
Primary	36	48	135
Only	19	29	93
Secondary	12	17	48
WASHINGTON			
Primary	25	30	68
Only	15	20	53
Secondary	10	13	34

EXHIBIT C-IV: DISTRIBUTION OF DRIVERS FOR VARIOUS PASSENGER ACCOMMODATIONS

	% CARRYING AT MOST X PASSENGERS		
	X=1	X=2	X=3
ALL DRIVERS	82	91	96
DRIVERS WITH CARS	85	92	97
PRIMARY DRIVERS	79	89	95
SECONDARY DRIVERS	84	92	97
ONLY DRIVERS	88	94	98

EXHIBIT C-V: PERCENTAGE OF DRIVERS REQUIRING FREEWAY OPERATION IN LOS ANGELES

ALL DRIVERS	33%
DRIVERS WITH CARS	35%
PRIMARY DRIVERS	52%
SECONDARY DRIVERS	20%
ONLY DRIVERS	33%

EXHIBIT C-VI: MAJOR OEM VEHICLE PERFORMANCE TARGETS

WEIGHT		
Curb	1800#	1650#
Gross	2200#	2000#
Passengers	2	2
RANGE		
EPA Urban	70 Miles	120 Miles
50 MPH Cruise	70 Miles	-
Top Speed	56 MPH	60 MPH
ACCELERATION		
0 - 30 MPH	10 Seconds	
0 - 45 MPH	20 Seconds	
0 - 50 MPH		14 Seconds
0 - 60 MPH		<20 Seconds
BATTERY		
Weight	550#	700#
WH/lb	32	40
W/lb	50	60
Life	3 Yr/22,000 Mile (300 Cycles - 100% DOD)	5 Yr/50,000 Mile (415 Cycles - 100% DOD)

EXHIBIT C-VII: GRAVIMETRIC ENERGY DENSITY VERSUS CAPACITY FOR HIGH AND LOW PROFILE: HIGH AND LOW VOLTAGE

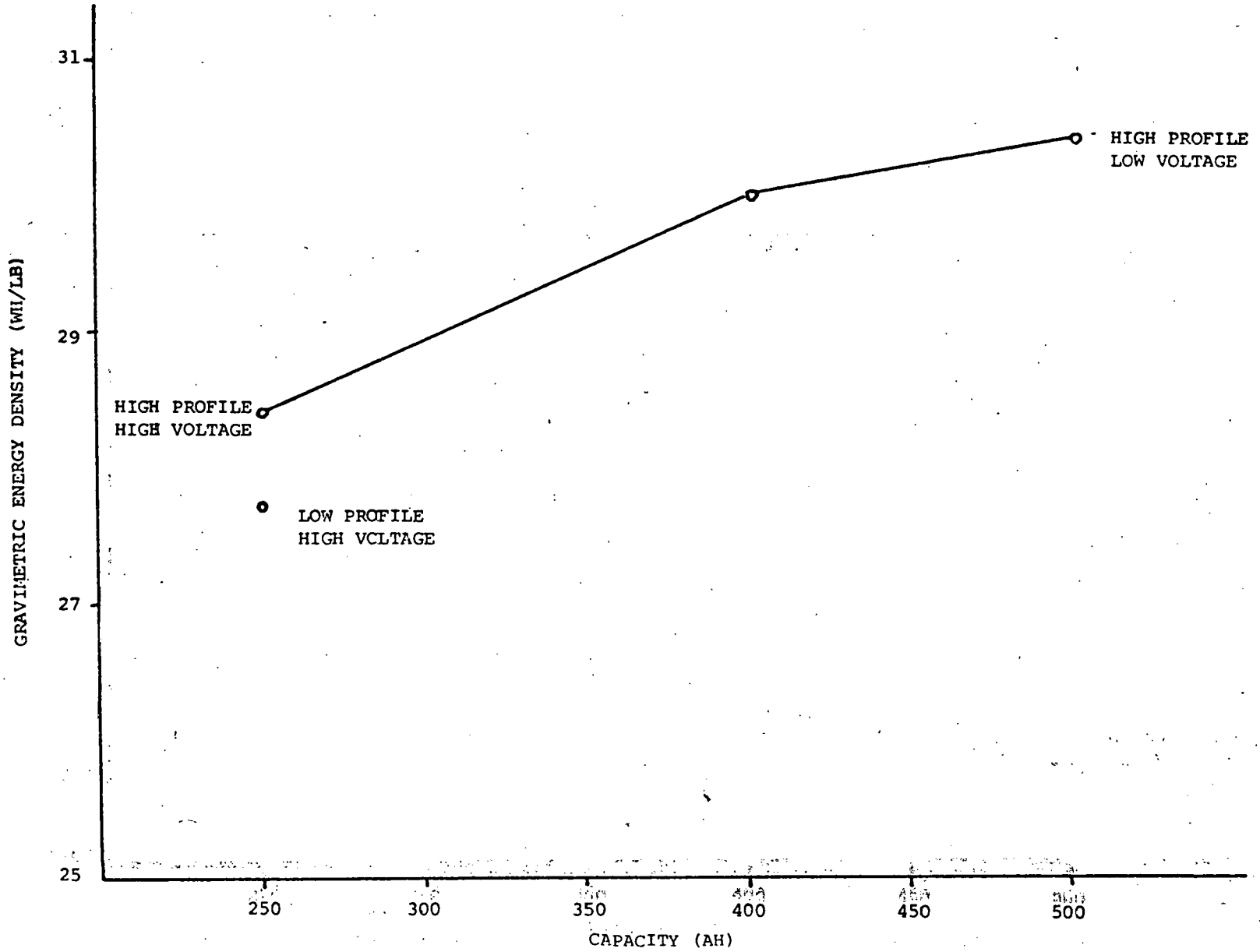

EXHIBIT C-VIII: VOLUMETRIC ENERGY DENSITY VERSUS CAPACITY FOR HIGH AND LOW PROFILE: HIGH AND LOW VOLTAGE

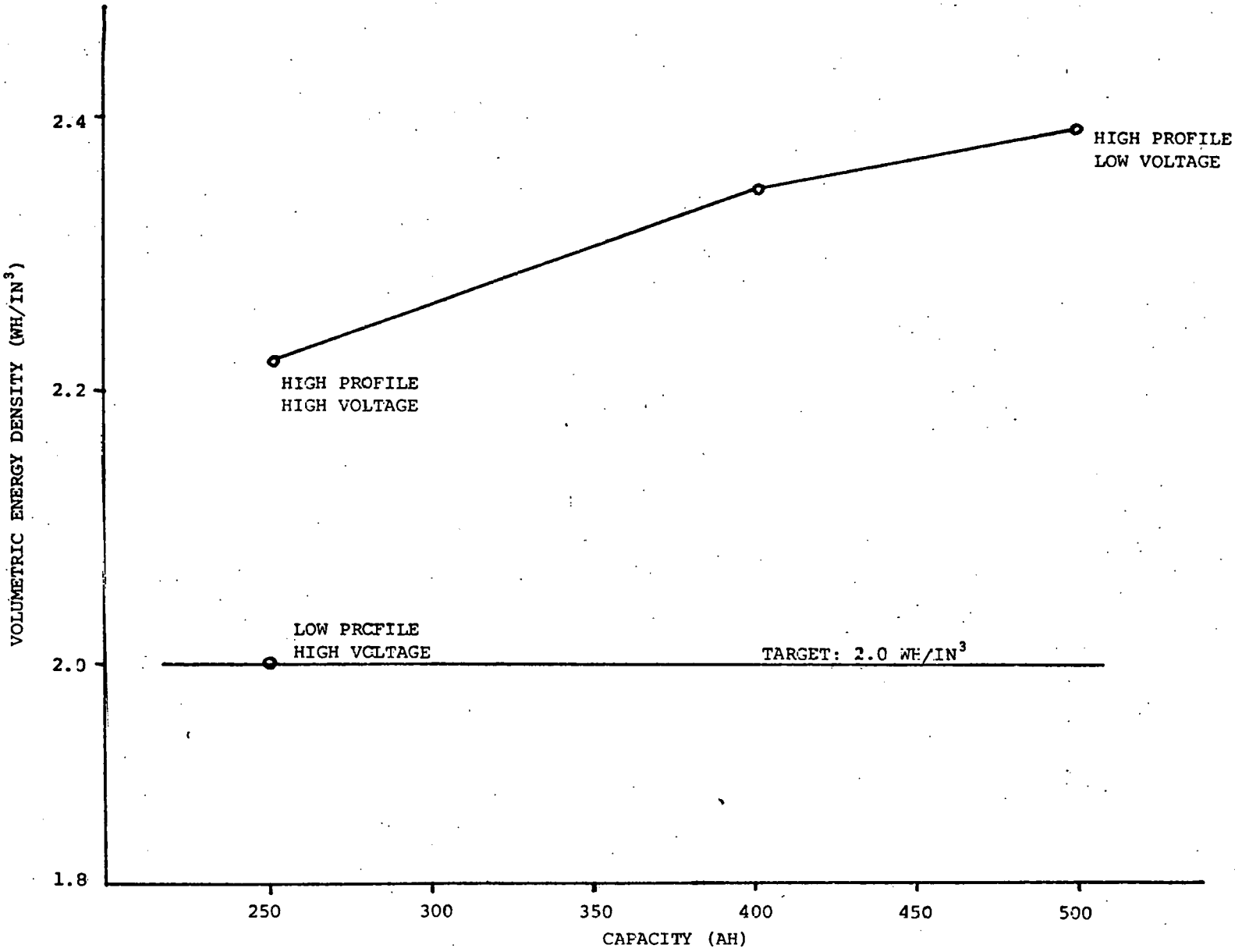

EXHIBIT C-IX: NICKEL-ZINC BATTERY DESIGN TRADE-OFF SUMMARY. DATA FOR GENERATION I DESIGNS ARE CHANGES RELATIVE TO THE GOLF CART DESIGN.

	LOW PROFILE	HIGH PROFILE (GENERATION I)	
	250 AH	250 AH	500 AH
BATTERY			
Cost/Kwh*	BASE	-34%	-42%
Cycle Life	BASE	>	>
Volumetric Energy Density	BASE	11%	20%
Gravimetric Energy Density	BASE	3%	10%
PORPULSION SYSTEM			
Cost	BASE	BASE	+ 3%
Efficiency	BASE	BASE	- 5%

*For labor intensive, pilot plant production

EXHIBIT C-X: PROJECTED PROPULSION SYSTEM CHARACTERISTICS LESS BATTERY

	LOW VOLTAGE	HIGH VOLTAGE
COST	+3%	Base
EFFICIENCY	-5%	Base
RELIABILITY	Equivalent (~50,000 Miles)	
PROBABILITY OF TECHNICAL SUCCESS	90%	

EXHIBIT C-XI: PROJECTED PERFORMANCE FOR GENERATION I DESIGN

		TARGET
LIFE CYCLE COSTS:	BEST EFFORT; NO COMPROMISE	400 CYCLES AT $75/Kw-Hr
VOLUMETRIC ENERGY DENISTY:	148 Wh/L	>120 Wh/L
PEAK POWER:	132 W/Kg	>125 W/Kg
GRAVIMETRIC ENERGY DENSITY:	60 Wh/Kg	>70 Wh/Kg
SUSTAINED POWER:	74 W/Kg	>45 W/Kg

EXHIBIT C-XII: MOST INFLUENTIAL DEISGN FACTORS REGARDING VOLUMETRIC ENERGY DENSITY

- CAPACITY
- MONOBLOCK CONSTRUCTION
- GRID MATERIAL SUBSTITUTION
- ZINC/NICKEL RATIO
- FREE SPACE (WIDTH)
- HEAD SPACE
- CELL HEIGHT

EXHIBIT C-XIII: MOST INFLUENTIAL DESIGN FACTORS REGARDING GRAVIMETRIC ENERGY DENSITY

- ZINC/NICKEL RATIO
- GRID MATERIAL SUBSTITUTION
- CAPACITY
- PLAQUE LOADING

EXHIBIT C-XIV: ARGONNE DELIVERY MODULE

GOULD

CELL NO: _____ RATED CAPACITY: _____

DESCRIPTION: _____

_____

THEORETICAL CAPACITY: _____ CELL WEIGHT: _____ CELL VOLUME: _____

INITIAL EFFICIENCIES:

AMP-HOUR: _____[1] _____[2]

WATT-HOUR: _____ _____

CYCLE	DAYS	RATES CHG	RATES D'CHG	END OF CHARGE VOLTS	END OF CHARGE IR (MΩ)	END OF CHARGE TEMP (°F)	END OF CHARGE INPUT AH	END OF CHARGE INPUT WH	END OF DISCHARGE VOLTS	END OF DISCHARGE IR (MΩ)	END OF DISCHARGE TEMP (°F)	END OF DISCHARGE OUTPUT AH	END OF DISCHARGE OUTPUT WH	EFFICIENCIES % AH	EFFICIENCIES % WH	% DECLINE IN CAP	% DECLINE IN ENER	AH EFF	WH EFF	REMARKS
1	1	8	80				320					140.0								
2	2	16	80				320					280.0								
3	3	20	80				360					-								
4	4	25	100				400					-								
5	5	25	100				520					362.0								
6	6	100	120				410					354.0								
7	8	90	125				440					394.0								
8	9	95	133				480					411.7								
9	10	100	133				460					412.2	89.6							
10	11	100					460													DELIVERED

[1]Efficiencies based on five consecutive cycles _____ thru _____. [2]Efficiencies based on cycle _____.

TASK D: CELL/MODULE/BATTERY TESTING

Objective

The objectives of this Task are to characterize and simulate the electric vehicle application to define appropriate laboratory testing regimes and to characterize the performance of hardware produced in the Pilot Plant under realistic manufacturing conditions.

Tri-Electrode Cells

Life cycle testing of the three NZNN Series cells resulted in cell NZNN-8 delivering 80% of weight gain capacity at 300 cycles of 100% DOD. This cell, inadvertently discharged to 30 mv on cycle 274, began losing approximately 0.4% of theoretical capacity per cycle at that time. In an effort to rejuvenate the cell, a maintenance cycle consisting of discharging the cell to near zero volts was attempted. No effect was noted on cell performance and the cell was removed from the cycler on cycle 314 even though it was delivering 65% of weight gain capacity. An extensive failure analysis is being planned to characterize the conditions of the electrodes and determine the cause of the abrupt decline in capacity.

Cell NZNN-4 had increased in delivered capacity from 50% at cycle 276 to 56.2% at cycle 300. This corresponds to 68.5% of its maximum observed capacity of 29.8 AH. The remaining cell, NZNN-1, had also increased slightly in delivered capacity and was delivering 25.1% of weight gain capacity before both cells were removed from the cycler at cycle 314 for comparative analysis with NZNN-4. A graph of the data for the three cells is shown in EXHIBIT D-I and tabularized in EXHIBIT D-II. It is clear that the cell with separator system #800 delivered exceptional performance. When compared to the remaining cells, NZNN-4, with separator system #805, had also reached 314 cycles with no appreciable degradation in delivered capacity since 80 cycles. Although the cell was delivering only slightly more than half of its rated weight gain capacity (36.3 AH), it has exhibited a greater portion of its observed peak capacity (29.8 AH). Apparently, the delivered capacity did not reach rated capacity because of the higher internal resistance of separator #805. The other cell, with separator #811, exhibited much more typical behavior with a gradual decay in capacity with cycle life, dropping from 80% rated capacity to less than 25% in 180 cycles.

An extensive analysis was performed to explain the very promising capacity retention performance of cell NZNN-8 in order to offer insight to improving the performance of full-size cells and batteries. The major differences appear to be related to temperature, ZnO to grid ratio, and cycle regime. Other differences are found in free space, electrolyte volume, and Zn/Ni ratio.

Several attempts to start new test series aimed at evaluating the major differences were unsuccessful due to problems resulting from poor nickel electrode performance. These major differences are now being evaluated under Tasks A and B of this contract.

A variety of tri-electrode tests have been conducted in support of the process development effort described in Task E to resolve the Pilot Plant problem with the nickel electrode. Tests are being conducted against both zinc and cadmium negative electrodes. The three-cycle test against cadmium previously found to

reproduce the Pilot Plant problem of excessive growth and cracking of the positive is used routinely. Electrodes have been tested to evaluate sintering conditions, impregnation, and new component designs. Most of the data, although listed in this Task, are discussed in Task E.

Full-Size Cells

A number of full-size cell tests were performed during the previous contract period to evaluate the cycle life of various components.

Ten 400 AH, 21 plate cells were placed on test. The parameters which were varied are listed below.

CELL ID	DESCRIPTION
43, 44	Separator System, #800 Zinc Electrode, #590 Terminal Design, #349
48, 49, 50	Separator System, #805 Zinc Electrode, #592 Terminal Design, #354
51, 52, 53	Separator System, #810 Zinc Electrode, #591 Terminal Design, #354
54, 55	Separator System, #805 Zinc Electrode, #591 Terminal Design, #354

After formation, the cells were placed on automatic cycling according to the DOE/ANL cycle life regime. All cells failed by massive shorting between cycles 23 and 50. Cells 54 and 55 achieved the highest capacities (420 AH or 105%) and the highest efficiencies with 89% AH efficiency and 73% WH efficiency. In every case, the short was at the cell edge and at a crack in the positive. Gross positive electrode growth and cracking was commonplace. This condition is not usually typical of the electrodes tested in Tasks A and B and, therefore, indicates either a design defficiency or a process problem encountered from scaling-up from laboratory to Pilot Plant production. Obviously, this positive problem prevented the determination of the cycle lives of the respective separator configuration and zinc electrode material.

Twelve 300 AH cells were also received from the Pilot Plant. Although they were not Preliminary Design cells, they were intended to provide information regarding cycle life at 50 and 80% DOD. It is quite clear that these cells have low gravimetric and volumetric energy densities due to the number of positives and, possibly, to the low number of impregnation runs. Due to their lower pressed densities, negatives with binder #801 did permit thicker positive electrodes or adequate free space at equivalent Zn/Ni ratios, both of which appear to be necessary from component test data.

Testing of these four-cell modules consisted of life cycle testing at 50 and 80% DOD. These modules should also verify the positioning of separator system #811

with regard to the negative electrode as two cells in each module have the positioning reversed from the remaining cells. Peak power tests were performed on the third module and sustained power testing was also conducted. Two cells from the 80% DOD module shorted at 25 and 60 cycles. The earliest failure may have been caused by inadvertent 180% recharge, however, the second failed cell shorted due to an edge crack in the positive. Autopsy of these cells indicate nonuniform use of the electrode. Causes of this mechanism are being evaluated. No relationship has been determined regarding the positioning of separator system #810 as one of each configuration has failed. The remaining cells are at 90% capacity at 63 cycles (100% DOD testing is conducted every 25 cycles to determine capacity). These data are shown in tabular form in EXHIBIT D-III and graphical form in EXHIBIT D-IV. It is clear that the capacity decline of the module being exercised to the lower, 80% DOD is at a higher average rate than the 50% DOD. Confirmation tests using the latest cell designs are planned.

Four 400 AH cells with vacuum sintered plaques/electrodes are also currently on the life cycle testing regime. Two of these cells using separator system #810 have peaked at 130% of weight gain capacity delivering 445 AH. The remaining cells, assembled with separator system #800, have delivered 113% of weight gain capacity during cycle 17 and are still increasing in capacity. The weight gain capacity is 340 AH.

Several design parameters were quantified and applied to the Generation I Design. They are the peak and sustained power densities. The peak power, illustrated in EXHIBIT D-V and D-VI, was shown to be near the estimated 0.7 W/In^2 of positive electrode surface for the NZ50, EV 400 AH, and EV 300 AH (nine positives/cell). It has also been confirmed that the peak power is positive-limited by monitoring reference voltages on the discharges. This value was incorporated into the computer algorithm described under Task C.

For comparative purposes, peak power tests were also conducted on Gould's PB220 golf cart battery and semi-industrial 66E-11 electric vehicle battery. Peak power levels and voltages for the golf cart battery are included as EXHIBITS D-VII and D-VIII. This data, along with the data generated from the testing of Gould's 330 AH semi-industrial electric vehicle battery, are shown as EXHIBITS D-IX and D-X. The semi-industrial lead-acid battery, similar to those in the U. S. Post Office Operating Fleet, has the lowest power rating of those tested. The overwhelming superiority of nickel-zinc over the semi-industrial and golf cart batteries can readily be seen, especially at the deeper depth of discharge.

The sustained power capability was also quantified on the Preliminary Design 400 AH nickel-zinc cells. This test is to remove as much power as possible in 20 minutes from a cell which has been reduced to 50% capacity at the C/3 rate. The power is, of course, very rate sensitive but it is also dependent on the cutoff voltage. It appears that for a 1.0 volt cutoff, the sustained power would be 45 to 50 W/Kg; however, verification is required. The dashed line in EXHIBIT D-XI shows the probable voltage curve. Comparative testing was also conducted with Gould's PB220 lead-acid golf cart battery. All golf cart batteries achieved approximately 140 AH (C/5) with cycling. EXHIBIT D-XII shows the sustained power of the golf cart battery compared to the EV 400 AH cell. The method used in EXHIBIT D-XII for comparison is believed to be more realistic because of the differences in voltage. The PB220s cannot run the necessary 20 minutes at currents over 150 Amps; and, in fact, the watt-hours decrease as the current is increased. At the peak sustained power level, the lead-acid golf cart battery only delivers 70% of the available capacity where the EV 400 AH

cell delivers nearly 100% of capacity at a low voltage cutoff. The superiority of nickel-zinc with respect to sustained power when compared to lead-acid golf cart batteries is obvious.

Further improvements in both peak and sustained power capabilities is expected due to a new tab design. Compared to the standard tab, the new tab reduces the resistance from 1.3 milliohms to 0.8 milliohms. This would increase nickel-zinc cell voltage by 0.11 volts at 100 Amps using the design and provide for an approximate 13% increase in peak power.

An upgraded version of the terminal was checked by measuring the voltage drop at 1,000 Amps. The voltage drop was 0.04 to 0.05 volts, which is similar to the 0.04 to 0.06 volts for the older terminal presently in use. The measurement was made from one corner to the top of the terminal and may not show the advantage of the new terminal as it will help to distribute the current more uniformly across the connector. Further improvements might be realized through additional design work in the area of materials, therefore, this effort will be continued.

Vibration Testing

The purchase and installation of a vibration test machine, splash shield, catch tray, hold down clamps, and instrumentation was completed on schedule during the reporting period.

The accelerometers were mounted and several trials made to establish the frequency and acceleration of the machine. The SAE J537h procedure calls for an acceleration of 5G and a frequency of 1,800 to 2,100 CPM. Trial runs were made with cells and a six-cell low profile battery.

After vibrating for two hours, no appreciable change in the battery performance was measured. In contrast, as SLI lead-acid battery cannot complete more than one cycle without shedding of the active material which will eventually cause shorting. Additional testing is scheduled to determine long-term effect on nickel-zinc cell performance.

Battery Tests

A 54 volt, 33 cell Preliminary Design battery was assembled and tested in the AMG-DJ5E postal vehicle. This was Gould's initial opportunity to produce components in volume in the Pilot Plant and to evaluate a full-scale battery in a vehicle. The battery required the fabrication of 363 negative electrodes and 330 positive electrodes and utilized over 1,320 ft^2 of separator. All 33 cells were found acceptable after formation cycling.

The 788 pound, 20 KwH (at C/3) battery, which is illustrated in EXHIBIT D-XIII and D-XIV, was assembled in the vehicle for a direct comparison on a chassis dynamometer to Gould's lead-acid battery 66E-11 (1,350 pounds, 15.5 KwH at C/3) currently used in the U. S. Post Office application. Vehicle characteristics are provided in EXHIBITS D-XV and D-XVI to aid in understanding the battery requirements during steady state cruises and the SAE J227a/B delivery schedule. Lead-acid baseline tests are shown in EXHIBIT D-XVII for comparison purposes. Results from the nickel-zinc tests, performed in accordance with

test requirements are summarized in EXHIBITS D-XVIII and D-XIX. The first two tests were performed at the same equivalent inertia weight settings as the lead-acid battery and are to be considered as trial runs only. The remaining tests were performed at an inertia setting that reflects the 562 pound lower battery weight. In general, the results reflect the superior high rate discharge efficiency of nickel-zinc compared to lead-acid. For the SAE J227a/B schedule, the nickel-zinc battery resulted in an 18% increase in range (38.2 miles versus 32.3 miles). Proportionally greater results are seen as the discharge current increases, e.g., 42% increase in range at the 30 mile per hour test. It must be noted that the vehicle's motor and controller prevent testing under a more realistic driving and acceleration schedule such as the EPA's urban CVS test cycle. In addition, a motor and controller designed for nickel-zinc use would have resulted in a much higher performance gain. Under these more difficult and realistic conditions, nickel-zinc's advantage over lead-acid will become much more pronounced.

Gravimetric and volumetric energy densities for the various steady state discharge rates of the tests are shown in EXHIBIT D-XX. These values are below those expected based on laboratory cell evaluations but still indicate a factor of two improvement over lead-acid in delivered WH/Lb. Design optimization of the tray will raise the volumetric energy density. As can be seen in the battery pictures, very extensive space was designed into the tray for maximum air cooling potential. The upper curve represents the maximum limit with these types of cells as it reflects only batteries with no tray. An additional explanation for the lower than expected values may be that the discharge efficiency is lower in constant power discharge (typical of vehicle use) than in the constant current discharge performed in the laboratory.

Cell temperatures were moderate after an air duct was fabricated to route cooling air to the air inlet of the tray. Typical electrolyte temperatures were less than 125° F, however, some positive terminals reached 135° F near the end of the 30 miles per hour steady cruise discharge rate. After only about 20 charge/discharge cycles, several cells during charge exhibited high temperatures. Open circuit and end-of-charge voltages also indicated that internal cell shorting had occurred.

Seventeen of the 33 cells were autopsied. Failure was due to excessive growth and cracking of the positive in a very similar manner to the 400 AH laboratory cells previously discussed. Data reduction and analysis of the nickel electrodes showed a close correlation between the volume change of the nickel electrode and the initial capacity (by weight gain) of the electrode.

Tape Dynamometer Testing

A tape-controlled dynamometer facility is functioning under manual control which will be utilized to determine the battery capabilities. Through the use of actual propulsion system components, battery testing will be conducted using the demand characterizations of the electric vehicle application as developed in Task C. Initial calibration tests are being conducted on the lead-acid 66E-11 traction battery.

Test Facility

A minicomputer based test facility was designed and built in-house. The computer system is a real-time sharing system utilizing the RSX-11M operating system. Presently, thirteen cyclers are interfaced to the PDP11 computer via CAMAC based interface designed and built by the Project. The computer system and some of the cyclers are shown in EXHIBITS D-XXI thru D-XXVIII. The facility also includes three mobile and one stationary environmental test chambers with temperature capabilities of -40° F to +180° F.

EXHIBIT D-I: NICKEL-ZINC TRI-ELECTRODES (36 AH RATED)

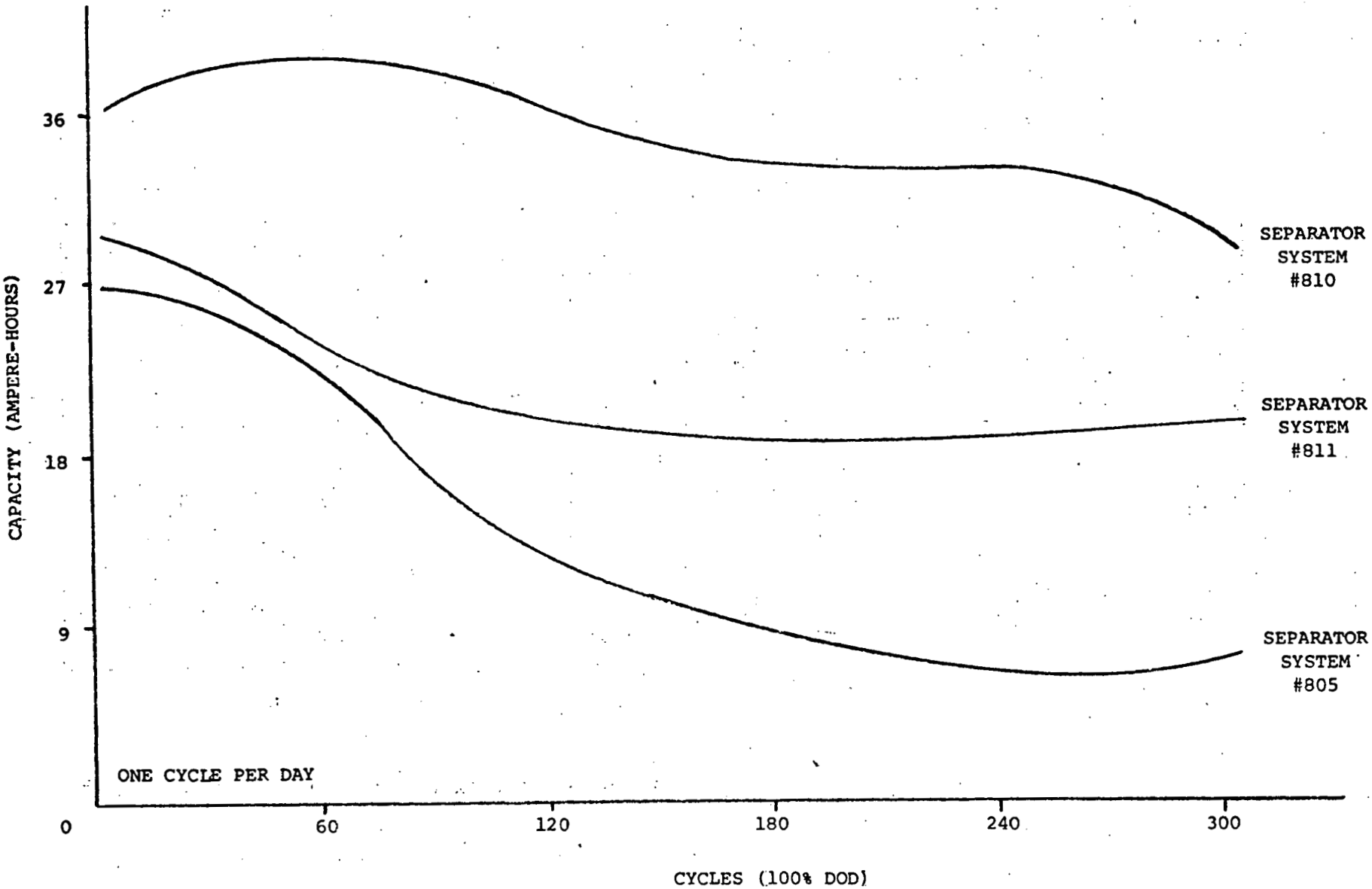

EXHIBIT D-II: NICKEL-ZINC TRI-ELECTRODES (36 AH RATED)

CELL/MODULE DESCRIPTION	RATED CAPACITY		RATES		INITIAL EFFICIENCY %		LIFE CHARACTERISTICS % DECLINE IN						REMARKS
	A-HR	W-HR	DISCHARGE	CHARGE	A-HR	W-HR	DAYS	CYCLES	CAPACITY	ENERGY	A-HR EFF.	W-HR EFF.	
NZNN-1	35.1		12 Amps,C/3	119%,C/15	63.6	47.9	391	319	71.3	71.0	71.2	70.1	
NZNN-4	36.3		"	"	61.4	42.7	"	"	24.8	28.4	32.7	28.5	
NZNN-8	36.0		"	"	86.6	72.8	"	"	30.0	29.9	30.1	29.9	

EXHIBIT D-III: 300 AH ELECTRIC VEHICLE MODULES

CELL/MODULE DESCRIPTION	RATED CAPACITY		RATES		INITIAL EFFICIENCY %		LIFE CHARACTERISTICS % DECLINE IN						REMARKS
	A-HR	W-HR	DISCHARGE	CHARGE	A-HR	W-HR	DAYS	CYCLES	CAPACITY	ENERGY	A-HR EFF.	W-HR EFF.	
EV Module 1	300	1920	100 Amps, C/3	20 Amps, 120%	84.7	68.2	60	61	22.6	26.4	22.6	24.0	One cell shorted cycle 25, 2nd cell shorted cycle 60
EV Module 2	300	1920	100 Amps, C/3	20 Amps, 120%	83.9	67.4	60	63	9.8	14.1	9.8	11.3	One cell shorted cycle 50
EV Module 3	300	1920	100 Amps, C/3	20 Amps, 120%	84.2	67.7	60	8	-	-	-	-	Power testing

EXHIBIT D-IV: 300 AH ELECTRIC VEHICLE MODULES

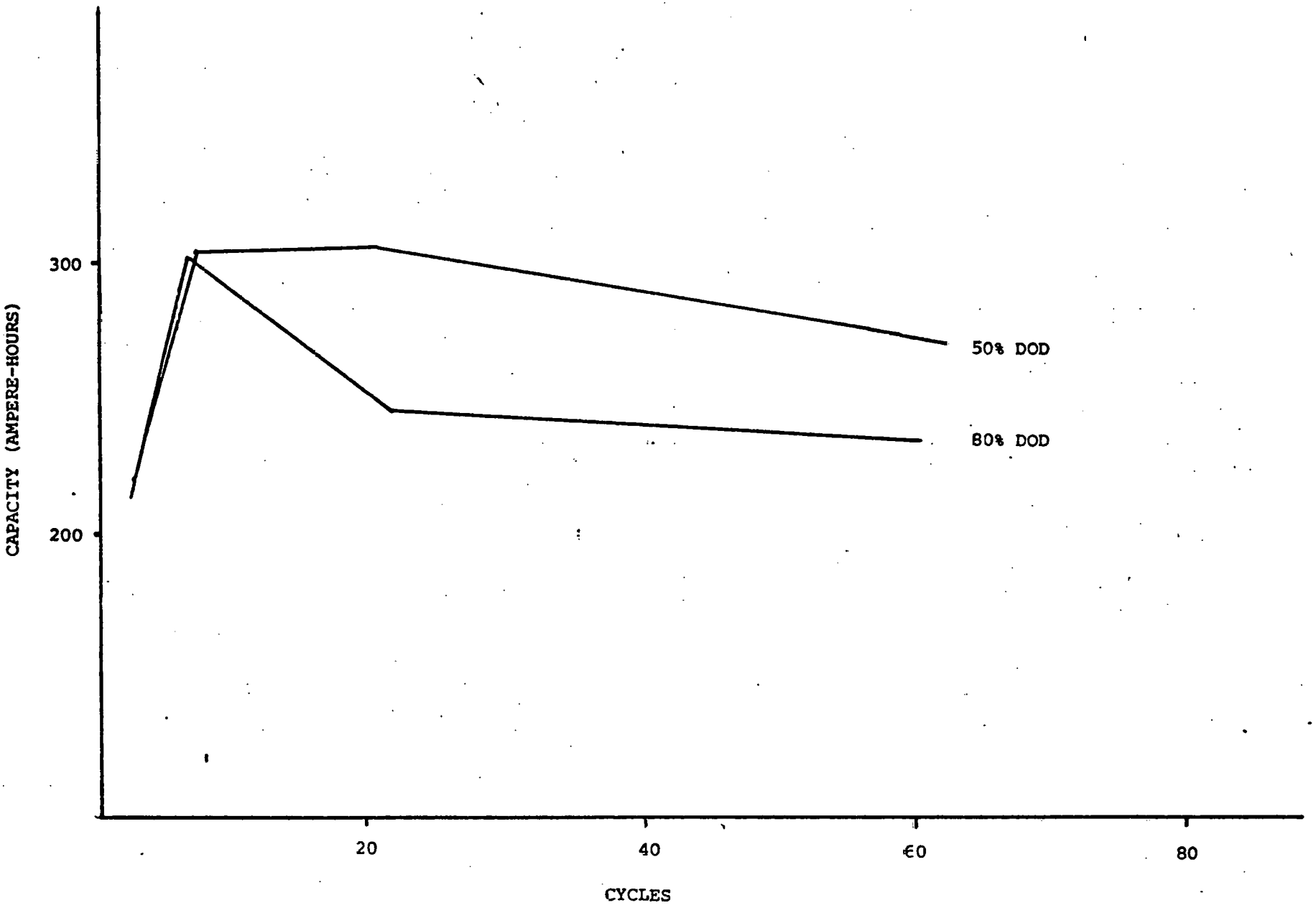

EXHIBIT D-V: PEAK POWER, 400 AH CELLS

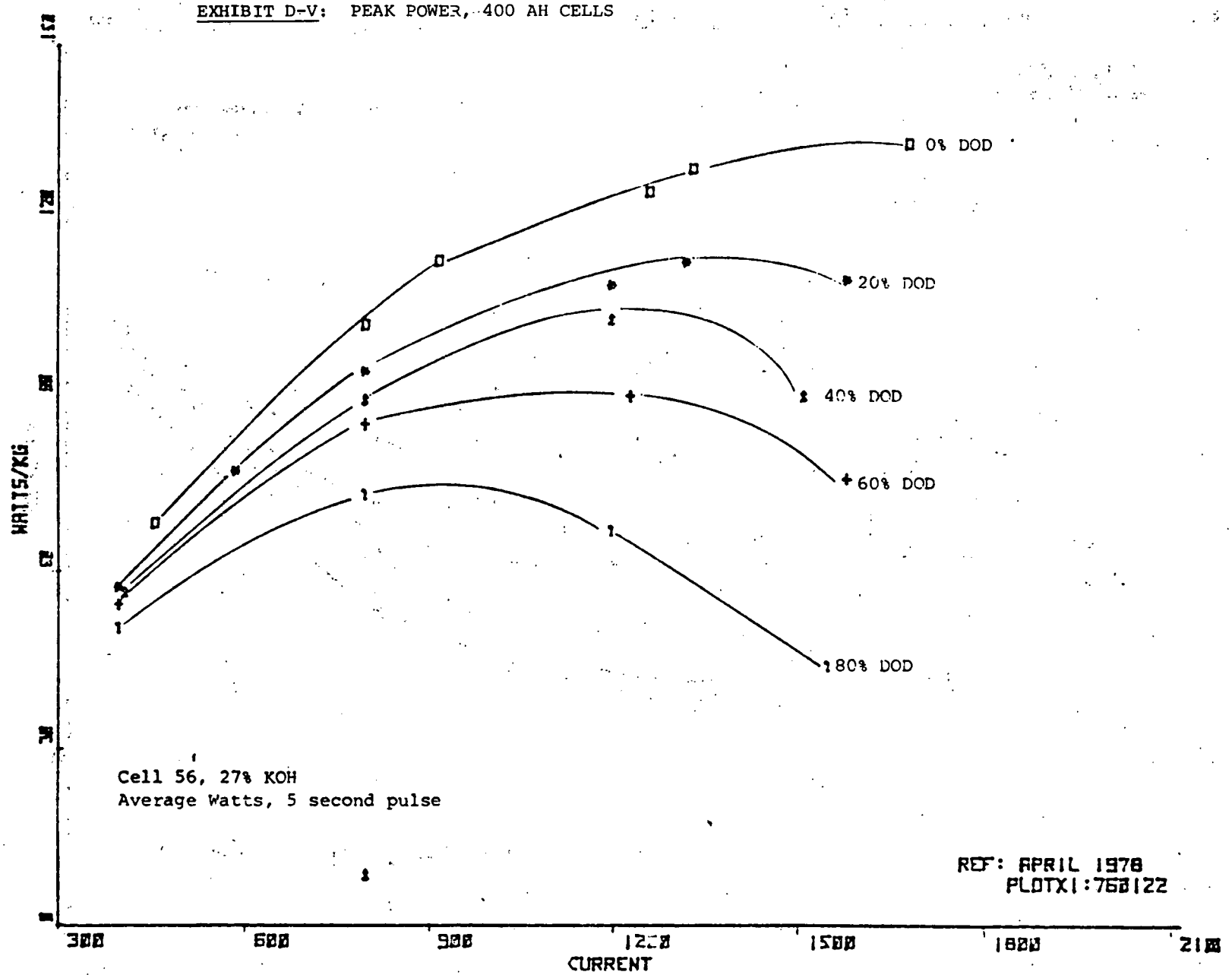

EXHIBIT D-VI: PEAK POWER, 400 AH CELLS, LOW KOH

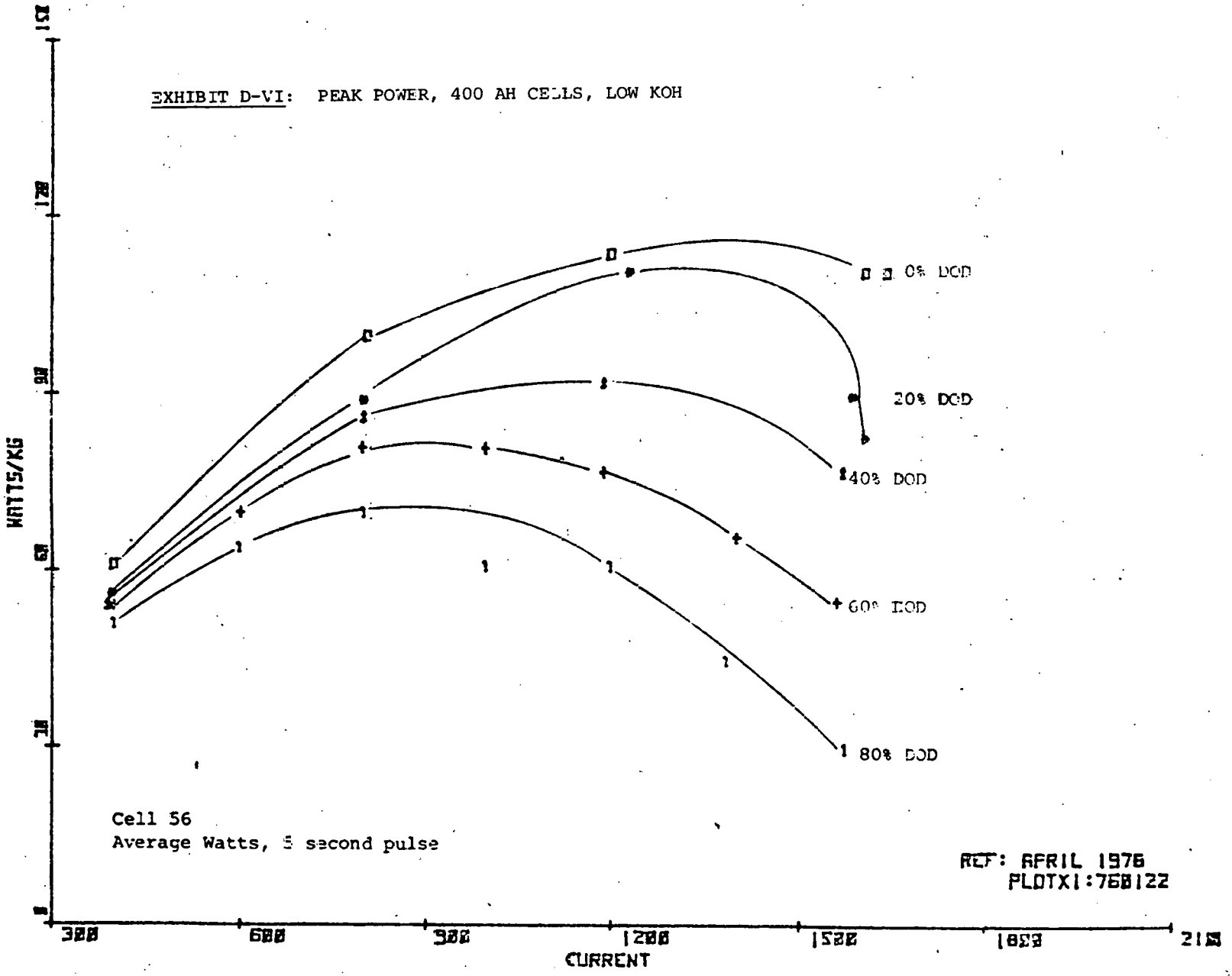

EXHIBIT D-VII: PEAK POWER, PB220 GOLF CART

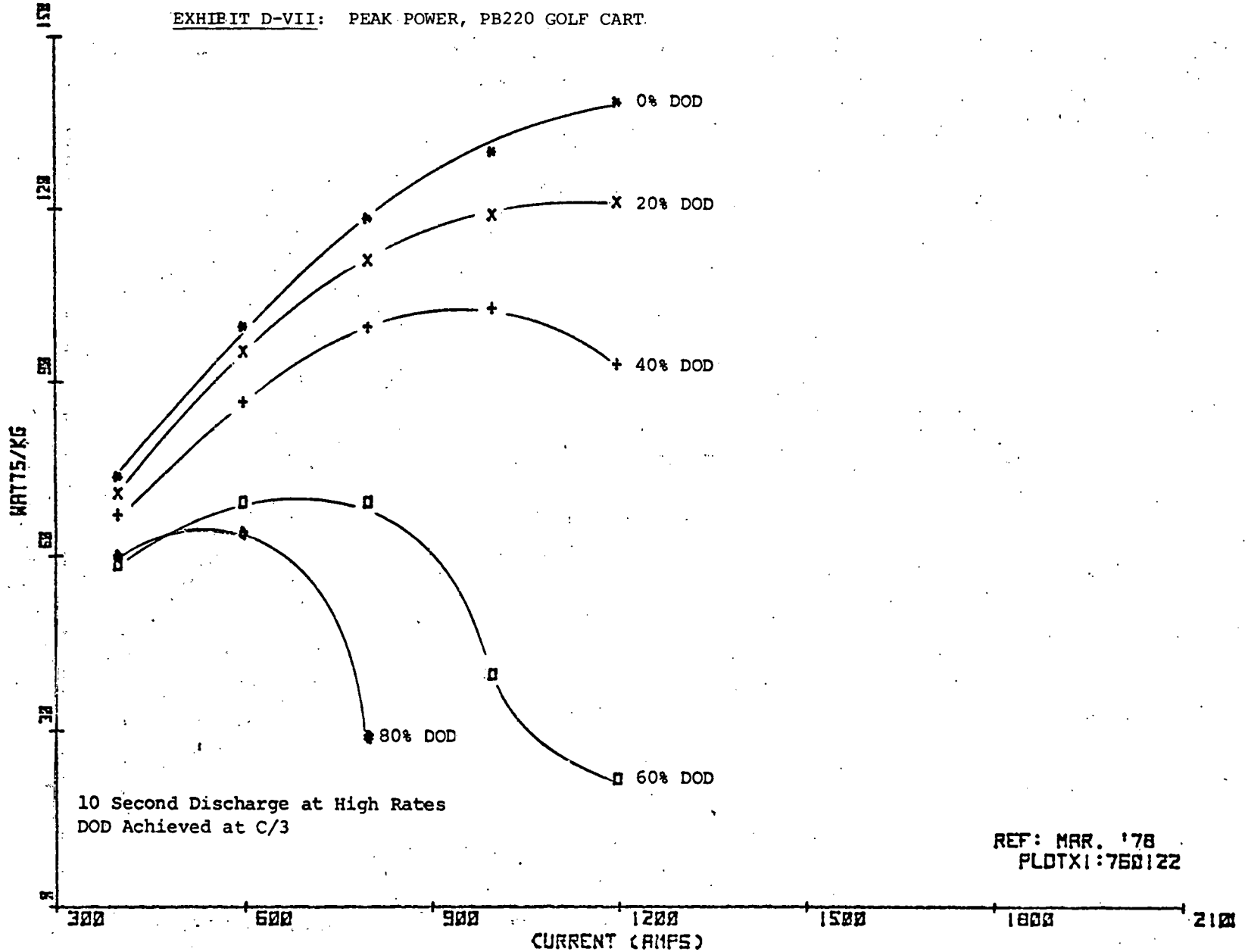

EXHIBIT D-VIII: PEAK POWER VOLTAGE, PB220 GOLF CART

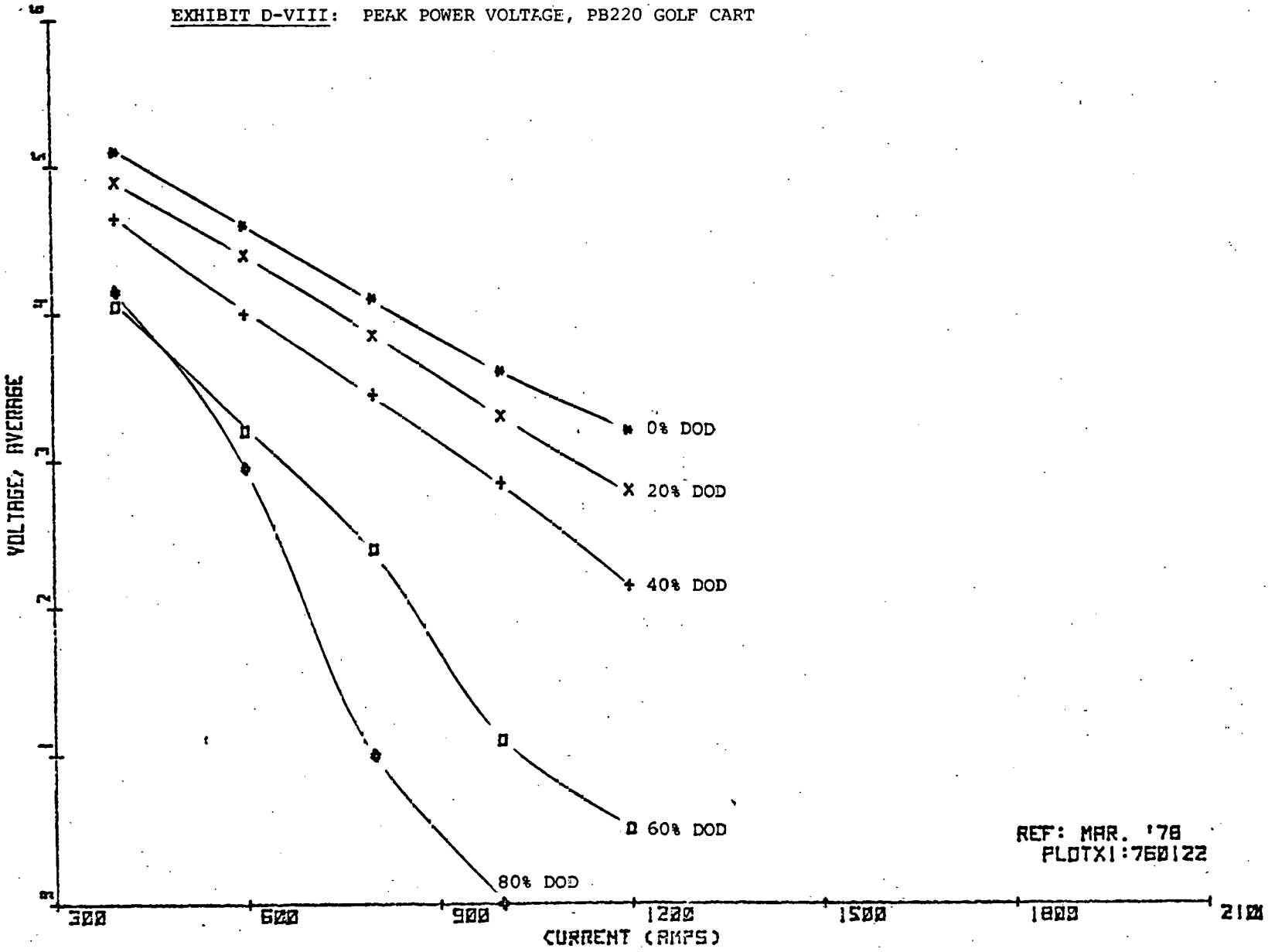

EXHIBIT D-IX: PEAK POWER COMPARISON, 0% DOD

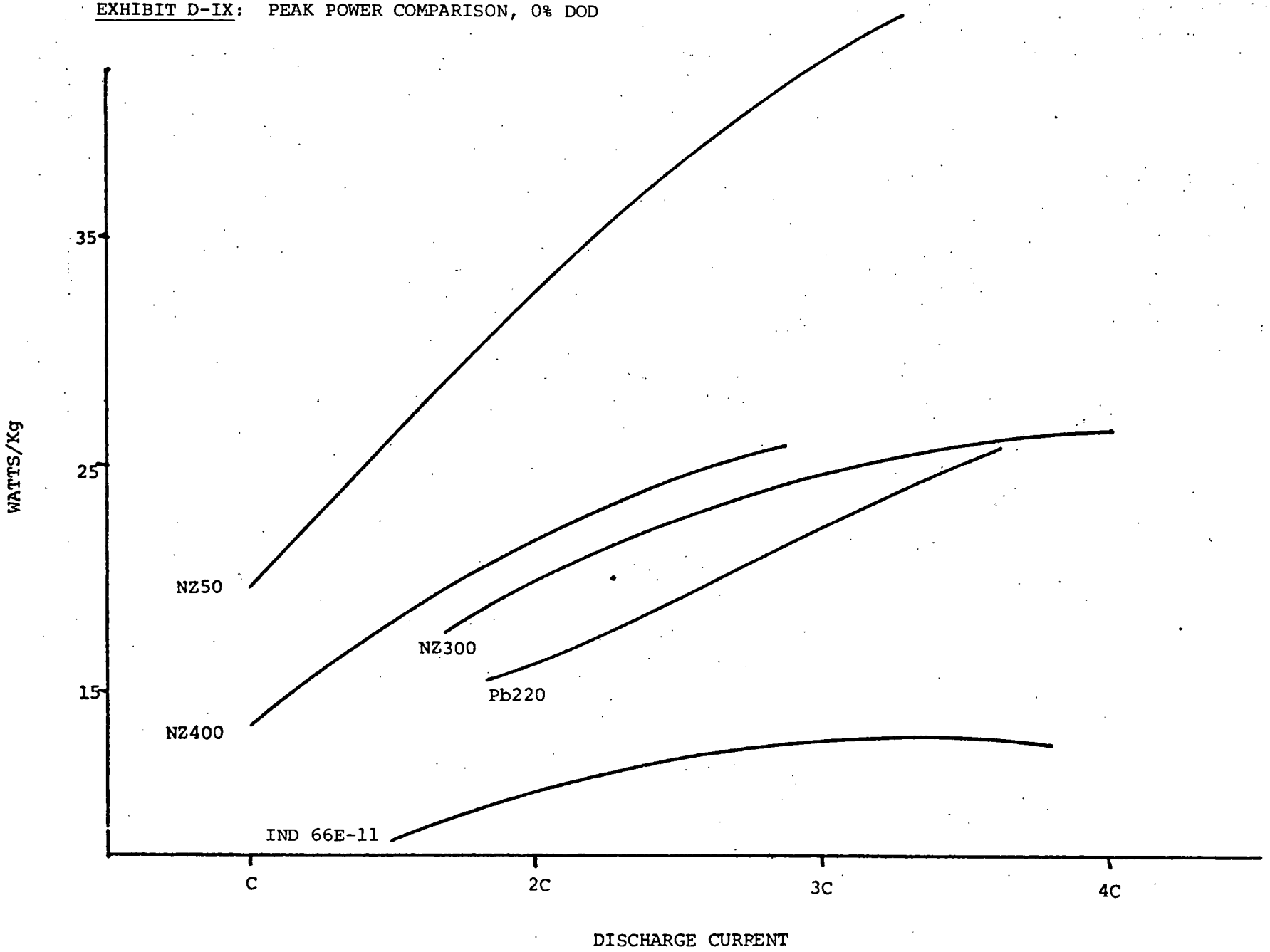

EXHIBIT D-X: PEAK POWER COMPARISON, 80% DOD

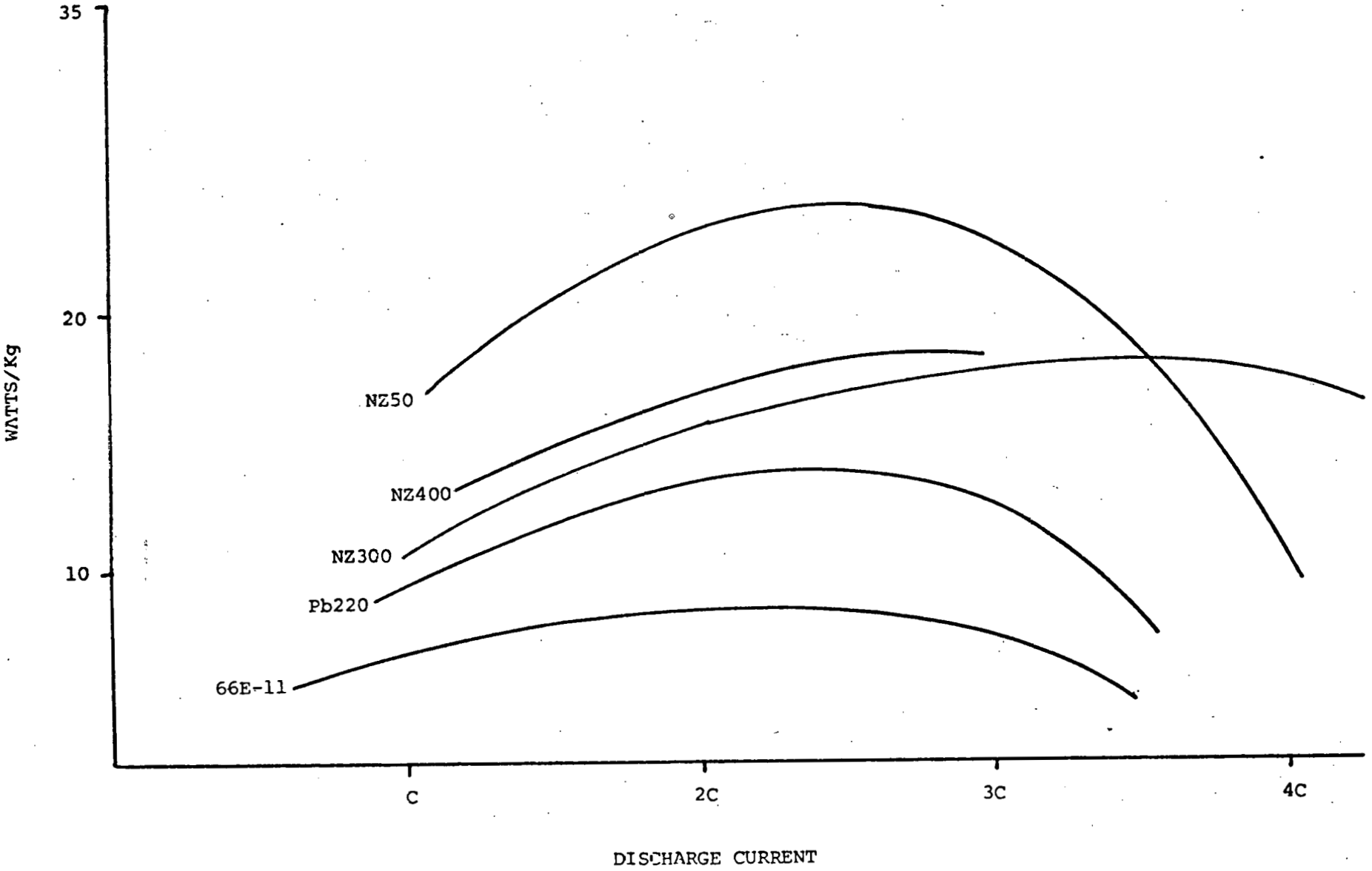

EXHIBIT D-XI: SUSTAINED POWER, 400 AH CELLS

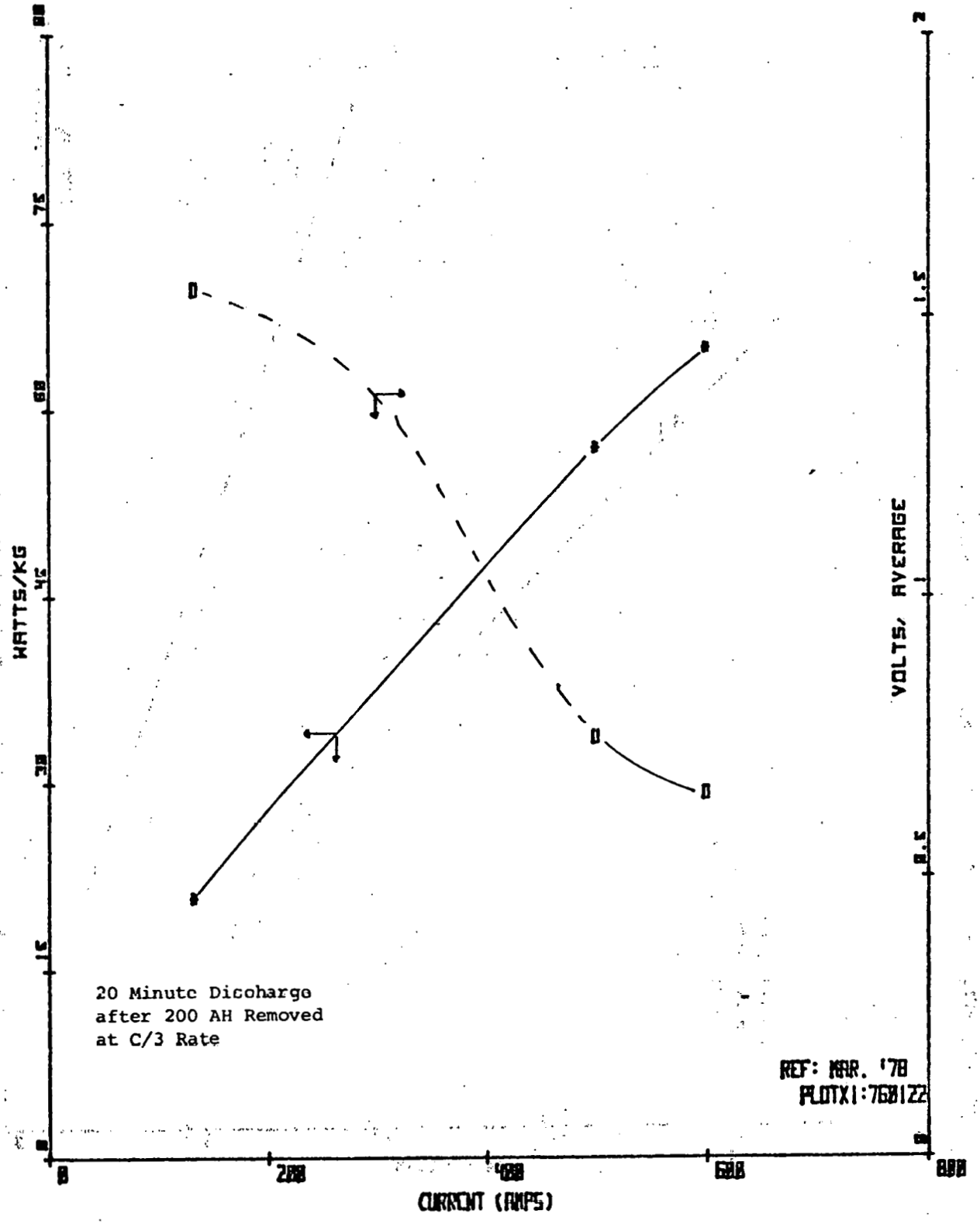

EXHIBIT D-XII: SUSTAINED POWER, LEAD-ACID VERSUS NICKEL-ZINC

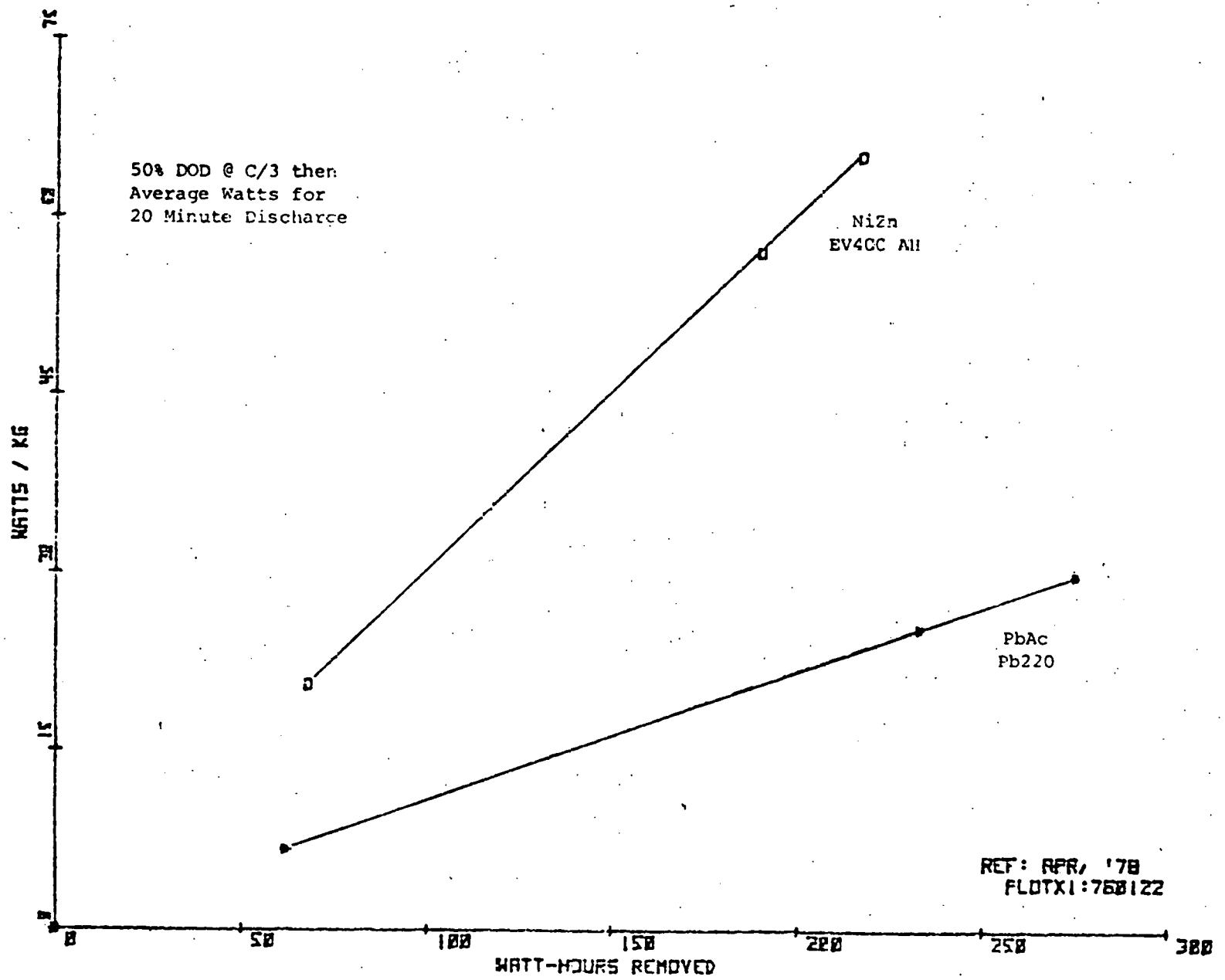

EXHIBIT D-XIII

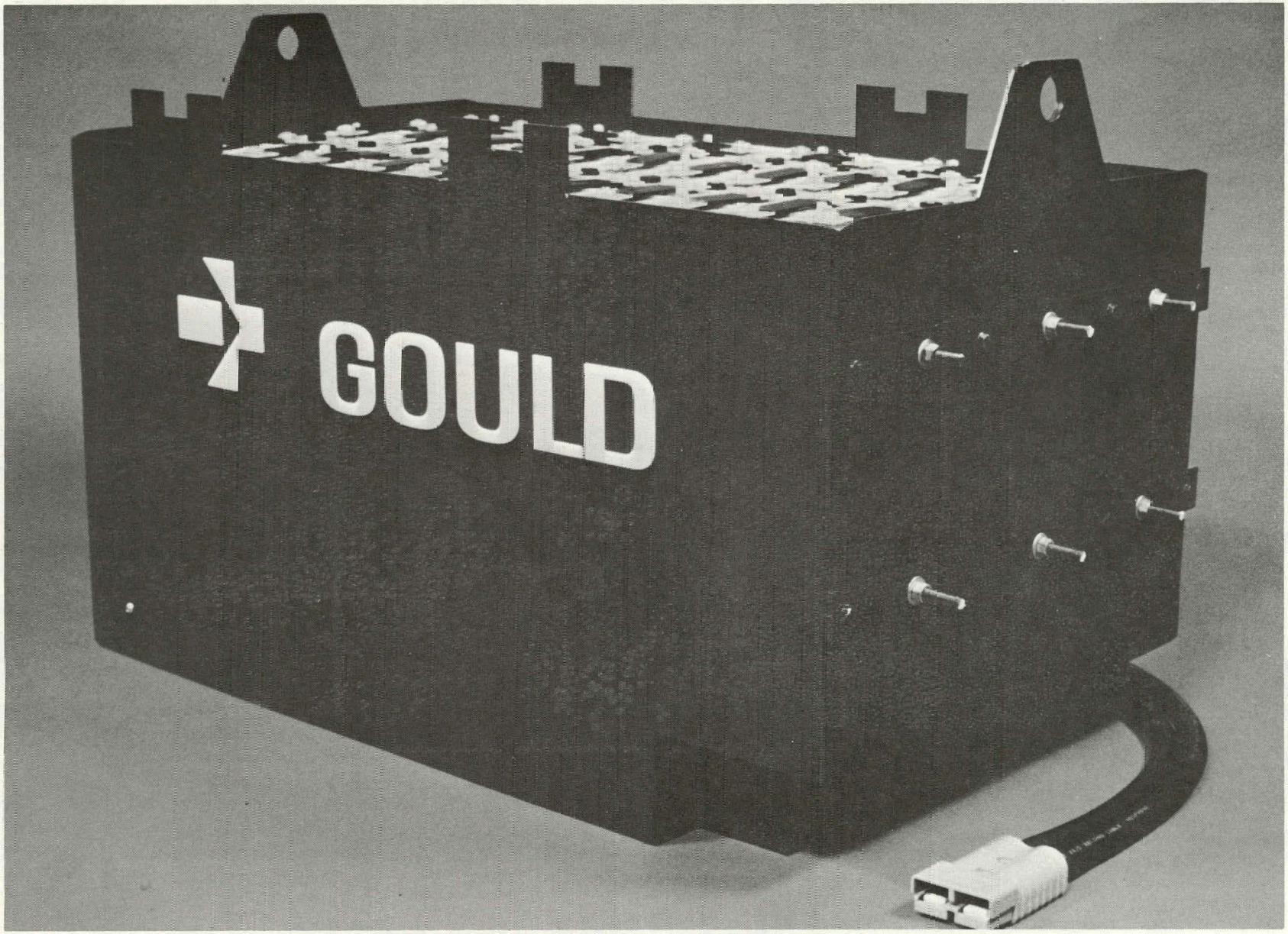

EXHIBIT D-XIV

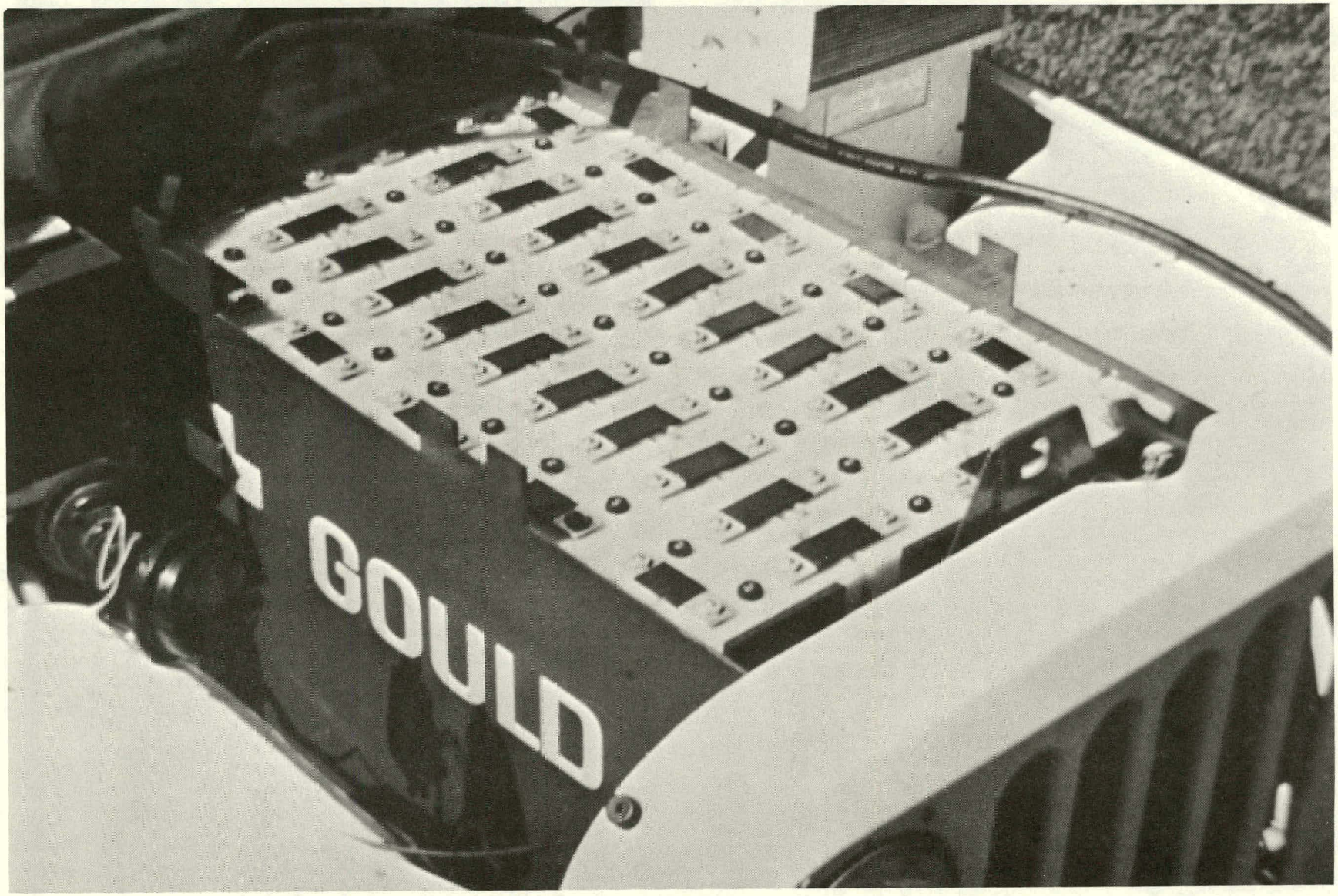

EXHIBIT D-XV: BATTERY CURRENT AT STEADY STATE VEHICLE SPEEDS

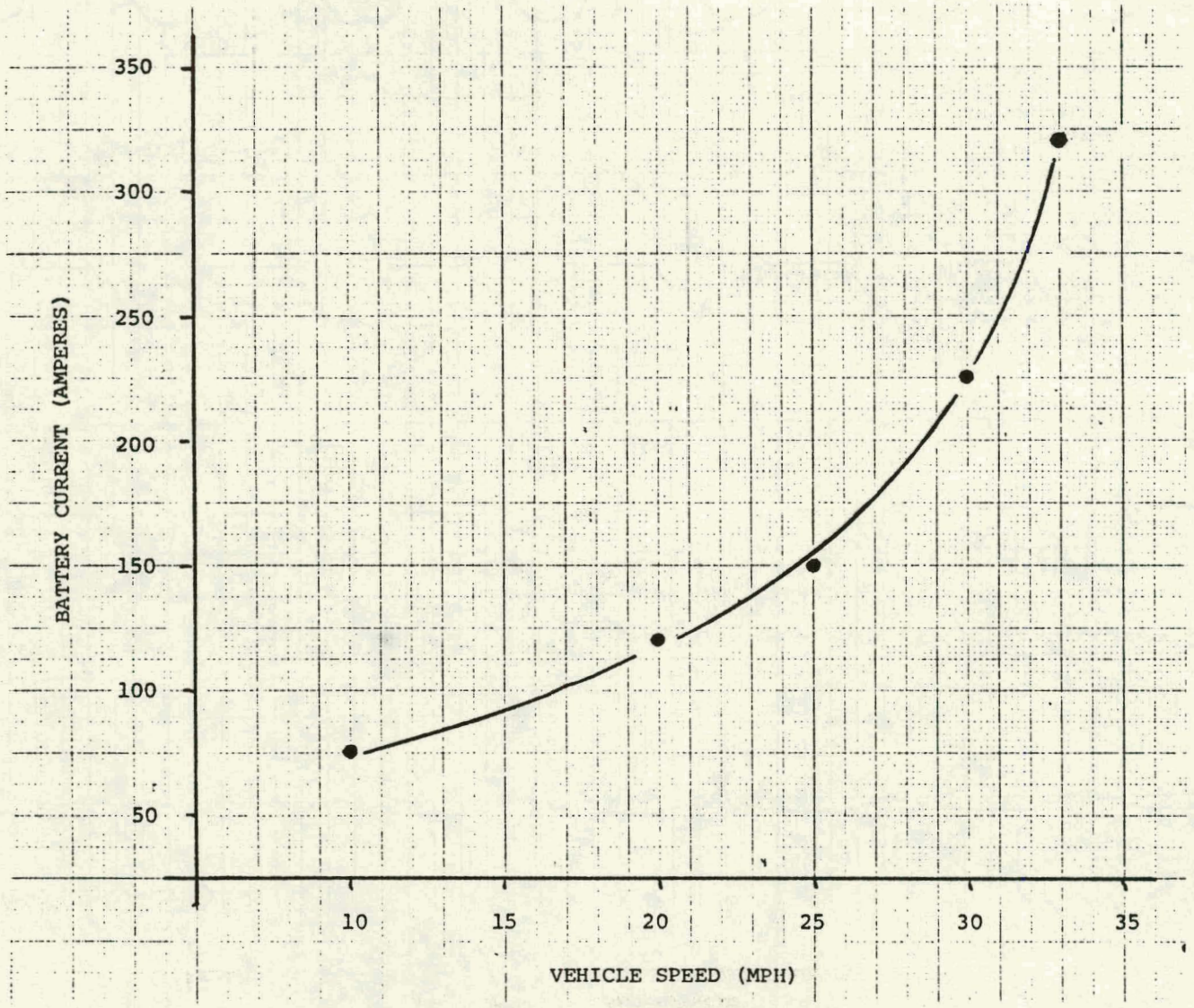

EXHIBIT D-XVI: BATTERY DISCHARGE CHARACTERISTICS FOR J-227a/B SCHEDULE

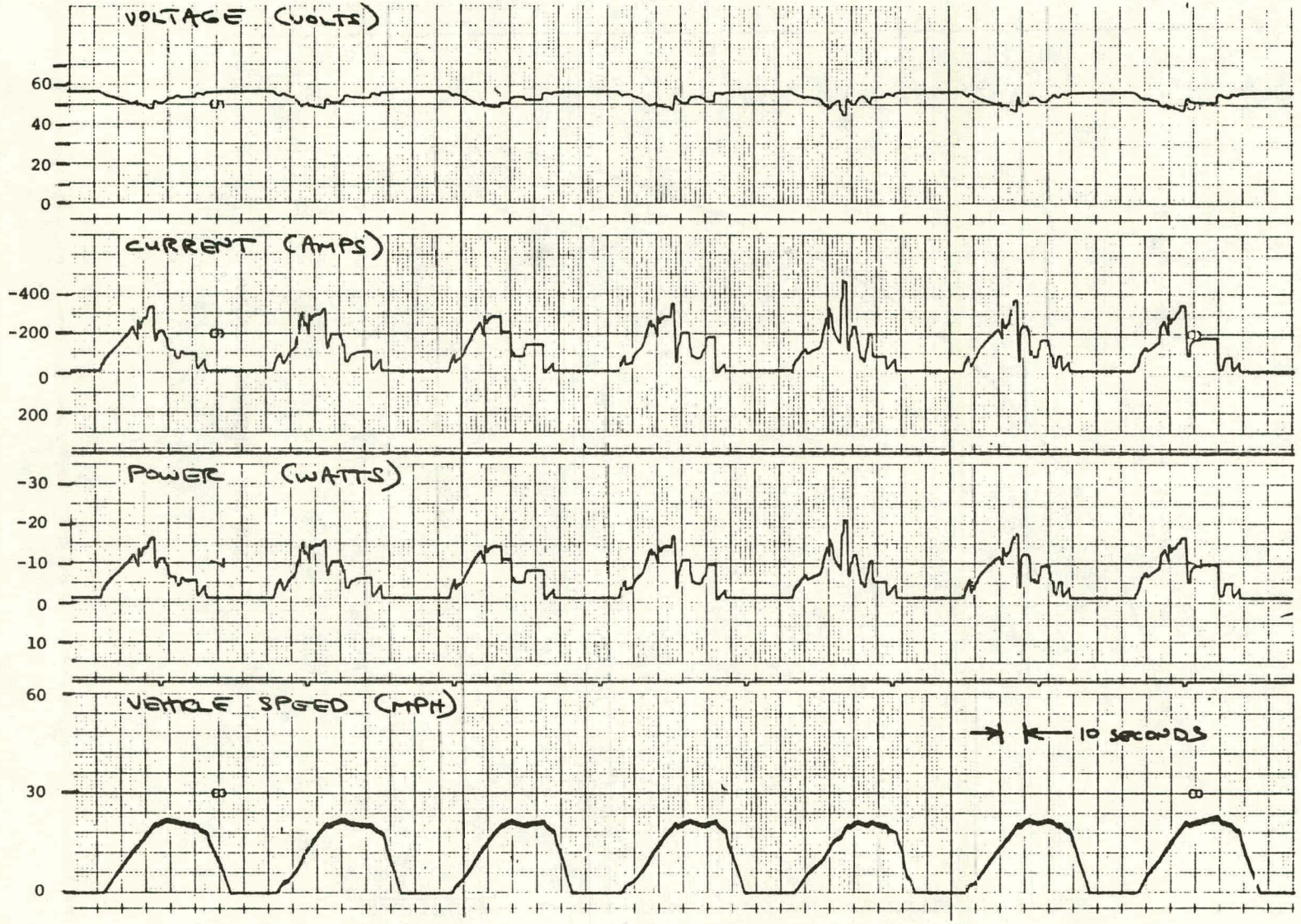

EXHIBIT D-XVII: LEAD-ACID BASELINE TESTS

TEST INFORMATION			ENERGY - KW-HR -		CAPACITY - AH -		RANGE	
TYPE	DATE	TIME	DISCHARGE	CHARGE	DISCHARGE	CHARGE	- MILES -	COMMENTS
10 MPH	7/19	6:30:00	18.95	27.41	-	-	68.9	
	7/22	6:27:00	18.89	31.67 *	-	-	68.7	
20 MPH	7/15	3:10:00	15.88	31.46 *	-	-	65.0	
	7/20	3:23:00	17.17	25.85	-	-	70.0	
25 MPH	7/12	1:48:00	12.69	19.48	-	-	46.5	
	7/18	1:45:00	12.35	19.4	-	-	45.1	
30 MPH	7/14	0:58:40	10.18	16.23	-	-	30.2	
	7/21	1:07:00	11.19	17.71	-	-	33.6	
33 MPH (Max. Speed)	7/25	0:29:00	7.21	12.04	136.2	181.9	16.7	Motor Overheat
227a/A	7/27	ABORTED - CONTROLLER PROBLEMS						
	7/28	7:15:00	10.85	18.02	208.0	286.4	11.2 (850)	To 54.0 V - No Performance
227a/B	7/13	3:30:00	13.16	21.62	-	-	31.6 (158)	Tc 52.24 OCV Cutoff
	7/26	3:20:00	13.38	20.38	263.5	326.3	32.0 (161)	
	7/29	3:35:00	14.16	28.66 *	274.6	451.6	33.4 (170)	
227a/C	8/1	CANNOT PERFORM SCHEDULE						

*Equalize Charge

EXHIBIT D-XVIII: NICKEL-ZINC ELECTRIC VEHICLE BATTERY TESTS

TEST INFORMATION			ENERGY -Kw-Hr-		CAPACITY -Ah-		RANGE		
TYPE	DATE	TIME	DISCHARGE	CHARGE	DISCHARGE	CHARGE	MILES	COMMENTS	
20 mph	8/15	3:03:00	18.023		342.4	405	65.9	4500#	
20 mph	8/16	3:00:00	15.713		296.7	460	58.3	4500#	
227a/B	8/17	3:57:00	16.798		342.3	458	38.4	4000#	(+18%)
30 mph	8/18	1:26:00	13.502		274.6	463	45.3		(+42%)
227a/B	8/19	3:55:00	16.268		314	465	38.0		(+18%)
25 mph	8/22	2:10:00	16.060		317	408	54.8		(+20%)

Battery Weight: 788 Pounds

EXHIBIT D-XIX: VEHICLE RANGE WITH LEAD-ACID SEMI-INDUSTRIAL BATTERY

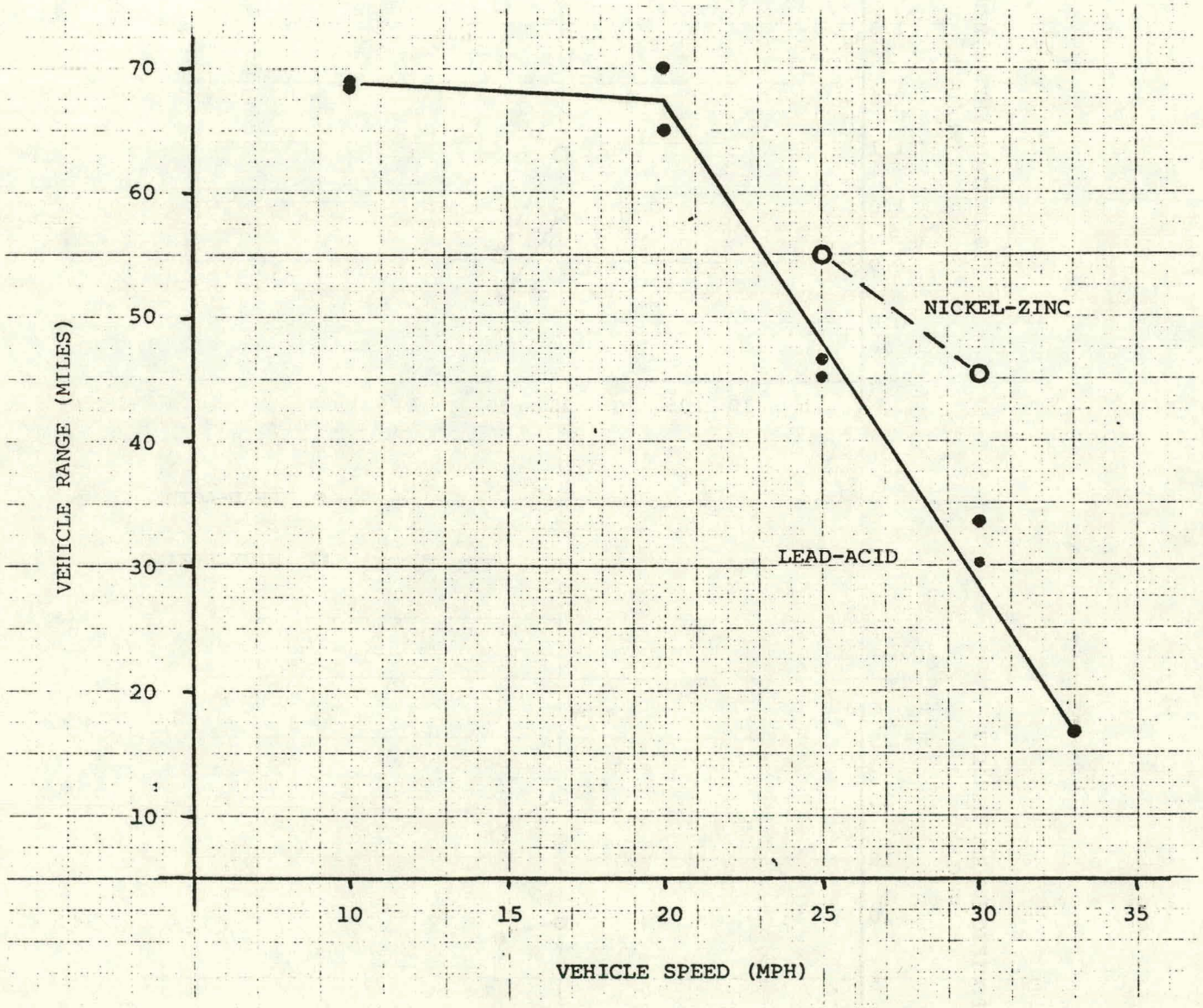

EXHIBIT D-XX; SPECIFIC AND VOLUMETRIC ENERGY DENSITIES FOR ELECTRIC VEHICLE BATTERY

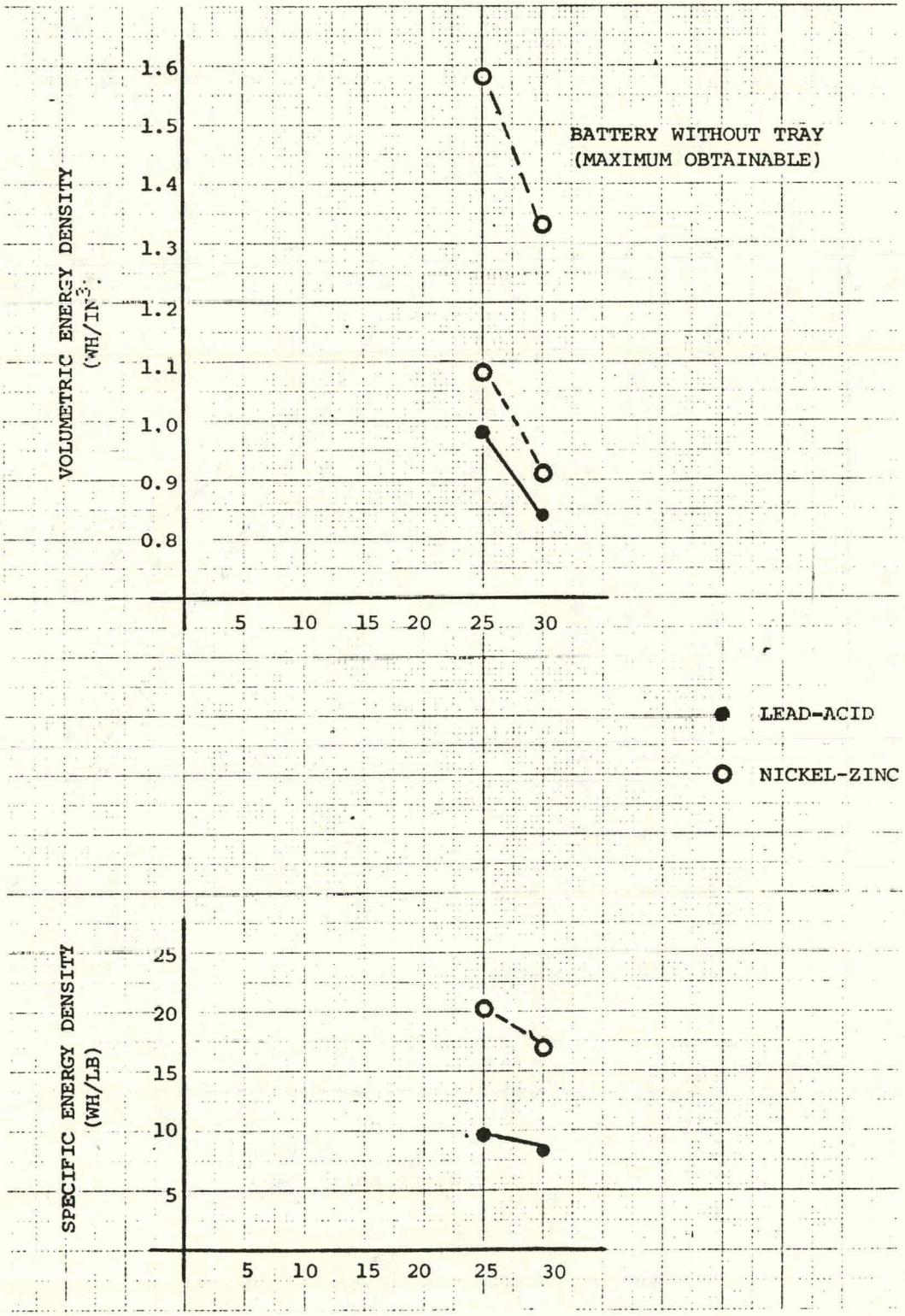

EXHIBIT D-XXI

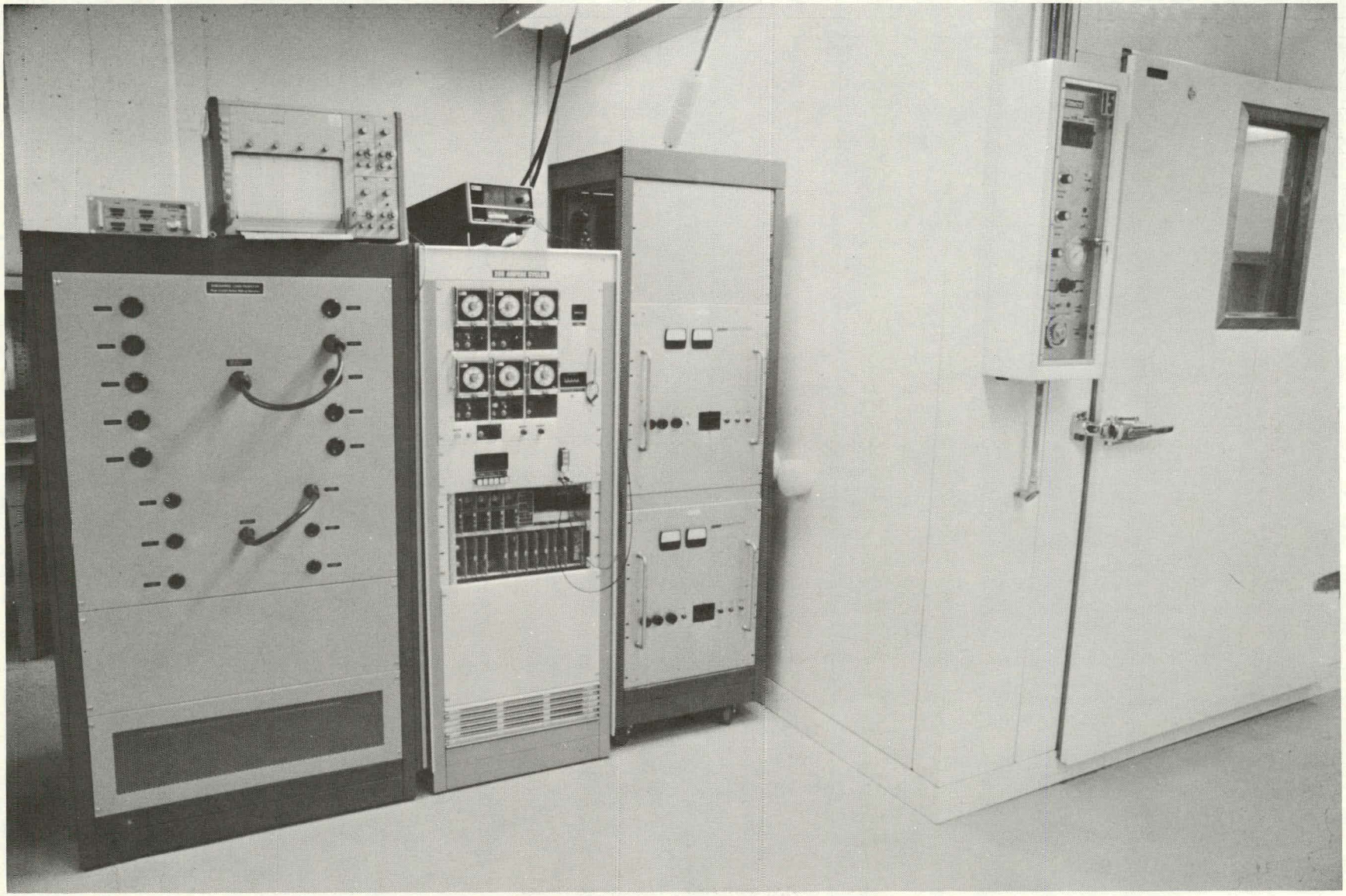

EXHIBIT D-XXII

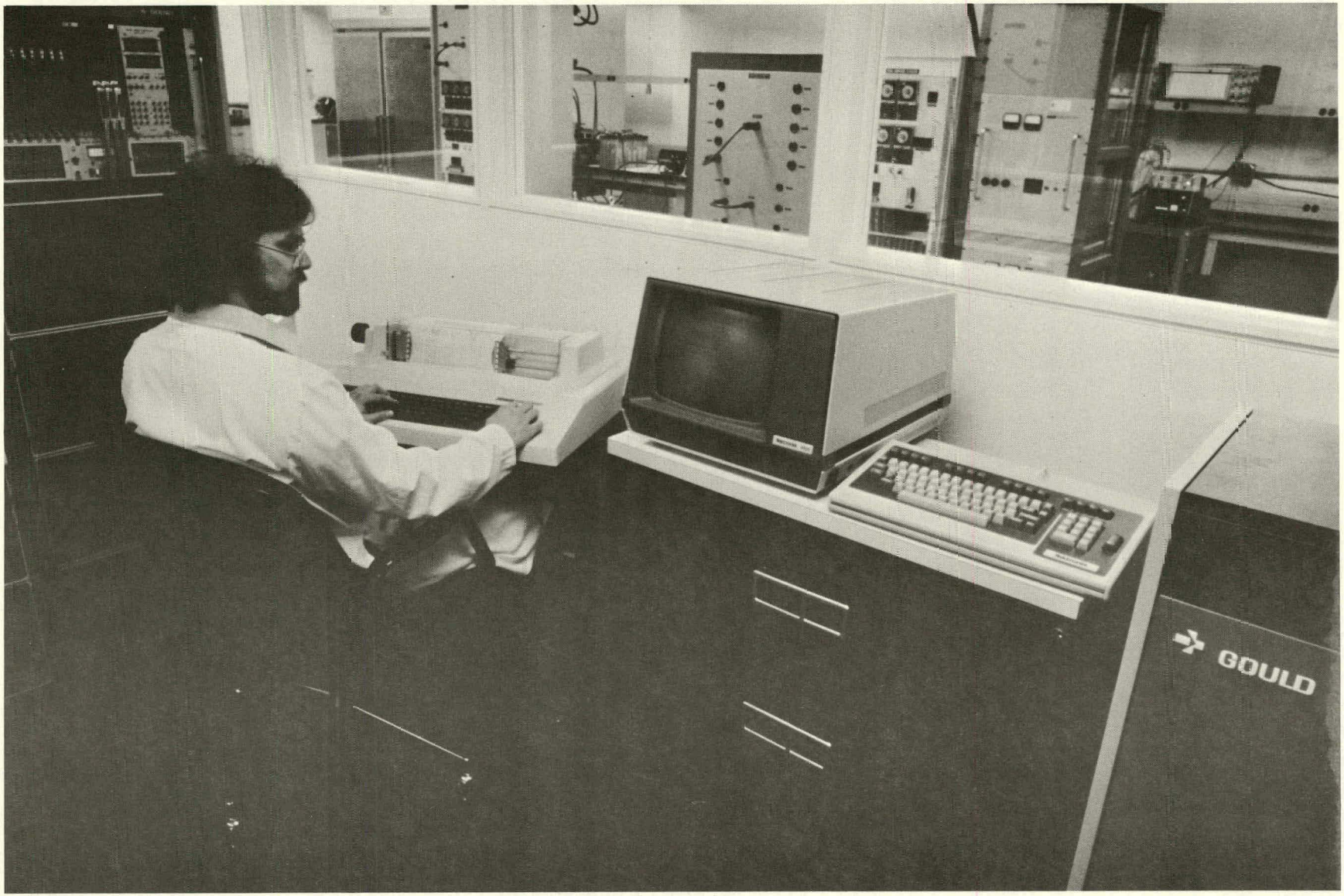

EXHIBIT D-XXIII

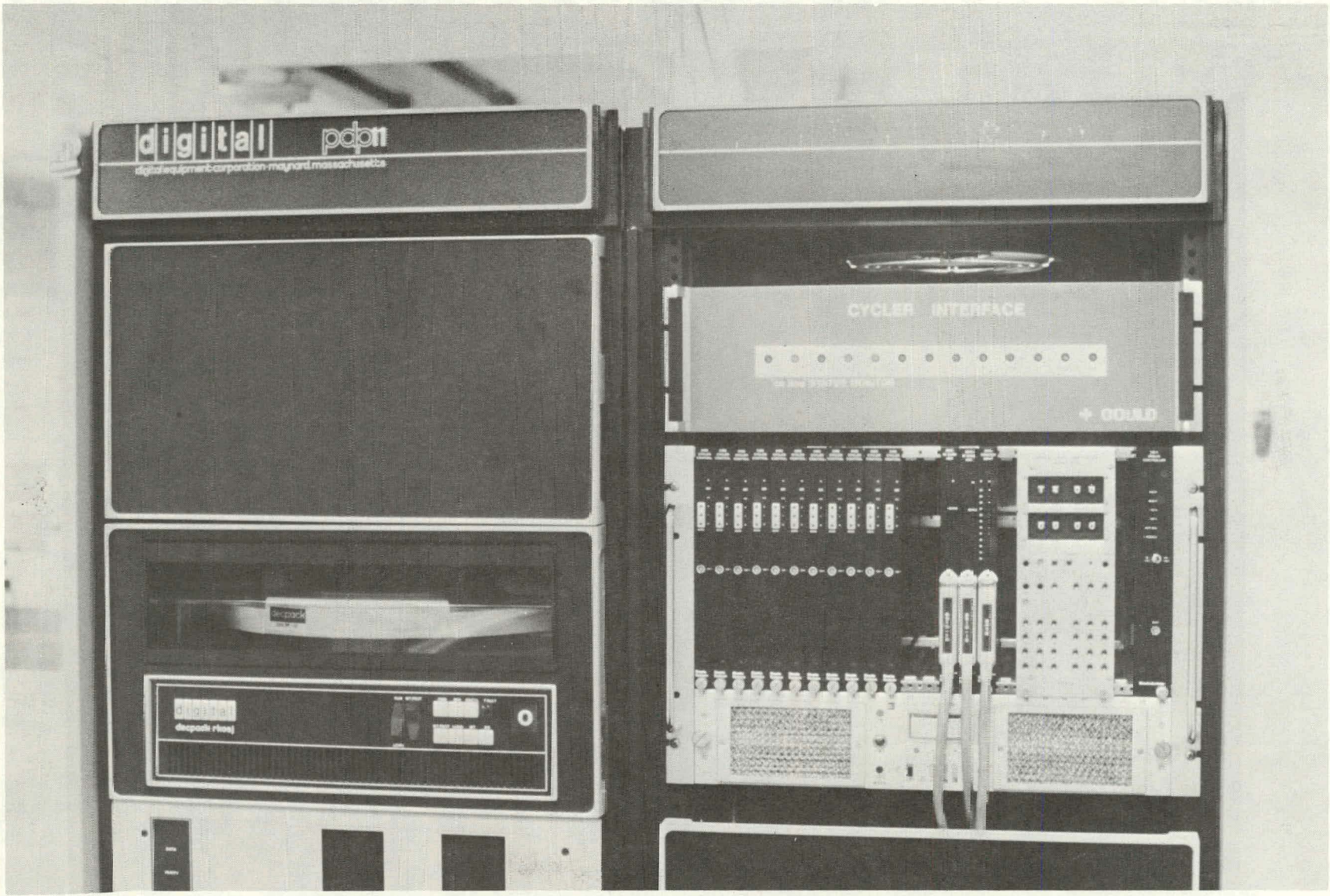

EXHIBIT D-XXIV

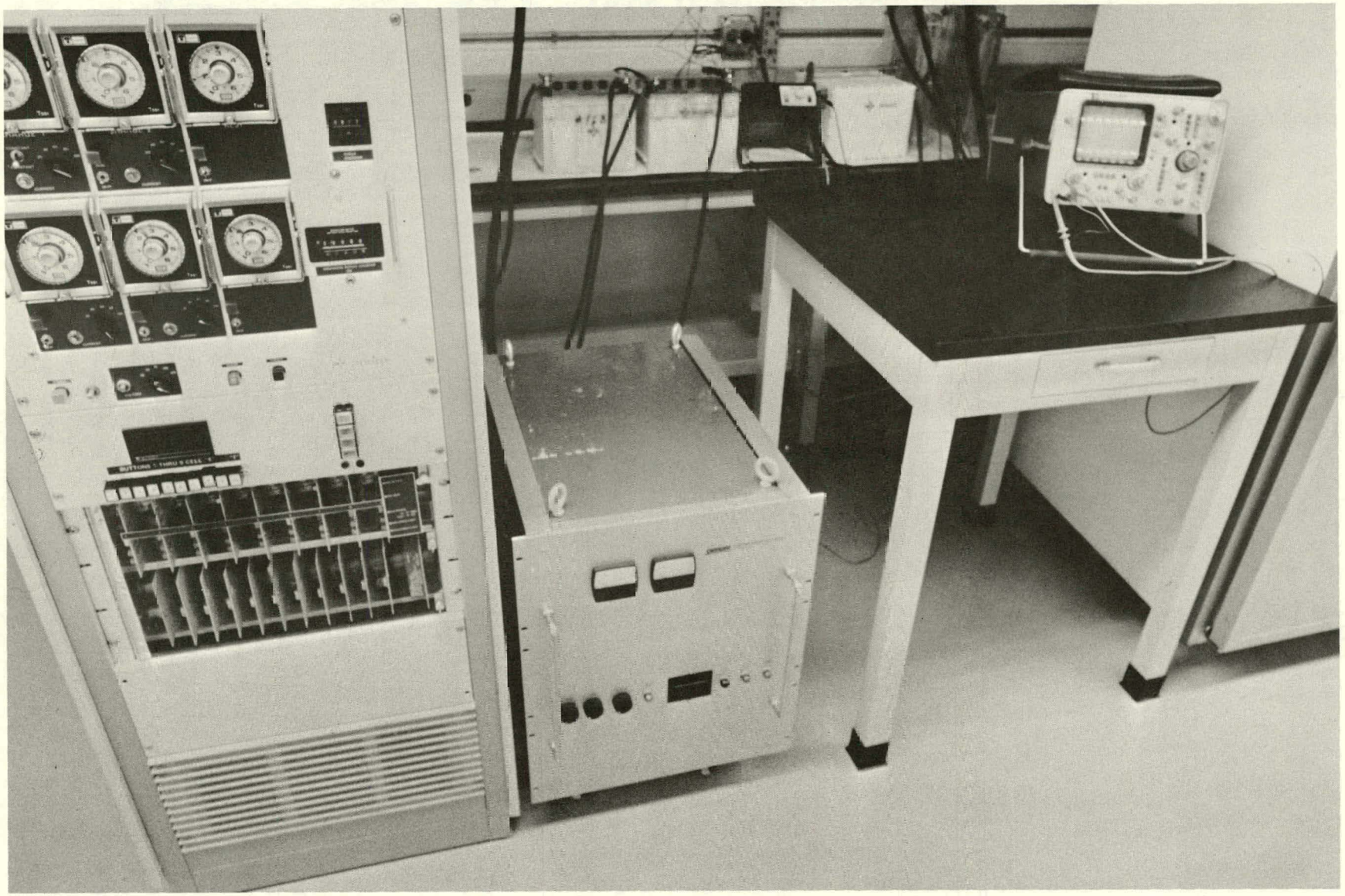

EXHIBIT D-XXV

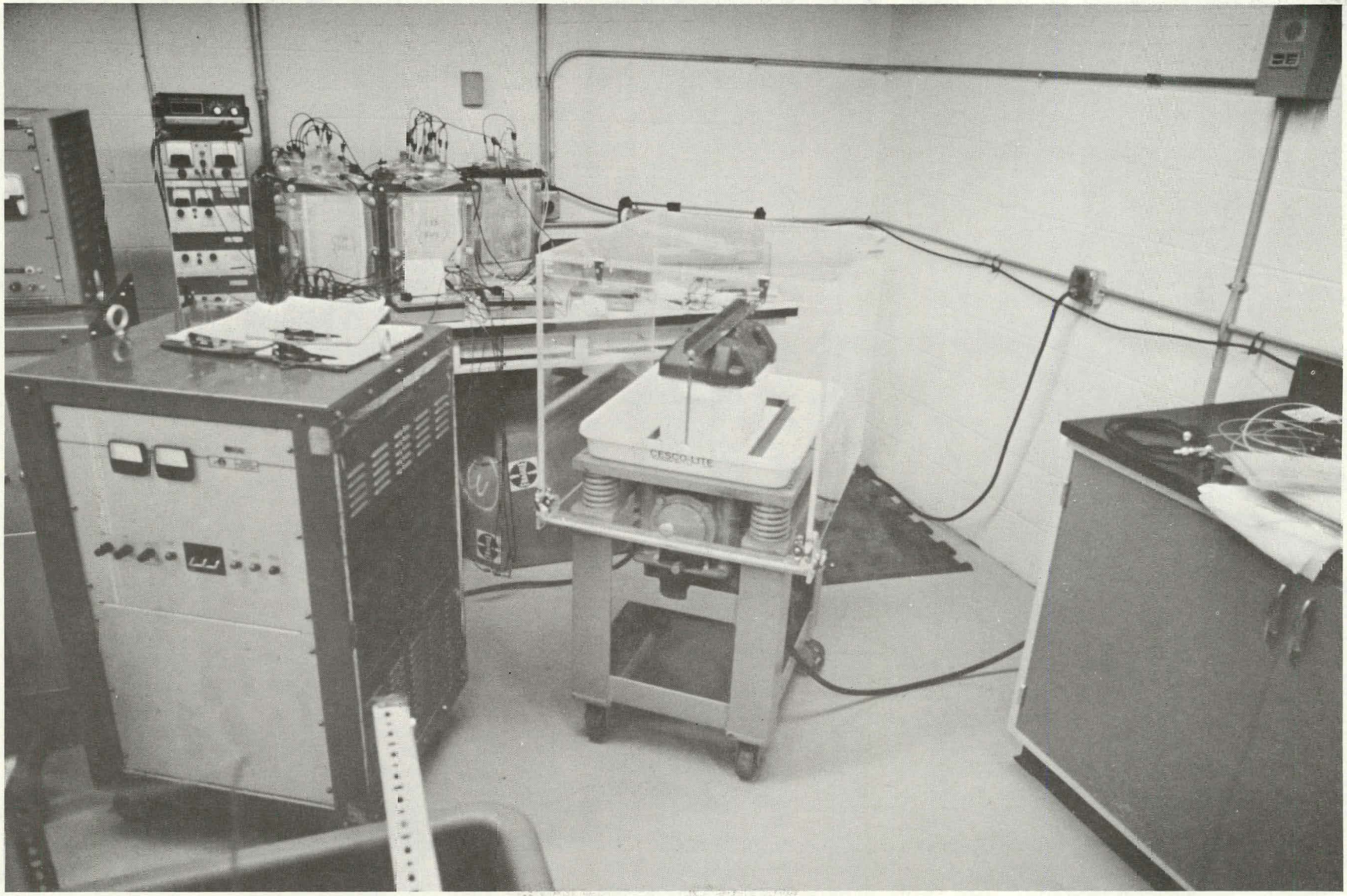

EXHIBIT D-XXVI

EXHIBIT D-XXVII

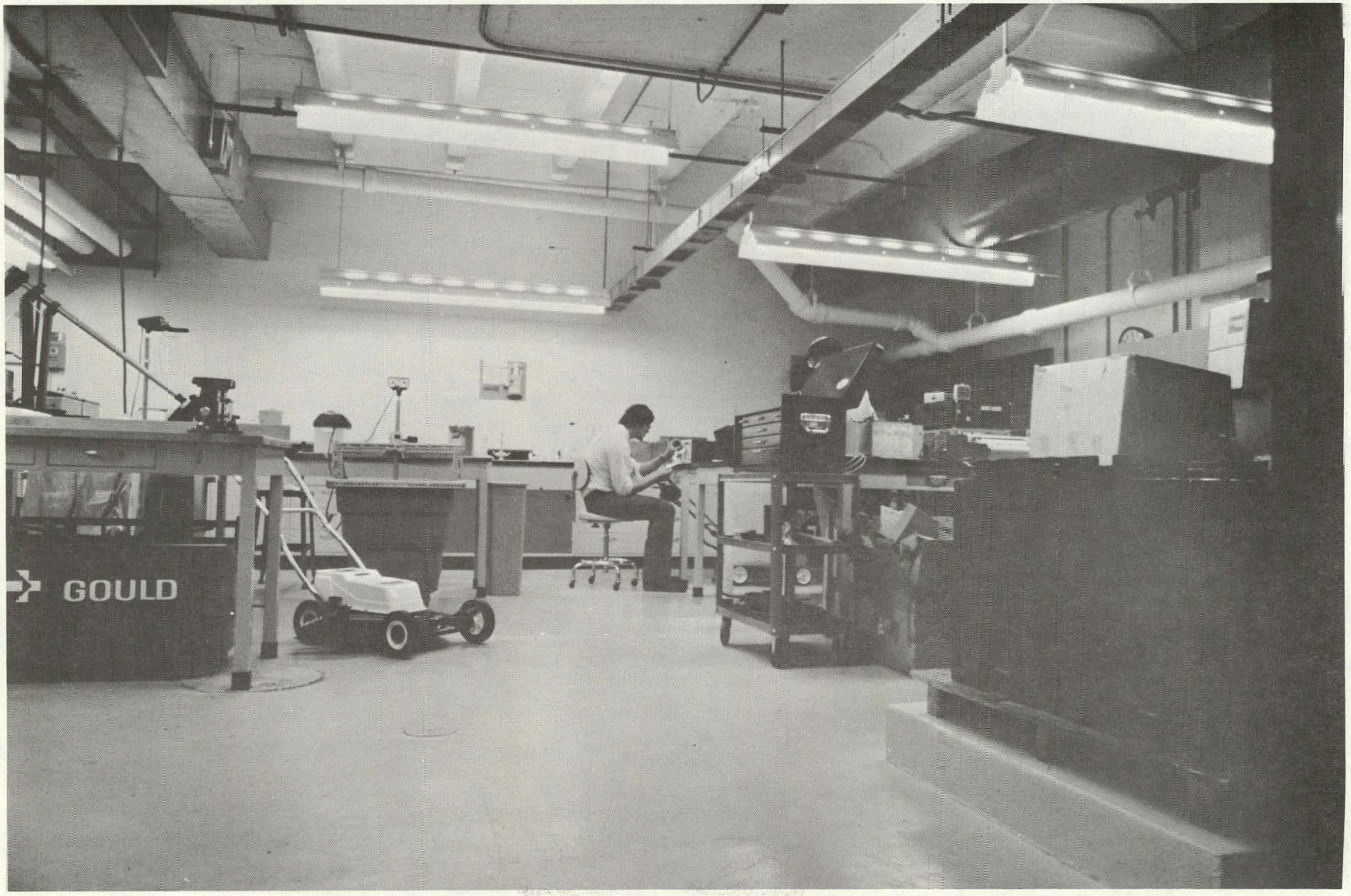

EXHIBIT D-XXVIII

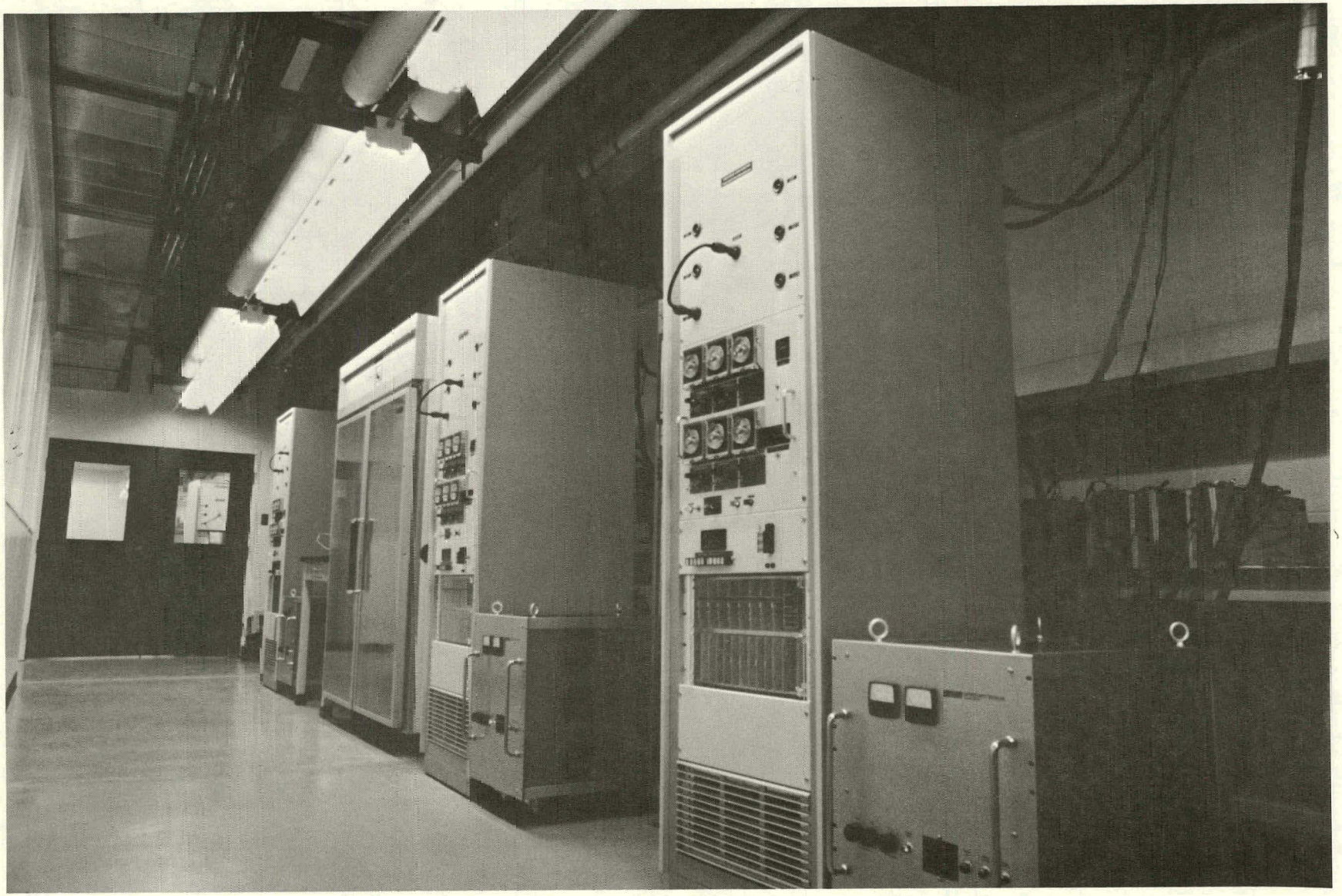

TASK E: PROCESS DEVELOPMENT

Objectives

The primary objectives of this Task are: 1) to implement applied research and product design innovations into the manufacturing environment and evaluate these innovations's manufacturability, 2) establish effective, accurate, and economical manufacturing quality control techniques; and 3) develop manufacturing processes to reduce the cost and increase reliability of the final product. Thus, process development ensures that laboratory developments proceed into a manufacturing environment with a minimum of technical hurdles.

Separator Process Development

The process development work on separator materials is divided into two main areas. The first is the manufacture of Gould's microporous separator. The second is the techniques and processes involved in manufacturing separator envelopes for the electrodes.

A process for volume production of Gould's microporous separator was fully operational by the end of April, thus meeting our milestone on target. Several 500 foot reels of this type of sepatator were made. Quality tests on these reels of material have shown that they meet specifications in terms of bubble prssure, i.e., pressure at which the first hole appears is 15 to 20 psi (EXHIBIT E-I) and electrical resistance 0.30 to 0.5 ohm-cm^2. However, optical microscopy reveals that the separator coating contains many small craters which are formed during the drying stage of manufacture. The raw material costs for the current formulation are listed in EXHIBIT E-II. From these data, it is estimated that the material cost per square foot is $0.027; with production scale-up, the total manufacturing cost should be below the $0.10/$ft^2$ target.

The processes for production of Gould's ELECTROPOROUS™ separator are reported under Task A.

The initial program of work on wrapping electrodes with separator was a literature survey. From this survey it became obvious that there is no "common" way to wrap electrodes and the separator-type determines the most appropriate technique. Therefore, it was imperative that a particular separator system be adopted; and hence, a program could be started on developing the relevant machinery.

For the separator material presently in use, the appropriate heat sealer was purchased to manufacture separator envelopes. Extensive sealing trials were implemented to determine the range of temperature, time, and pressure to produce an optimum seal. The "optimum" seal was determined by both hand and machine pull tests. It was found that there are three broad levels of seals when the polymer has become transparent in the heat zone. Once having established the conditions for good seal, the next step was to determine how to repeatedly make good seals since the heat seal device takes some time to reach a dynamic equilibrium. By incorporating some fairly sophisticated instrumentation on the sealer unit, it was possible to reproduce good seals at a reasonable production rate for a manually operated machine. A further improvement has been achieved in the separator envelope manufacture in that it is possible to make multi-layer bags by a single operation. A prototype machine has now

been built and is operational in the Pilot Plant to manufacture single-layer bags, this machine also incorporates inspection and cutoff stations.

Molding of Negative Electrodes

The laboratory process developed for the molding and pressing of zinc oxide electrodes is a very time consuming process. Therefore, it was essential that a faster production method be found. Gould has developed a preform/marry concept based on its depth expertise in traditional powder metallurgical mass production techniques, this technique has increased the production rate by a factor of eight over previous pressing methods.

It is planned that zinc electrodes be made by first making two preforms which are then pressed together around a metal current collector. This method of electrode manufacture necessitates special tooling which can withstand high pressures. Although the concept of preform/marry is simple, the actual execution of the technique proved more difficult. The first indication of a problem was when the two preforms were married together and the pressure released. This resulted in large blisters occurring in the electrodes, particularly in the "end" type electrodes. A thorough investigation of the problem brought several important observations to light. Probably the most important being that initial powder characteristics had to be very closely controlled, especially with the new binder which was introduced in the early stages of this work.

Several batches of agglomerated zinc oxide made in the "in-house" spray dryer were analyzed for binder level, moisture content, and agglomerate size distribution, these results are reported in EXHIBITS E-III thru E-VI.

The binder contents of the five individual lots ranged from 7.7 to 10.3 W/O with an average of 8.7 W/O, with the moisture contents from 2.3 to 3.0 W/O. The screen analyses showed a significant variation in agglomerate size distribution. The variations greatly effect the powder diefill weight and the preform expansion rate. Hence, it is essential to blend the small 25 pound lots into larger 200 pound lots to produce a uniform negative electrode preform.

Once demonstrated that the preform/marry concept was successful then special preform tooling and powder feed shoe were built for the press. This greatly improved production so that it was possible to make approximately 2,200 electrodes in three weeks.

Advanced Nickel Electrode Molding

Porous nickel plaques are currently molded in the Pilot Plant on an individual basis. In order to achieve the target costs for this component, scale-up to multiple piece molding or continuous molding is essential.

The initial program of work was directed at a multiple process. Early trials indicated that the molding and sintering of a low profile piece caused no great problems, however, the separation into individual pieces was an area for further investigation, both in technical and economic aspects. These further investigations were completed and a favorable route was handed over to the Pilot Plant.

As a longer term objective for mass producing nickel electrodes, a further program was initiated to continuously deposit nickel powder layers.

A series of trials has been completed to investigate the range of powder thickness which can be reproducibly deposited by this technique with different nickel powders. The minimum powder thickness which maintained good quality surface was 0.015". In general, the surface quality improves as the layer thickness decreases. The 0.5" to 0.2" thick layers require lower belt speeds than the thinner layers. Preliminary weight reproducibility trials have been carried out. These show the weight to vary ±2% from layer-to-layer.

Positive Electrode Manufacture

The major objective of this effort was to determine the cause of the poor performance of the nickel electrode made in the Pilot Plant and implement the required improvements to restore the positive electrode to the expected 500 to 1,000 cycle capability. Initial work was concentrated on improving the nickel plaque prior to impregnation. The reason for adopting this line of attack was that a paper analysis of the nickel electrode manufacturing route indicated that several changes had occurred from the laboratory process prior to impregnation.

Initial experiments on the nickel plaques prior to impregnation brought about only a minor improvement when the electrodes were tested in accelerated nickel-cadmium tri-electrode cell tests.

As a result of these findings, efforts were redirected to thoroughly examine the impregnation process. Two possible causes of poor electrode performance were postulated as a result of improper impregnation.

Experimental work on the impregnation loading of nickel plaques revealed several important results.

From all the data generated, it was possible to design a nickel electric vehicle cell electrode which should deliver 40 AH.

A batch of nickel plaques were made. The sintering was carried out in a cracked ammonia atmosphere after which the plaques were subjected to the required impregnation runs.

The average data for this batch of plaques was as follows:

Nickel Powder Weight	203.2 ± 3.6g
Weight Gain	102.8 ± 4.0g
Weight Gain Capacity	33.7 ± 1.1 AH
Thickness	105.3 ± 1.4 mil

If a capacity factor of 1.2 is assumed, then these electrodes will deliver 40.4 AH when cycled if they are given a charge of 145% that of the weight gain capacity.

Some of these cracked ammonia sintered electrodes were compared in tri-electrode cell tests to identical electrodes which had been vacuum sintered. The vacuum sintered electrodes proved superior in terms of minimum growth and delivered capacity.

It was decided that the improved current collector/tab designs be used to improve the current distribution and thermal transfer within the electrodes. These were discussed in detail in Task B.

EXHIBIT E-VII shows cadmium tri-electrode cycled nickel electrodes; one is from about six months earlier showing all the defects of the "mushy" surface, blistering, edge spalling, and cracks and the other shown is a current cracked ammonia sintered nickel electrode, the improvement is obvious in all respects.

In view of the superior quality of the vacuum sintered nickel electrodes over the cracked ammonia sintered electrodes, it was decided that a program of work be carried out to fully characterize our nickel plaques to ascertain what constitutes a good nickel electrode.

To establish a baseline, in this program, vacuum sintered and ammonia sintered plaques were compared with respect to microstructure, transverse rupture strength, surface area, and pore size. EXHIBIT E-VIII shows strength, surface area, and mean pore size data for these parts. The results show the vacuum sintered baseline parts are substantially stronger and exhibit lower surface area than the ammonia sintered baseline. The mean pore size of the vacuum sintered parts is higher than that of ammonia sintered baseline.

EXHIBITS E-IX and E-X show SEM micrographs of vacuum and ammonia sintered plaques. The vacuum sintered parts exhibit much smoother particle surfaces and generally appear to be better sintered.

In order to characterize the influence of some sintering variables, several sintering runs were made with a grid at the base of each sample. The major result of these tests was an observation of the effect of dewpoint on micorstructure of the sintered samples.

In mid-April, the furnace used for production ammonia sintering of nickel electrodes failed. Tear-down revealed a cracked weld at the mid-point of the furnace muffle. The muffle was rewelded and reinstalled, the heating elements were rebalanced, several heating elements being replaced, and the first section of the cooling jacket was replaced.

EXHIBIT E-XI shows SEM micrographs of a nickel plaque after the furnace repair. The surfaces of the nickel are quite smooth and the structure closely resembles the vacuum sintered product. These results indicate performance of these plaques should be comparable to vacuum sintered plates.

The post-furnace repair nickel electrodes tested in tri-electrode cell tests preformed somewhat better than the pre-furnace repair electrodes; edge cracks were eliminated and surface appearance was superior. Growth was less than one percent for both groups of electrodes.

As another part of this characterization program, the morophology of the nickel powder was examined. Current practice is to blend the as-received powder. This practice enables the use of constant mold settings, in spite of batch-to-batch variations in the incoming powder. However, blending times can be up to one hour duration. Different blending times will have differing influences on this change. The effect of this variation on sintering behavior is yet to be determined.

EXHIBIT E-I: CHARACTERISTICS OF CONTINUOUS MICROPOROUS SEPARATOR

	SAMPLE NO.	WEIGHT GAIN (G/FT^2)	AVERAGE THICKNESS (MILS)	BUBBLE TEST PSI OF 1ST HOLE	OHMS-CM^2
ZL-36	1	12.73	4.7	21	.54
	2	12.72	4.7	16	.45
	3	12.88	4.7	25	.50
ZL-37	1	12.27	4.7	12	.37
	2	12.86	4.8	14	.36
	3	12.89	4.7	16	.35
ZL-38	1	12.46	4.7	20	.42
	2	12.55	4.7	20	.37
	3	12.89	4.6	30	.40
ZL-40	1	11.67	4.7	15	.49
	2	11.83	4.6	18	.49
	3	11.82	4.6	17	.50
ZL-41	1	11.78	4.7	20	.35
	2	12.07	4.7	18	.33
	3	12.02	4.6	21	.35
ZL-42	1	12.56	4.8	15	.31
	2	12.45	4.7	16	.30
	3	12.77	4.7	20	.27
ZL-43	1	12.59	4.6	15	.30
	2	12.89	4.7	16	.38
	3	13.12	4.7	24	.40
ZL-44	1	12.07	4.6	16	.43
	2	12.36	4.6	17	.38
	3	12.28	4.6	11	.38
ZL-45	1	12.04	4.7	16	.38
	2	12.30	4.7	18	.36
	3	12.34	4.6	25	.46

EXHIBIT E-II: MICROPOROUS SEPARATOR MATERIALS COSTS PER SQUARE FOOT

Substrate	$.0001
Matrix Polymer	.0077
Inorganic Additive	.0079
Pore Former	.0005
TOTAL	$.0271

EXHIBIT E-III: AGGLOMERATE SIZE DISTRIBUTION OF VARIOUS LOTS OF SPRAY-DRIED ZnO

Mesh Size	% FINER									
	Lot 1	Lot 2	Lot 3	Lot 4	Lot 5	Lot 6	Lot 7	Lot 1-5	Lot 1-7	Ideal
(-) 20	100	100	100	100	100	96.7	95.7	100	98.9	
30	100	100	100	100	99.2	83.5	87.8	99.8	95.8	
40	98.8	98.9	99.3	98.8	96.7	75.45	74.9	98.5	91.8	
50	93.9	91.1	92.9	90.3	88.1	70.3	66.5	91.3	84.8	100
60	90.2	85.3	88.1	83.8	81.6	63.2	61.1	85.8	79.1	95
70	84.6	81.2	84.5	78.9	77.1	55.9	53.5	81.3	73.7	90
80	80.7	75.8	79.6	72.0	70.9	13.8	46.9	75.8	62.8	70
100	68.3	69.7	73.7	64.3	64.5	9.2	16.6	68.1	52.3	50
140	50.1	56.3	54.6	39.5	47.6	2.1	4.5	49.6	36.4	45
200	28.6	38.6	10.6	1.7	17.6	0.6	1.7	19.4	14.2	30
325	1.2	13.2	1.3	0.6	1.6	0	0.1	3.6	2.6	0
% Binder	10.3	8.3	9.2	8.1	7.7	4.4	6.2	8.72	7.74	--
% H_2O	2.5	3.0	2.5	2.3	3.0	6.0	4.0	2.7	3.3	--

EXHIBIT E-IV: AGGLOMERATE SIZE DISTRIBUTION OF VARIOUS ZnO POWDER LOTS SPRAY-DRIED

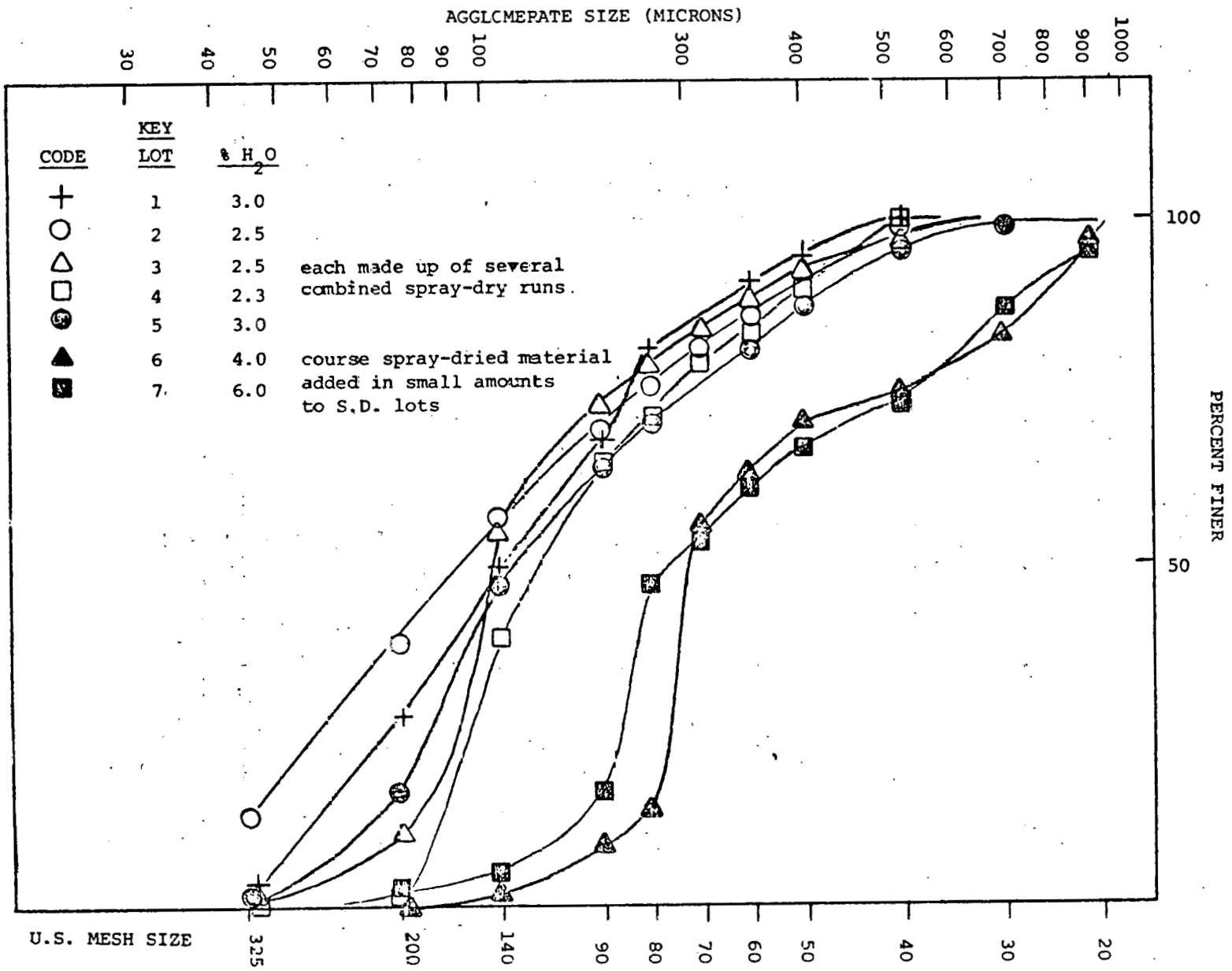

EXHIBIT E-V: AGGLOMERATE SIZE DISTRIBUTION OF VARIOUS ZnO POWDER LOTS SPRAY-DRIED

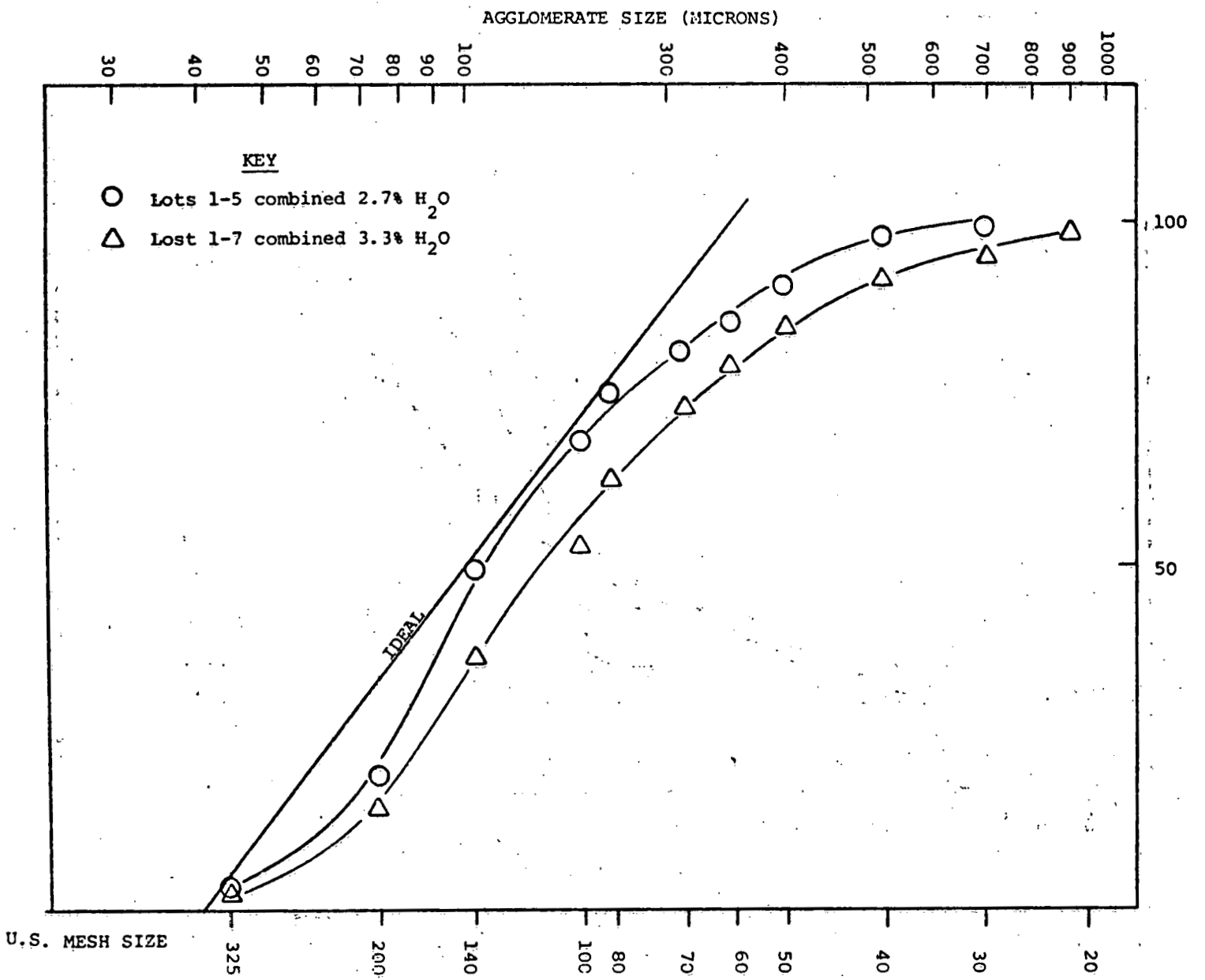

EXHIBIT E-VI: AGGLOMERATE SIZE DISTRIBUTION OF ZnO POWDER SPRAY-DRIED WITH TWO DIFFERENT BINDERS

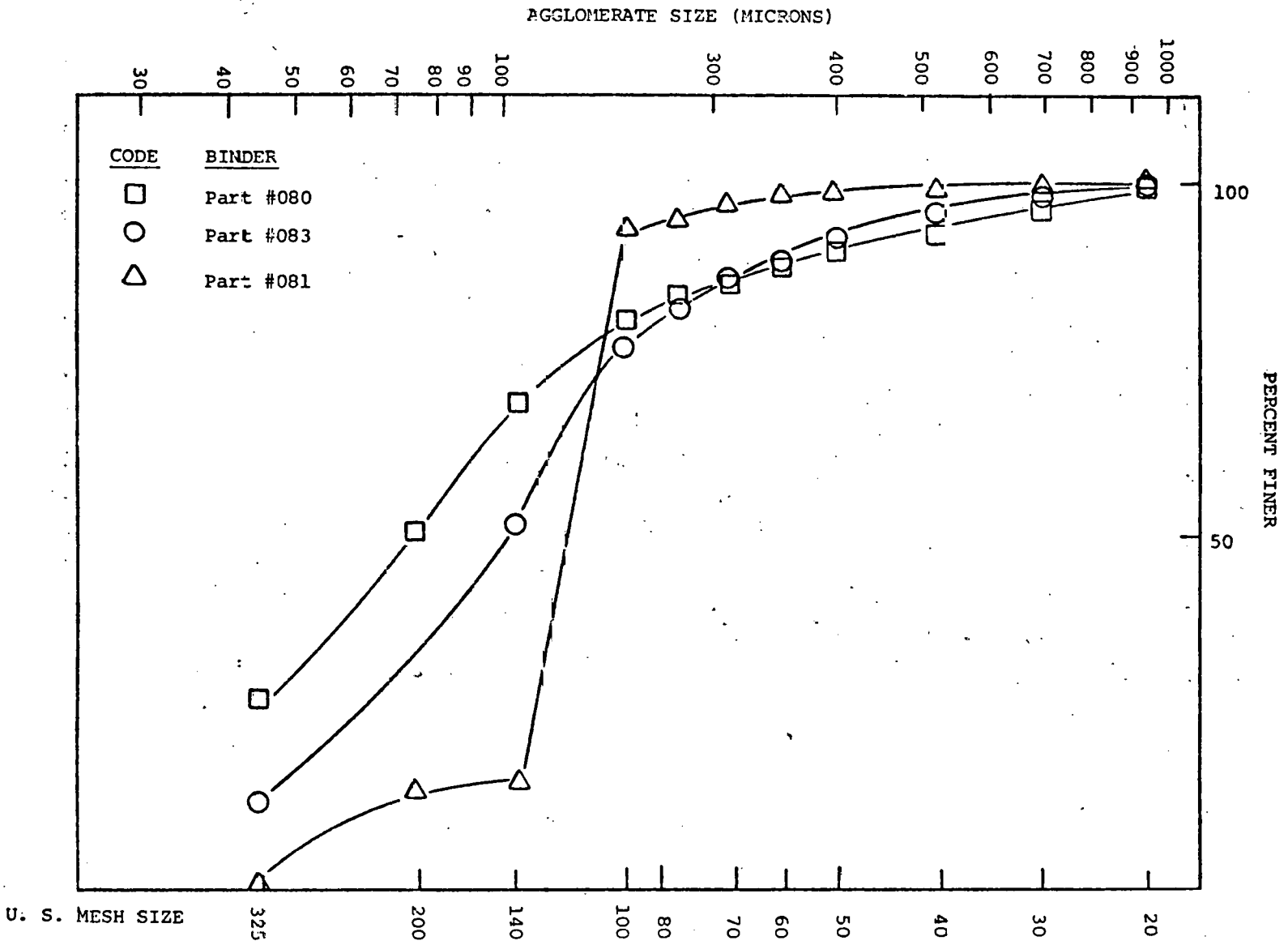

EXHIBIT E-VII: SINTERED NICKEL ELECTRODES

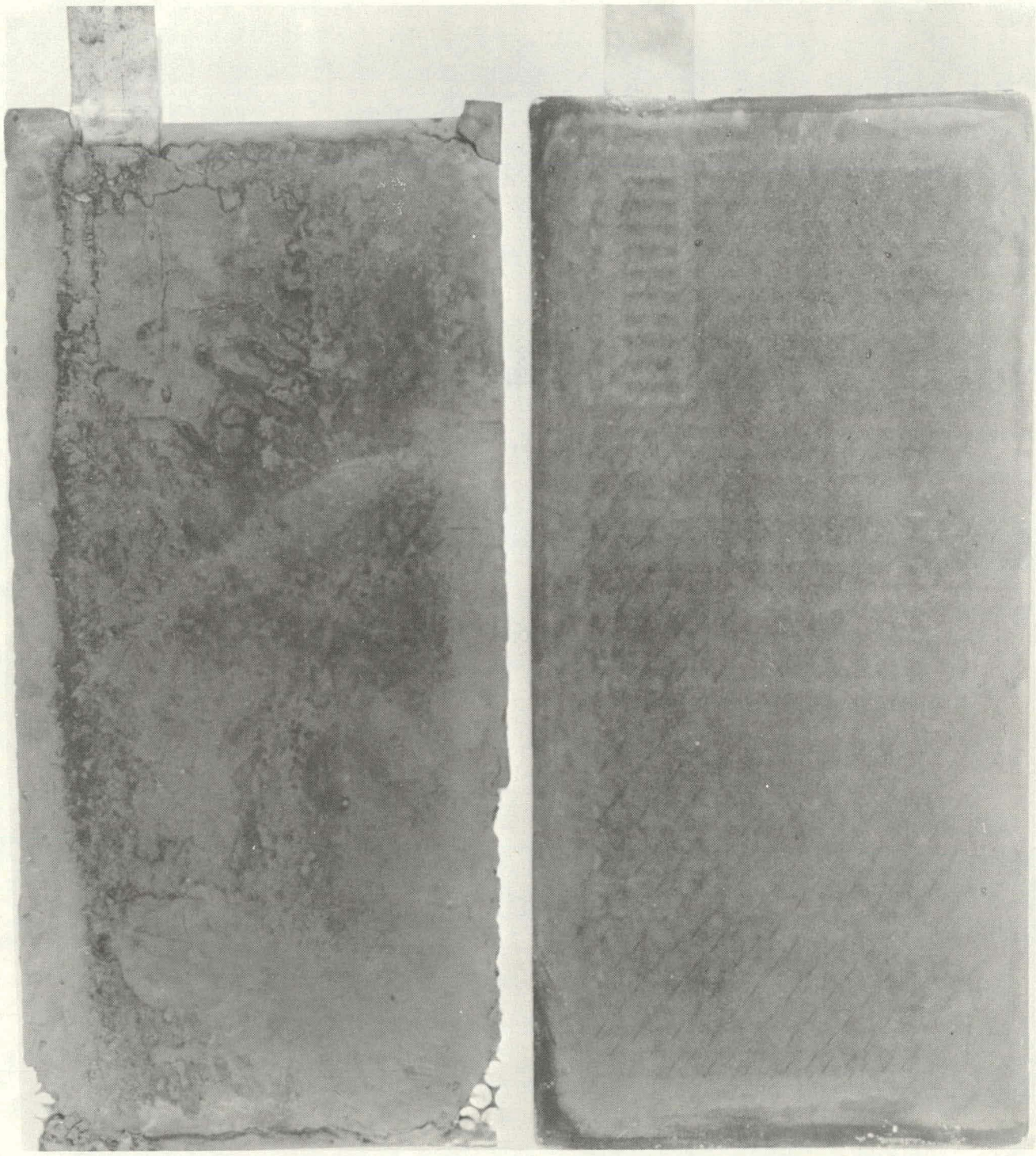

EXHIBIT E-VIII: BASELINE DATA FOR VACUUM AND NH_3 SINTERED ELECTRIC VEHICLE ELECTRODES

	VACUUM	NO. OF TESTS	NH_3	NO. OF TESTS
Average Transverse Repture Strength (psi)	984	9	455	8
Standard Deviation Transverse Rupture Strength	49	-	44	-
Surface Area (m^2/g)	0.144	4	0.225	2
Average Mean Pore Size (μ)	16.5	12	8.0	8
Range of Average Mean Pore Size (μ)	14.0-18.5		7.6-8.7	

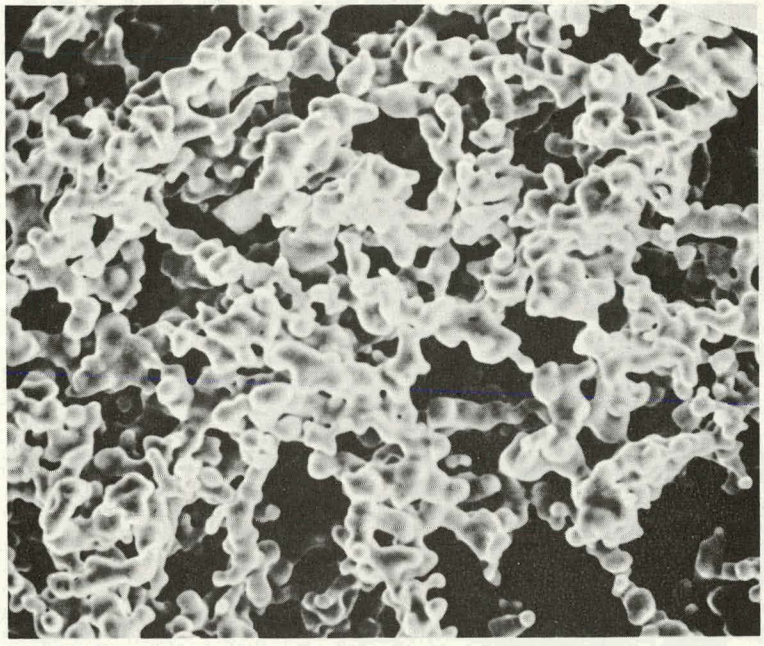

1000X

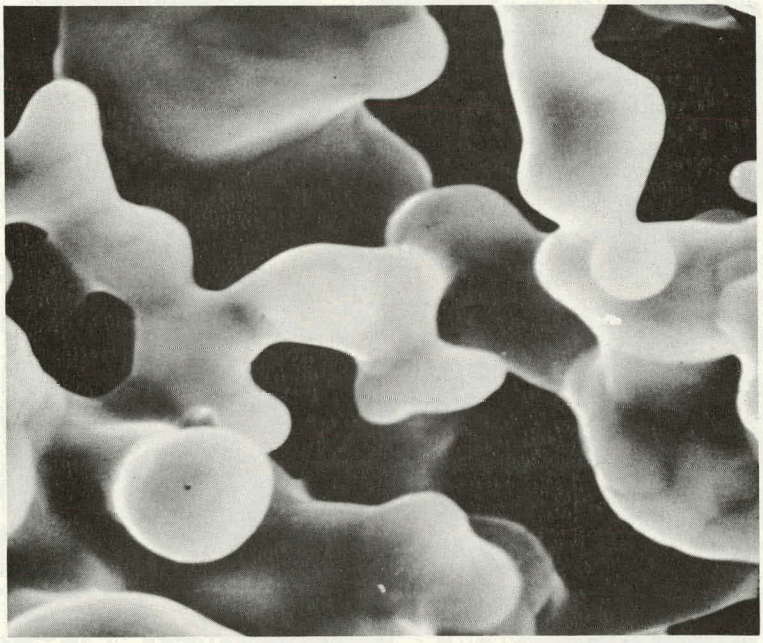

6000X

EXHIBIT E-IX: SEM photographs of a vacuum-sintered E.V. electrode (654) sintered at Rolling Meadows. Note the smooth particle surfaces.

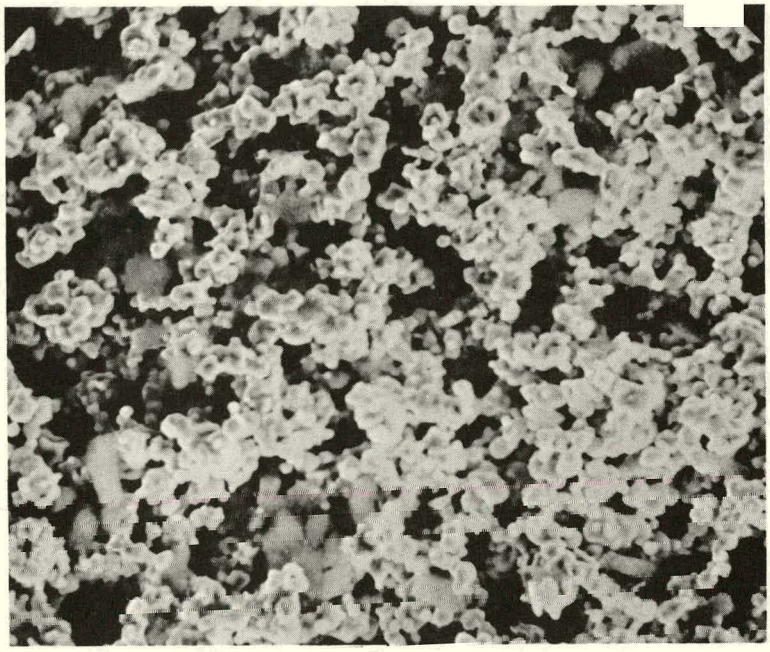

1000X

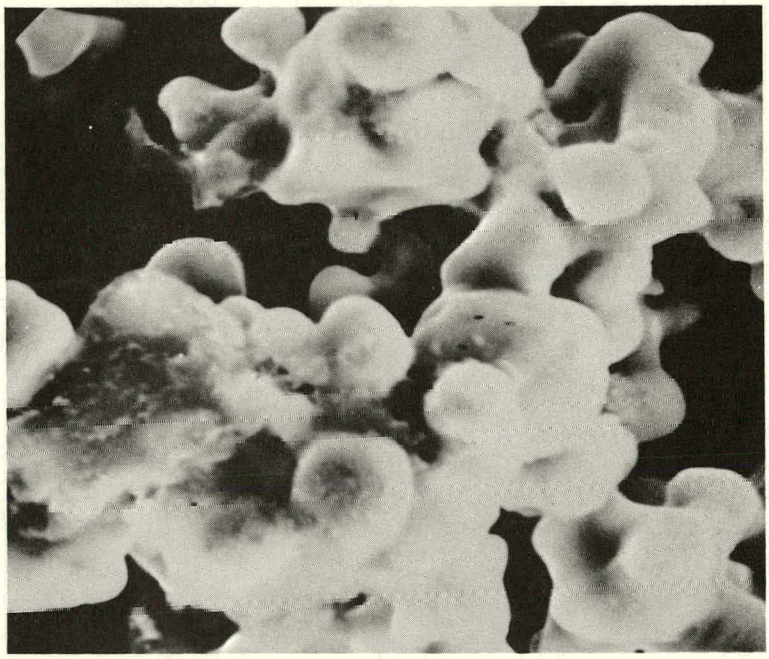

6000X

EXHIBIT D-X: SEM photographs of an NH_3-sintered E.V. electrode (N-16) produced in the Harper belt furnace before repair. Note the roughness of the particle surfaces. The structure is also much more blocky and less elongated than the vacuum-sintered base.

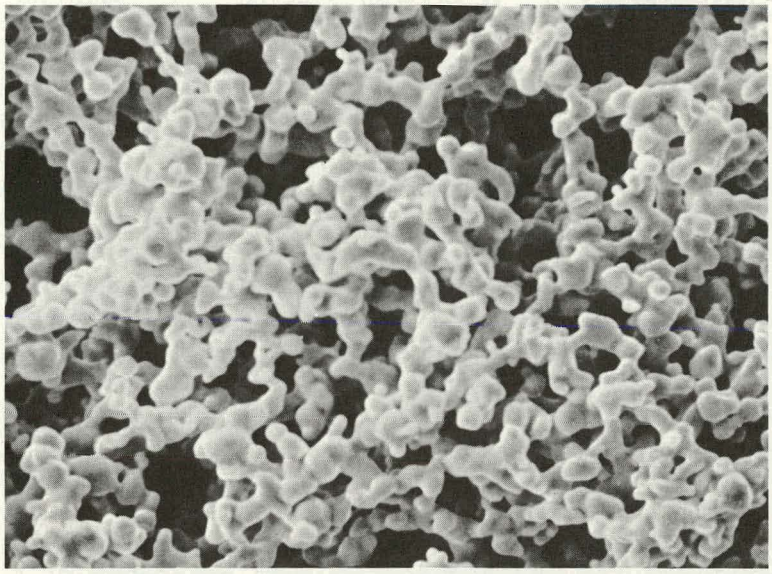

1000X

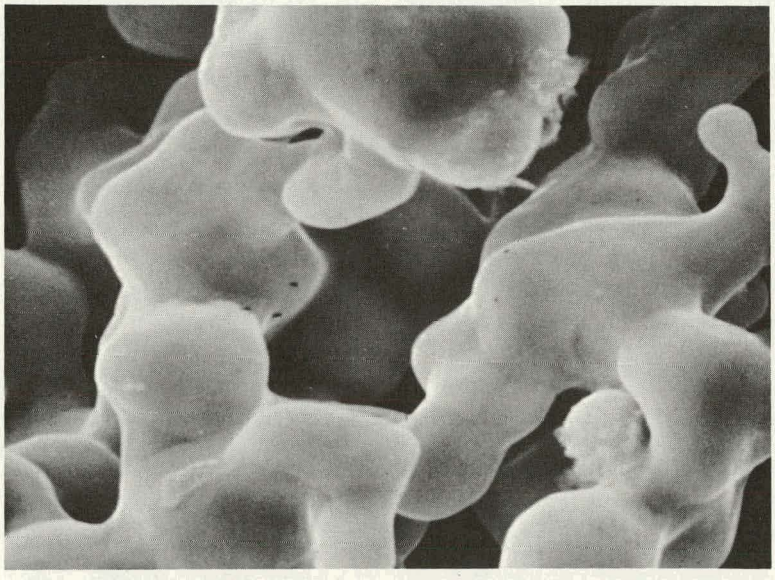

6000X

EXHIBIT E-XI: SEM photographs of an NZ-160 electrode sintered after the Harper furnace repair. Note that the smoothness of the particle surfaces is comparable to that of the vacuum-sintered product.

TASK F: PILOT MANUFACTURE

Objectives

The primary objectives of this Task are: 1) produce a series of improved cells, modules, and batteries for Gould internal and Argonne testing; 2) establish manufacturing reproducibility and forecast manufacturing economics; 3) perform a comprehensive materials availability study; and 4) produce pilot quantities of batteries for external demonstration. An operational Pilot Plant enables Gould to produce quantities of nickel-zinc hardware under realistic manufacturing conditions to satisfy all testing requirements while simultaneously performing product and process developments. Furthermore, this Pilot Plant is capable of producing batteries in quantities to support the electric vehicle requirements under the demonstration of PL 94-413. Gould feels strongly that pursuing the Pilot Plant phase at this time is essential for two reasons. One, to accurately evaluate the status of technology and its feasibility in the electric vehicle environment, the data must be generated in a manufacturing mode as opposed to one-of-a-kind-laboratory-hand-built operation. Secondly, lead time considerations for the acquisition and check-out of major capital equipment are of the order of two years. Even then, the product made in the Pilot Plant would have to be fully evaluated. If there were no scale-up problems, an invalid assumption, at least an additional year is required. Since it is Gould's desire to participate in the 1981 demonstration program, a corporate commitment was made to move immediately into the Pilot Plant stage. Gould is well aware that the inevitable scale-up problems will arise; however, it is more expedient and judicious to resolve them now than to wait until production quantities of cells/modules/batteries are required.

Pilot Plant Process Implementation

The major part of the effort in this Task has been aimed at the translation and implementation of laboratory-scale processes to production level activity. In addition, effort has been directed at modifying processes that, at some point, were production bottlenecks.

Specifically, some of the areas that have received attention and problems have been solved or alleviated are listed along with the actions taken.

PROBLEM	EFFECT	SOLUTION	COMMENTS
1) Inadequate waste management system	Delay in installation of positive electrode impregnation equipment	Redesigned and installed new, self-contained waste management system	
2) Unreliable welds because of poor fixtures	High resistance welds, poor electrode performance	Improved welding fixtures designed and installed; new Tab bending process installed	More reliable cell performance

PROBLEM	EFFECT	SOLUTION	COMMENTS
3) Negative electrode (with new binder) blistering and delamination from current collector	Unusable negative electrodes	Improved spray dry and pressing processes	Manufacture of good usable electrodes
4) Limited welding capability	Production bottleneck	New welder purchased, installed, and debugged	Improved cell production rate
5) Potential OSHA problem with foot pedal switch of welder	Possible safety hazard	Problem corrected	Removal of safety hazard
6) Separator bag production very slow; production bottleneck	Separator bag fabrication machine designed and built	Several fold increase in separator bag production rate	Machine enables QC of film before bag manufacture
7) Heat seals in separator bags not reproducible	Unreliable cell performance	Study conducted, new heat sealing system developed and installed	Excellent seals with multiple layers of separator
8) Leaking cell cases at the seals	Electrolyte spillage	Improved sealing techniques implemented	Better reliability, reduction in carbonation, improved safety
9) Nickel plaque molding too slow	Bottleneck in nickel electrode production	4X plaque molding process developed and implemented	Nickel electrode production rate increased by a factor of four
10) Nonuniform nickel plaques because of nonuniform mold fill	Unreliable positive electrodes	Design and installation of new filling molds	Improved uniformity and reliability
11) Slow tab production	Bottleneck in electrode (positive and negative) production	Tab blanking press for 10 and 20 mil stock put in operation	Improved electrode production rate
12) Sintering furnace inoperational	Stop nickel electrode production for two weeks	Repair muffle, water jacket, and heating elements	Resumed production
13) Design defficiency in impregnation equipment	Delay of operation of nickel plaque impregnation equipment	Defficiency corrected	Production delay

Overall, the Pilot Plant operation is still pretty much manual, primarily because of the diversity of components that must be produced to accommodate the entire Project; however, the learning gained in this process is absolutely invaluable. And, in developing and implementing the operations, areas of mechanization and automation are being identified and pursued vigorously. This is something that cannot be predicted or identified in a laboratory environment.

It is to be emphasized that, in spite of the difficulties and hurdles associated with the start-up of any new operation and the operations and equipment difficulties, especially with new personnel, the Pilot Plant has met all the internal and external (ANL) production goals on time, and it is anticipated that, with the vast amount of production knowledge being generated, the efficiency and response to production request will increase dramatically.

Cell/Battery Production

Although component and cell and battery production rates have been steadily increasing, the principal highlight was the delivery (to ANL) of the four-cell module which incorporates several new concepts and components developed during the previous several months and produced in the Pilot Plant. Several thousands of negative and positive electrodes, separator bags, grids, tabs, etc. were fabricated and several hundreds of full-size electric vehicle (400 AH) and 50 AH cells were built to support the other Project activities in spite of the fact that the full-scale impregnation equipment was still not operational and the nickel plaques being impregnated by the batch process. Although considerable mechanization still needs to be implemented with the present processes, the Pilot Plant could meet component production and delivery requirements for 100 electric vehicle batteries per year.

Significant is the fact that there is a great deal of diversity for cell requirements necessitating the use of several different dies for the fabrication of the zinc electrode, different molds for the positive electrodes, while simultaneously implementing new processes to fabricate improved components as they are being developed. In spite of this fact, production schedules are being met.

Materials Utilization Study

This study was submitted to Argonne in report form on June 19, 1978. The study includes a manufacturing flow design, the projected materials usage in kilograms per kilowatt-hour, and projected market size through the year 2000.

Manufacturing Economics

In order to accumulate sound data from which reliable manufacturing economics analyses can be made, a cost accounting system was instituted for the entire operation. The system covers variables such as materials costs, nickel plaque impregnating assembly, separator production, sintering costs, pressing costs, stamping, etc. Additionally, in conjunction with Gould's Automotive Battery Division, detailed breakdown of cost categories common to both nickel-zinc and automotive battery business has been generated. A standard materials cost has

been generated for the Preliminary Design cell configuration for a 22.4 KwH battery. A more detailed analysis follows.

MANUFACTURING ECONOMICS ANALYSIS

This part of Task F is in response to the milestone for August requiring an analysis of the manufacturing economics for nickel-zinc electric vehicle batteries.

As part of the data requirements of Contract No. 31-109-38-4200, estimates of the current and projected manufacturing costs are required each year. The following analysis is the first yearly summary of the manufacturing economics of the Gould nickel-zinc battery and is included in this January-July, 1978, Progress Report as part of Task F.

Market Realities

In discussing present and future manufacturing costs and selling prices, the most important factor to emphasize is that for a given developed product of this type, costs will be greatly dependent upon the magnitude of market pull. For nickel-zinc electric vehicle batteries, there are two major problems. First, the product is still being developed and, therefore, even current and definitely future costs are at best gross estimates. Second and most important, there is no present or short-term market pull. The electric commuter vehicle will probably not be cost and performance competitive with the comparable ICE powered vehicle prior to 1990. The electric powered commercial vehicle may be cost competitive by 1985, however, its potential market is at least an order of magnitude smaller than commuter vehicles. Thus, in a free market scenario, there is little incentive for Gould or other battery manufacturers to employ massive capital in the near term to mechanize production and expand capacity.

The federal government may play a mid-wife role and provide the needed economic incentives during this subeconomic period of the 1980s. However, the current Department of Energy program in response to PL 94-413 is insufficient in stimulating production capacity for electric vehicle batteries. Thus, at the present time, there is not market pull to reduce manufacturing costs and increase capacity. This is reflected in the following analysis which will indicate that it will take significant government action to achieve target manufacturing costs in the 1980s.

Gould Pilot Plant

Late in 1976, Gould decided to invest over $1 million to move nickel-zinc from laboratory-scale to pilot plant production. The purpose in establishing this facility was three fold; first, to determine the true state of technology by producing reproducible components under realistic manufacturing conditions; second, to provide for the large number of test cells and batteries required for various product development programs including Contract No. 31-109-38-4200; and third, to provide information to estimate current and future manufacturing costs and process requirements. The 9,500 ft^2 Pilot Plant has been operational since the beginning of this contract; however, as described extensively in Tasks E and F of this report, improving productivity and reducing materials costs is a continuous process.

Present Pilot Plant Processes

The basic process in the manufacture of Gould's sintered nickel electrode are shown in EXHIBIT F-I. Nickel powder is molded onto a grid to form a substrate. This substrate is sintered under conditions to provide the required porosity in preparation for impregnation. The physical properties of the substrate (pore size and distribution, porosity, nickel powder content, strength) can be directly controlled and specific substrates can be produced to a particular re-requirement. The impregnation of active mass (nickel hydroxide and additives) proceeds directly in the pores of the substrate from a nickel solution that is readily prepared from raw materials by straightforward techniques.

The manufacturing processes of Gould's zinc electrode are shown in EXHIBIT C-II. The basic processes are the preparation of the zinc mass (blending zinc oxide and additives) and the compaction of the zinc mass onto a grid. The compaction of the zinc mass is generally accomplished in two steps using mechanized powder metallurgical presses. These compaction steps can be modified for high volume and low cost production.

Gould has been developing new separators for the nickel-zinc battery, including inorganic/organic microporous types. The key steps in the manufacture of this material are given in EXHIBIT F-III. The process involves relatively few simple operations, although certain steps (e.g., those in the materials formulation and handling) require that they be carried out precisely to achieve a quality product with the desired physical properties. The important point is that the application demands a uniform pore size separator to assure long cycle life. The less complex the process, the more reliable the product should be in mass production. Other continuous processes have been developed for the production of electroporous separators. These are discussed in detail in Task A of this report.

Ultimately, the assembly of the nickel-zinc cell poses no greater obstacles than other volume production batteries such as the automotive lead-acid type which can be manufactured at low cost. However, past battery manufacturing experience at Gould dictates an evolution of proudct design and manufacturing processes. Due to the nature of any new product, changes in the product that could require modifications in the assembly techniques or new processes are likely in the early years of production and thus mechanization of the overall assembly process is lagging the balance of the Pilot Plant. The selected electrode configurations, separator system, cell design, and hardware design will influence the assembly process. While certain assembly processes cannot be specifically defined at present or are in the conceptual stage, the fact that many process approaches are derived from Gould's knowledge of the manufacture of batteries in large volume (e.g., automotive and industrial lead-acid batteries) and from our manufacturing operations in the nickel-cadmium and silver-zinc cells, lends Gould the in-house expertise to solve the anticipated problems in stabilizing a production process.

Current Cost Estimates

Several thousand of each type of electrode and hundreds of cells have been produced in the Pilot Plant. This experience has permitted the first calculation of the actual manufacturing cost. These costs have been calculated using a totally dedicated cost accumulation system which accurately includes

all direct labor and materials costs. A standard overhead rate of 150% is assumed which includes plant and equipment depreciation. The results to date indicate a current manufacturing cost of about >$400/KwH for the 400 AH Preliminary Design cell produced in a four-cell module configuration.

Future Cost Estimates

From the above data, it is obvious that the current costs which represent the first stage pilot production far exceed the estimated selling price target of $75/KwH. To achieve the target selling price, the following items are essential:

1) Heavy investment in mechanization to reduce the labor cost.

2) Improve process yield to reduce scrap rate theregy reducing materials cost.

3) Recycle process scrap and used batteries to reduce materials cost.

4) Improve materials utilization in both negative and positive electrodes to reduce materials cost.

Gould believes that the target selling price can be achieved but it will take heavy investment in plant and equipment and process development beyond the scope of the current contract. As previously discussed, there is no market pull to encourage Gould to make the necessary investment at this time, so a projection of the time table to achieve the costs, in a free market scenario, is impossible. On the other hand, if the federal government decides to stimulate the electric vehicle marketplace through the 1980s by virtue of significant funding for product and process development beyond the present contract and guaranteed battery purchases, the $75/KwH selling price can be achieved by 1986. This goal would be achieved by going through three stages of plant expansion requiring many millions of dollars in capital. The very high volume which is required to achieve the target price is greatly dependent upon the assumption that the return on investment be recovered within two years. This is required because in a subeconomic market, stimulated solely by the government, either the Department of Energy or Congress can eliminate the marketplace at will.

EXHIBIT F-I: MANUFACTURE OF NICKEL ELECTRODE FOR ELECTRIC VEHICLE NICKEL-ZINC BATTERY

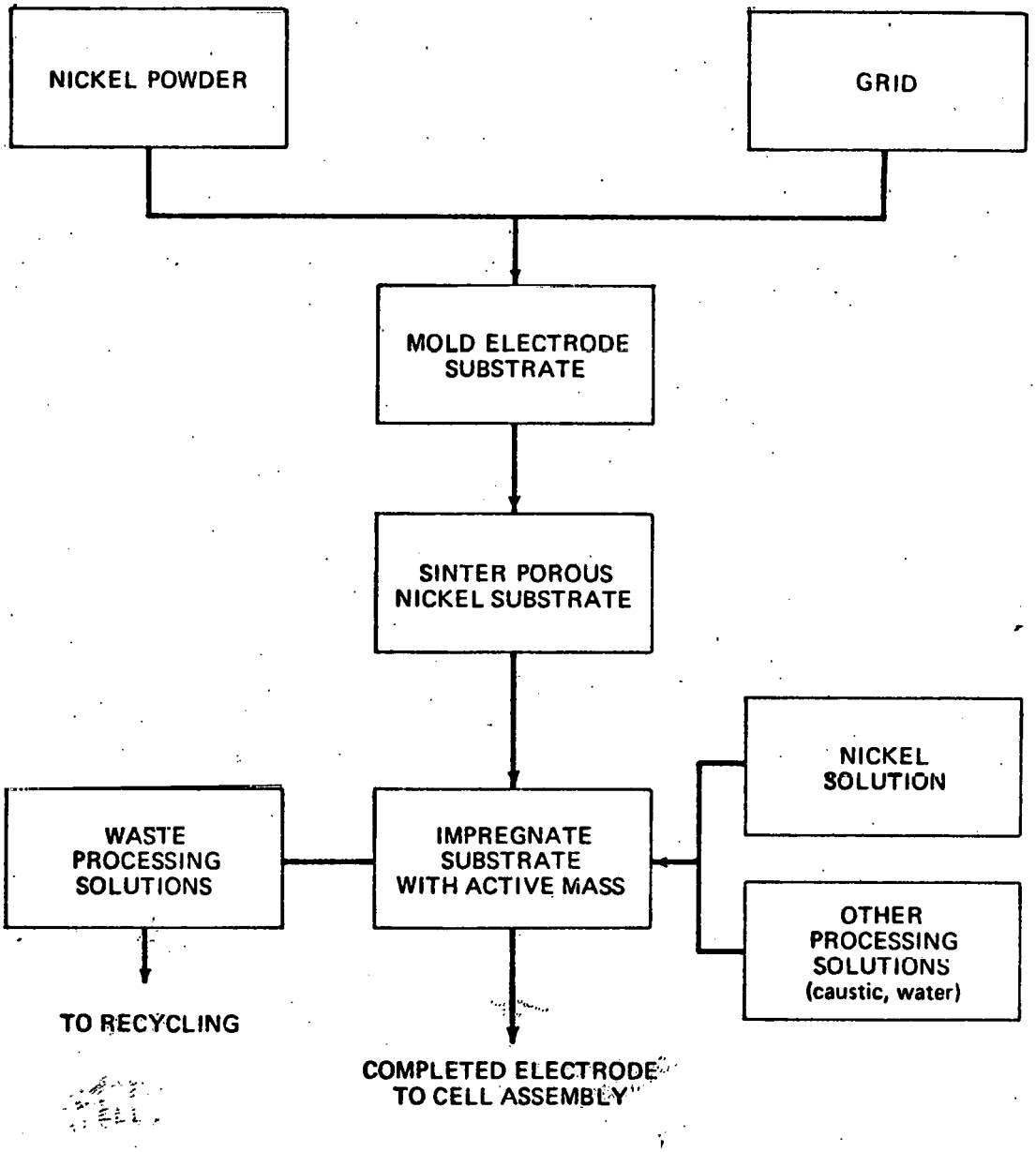

EXHIBIT F-II: MANUFACTURE OF ZINC ELECTRODE FOR ELECTRIC VEHICLE NICKEL-ZINC BATTERY

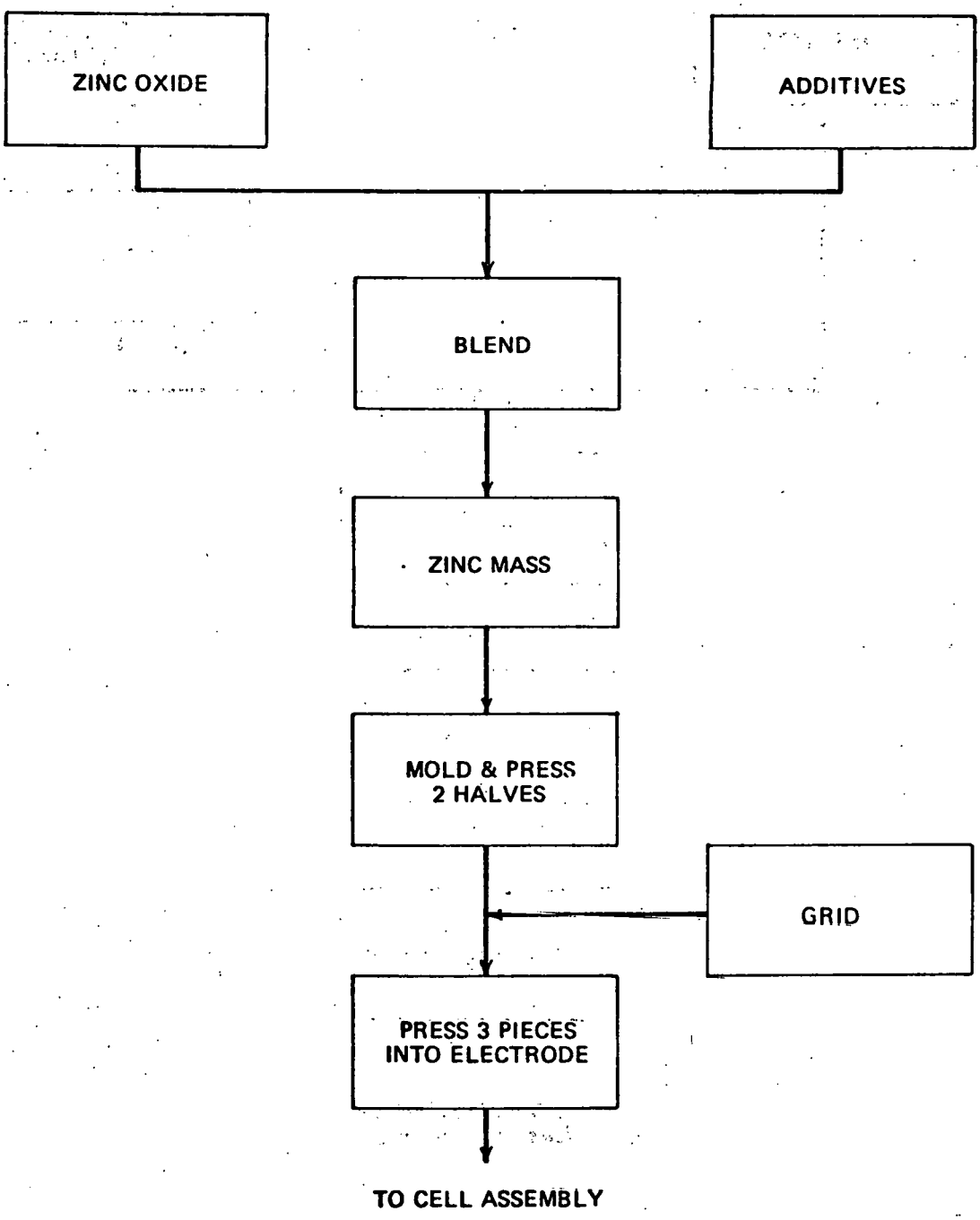

EXHIBIT F-III: MANUFACTURE OF FLEXIBLE INORGANIC/ORGANIC COMPOSITE SEPARATOR

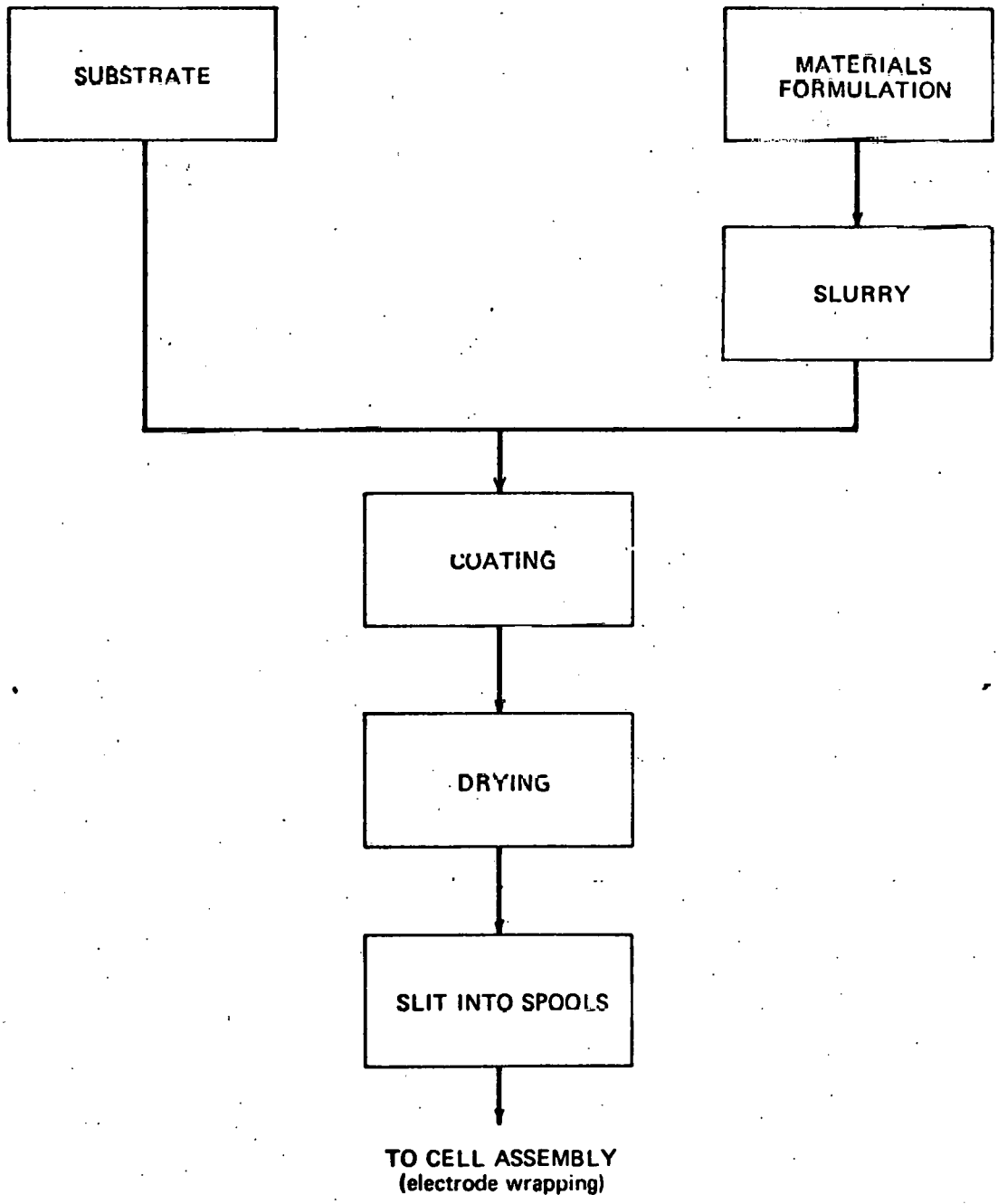

TASK G: QUALITY ASSURANCE

A highly experienced professional assumed responsibility for Quality Assurance for the Project. Toward this end, an initial task was to incorporate the quality assurance requirements of the recently revised statement of work into the mainstream of the Project. The initial work was to produce a clarification of the specifications of the various electrode types and a series of fixtures designed to facilitate consistent grid-tab alignment. In addition, various pieces of test equipment have been ordered and several qualification tests have been evaluated. The parts list used in the Cost Control Program was updated and simplified so that it could be used as a guide for ordering components from the Pilot Plant.

As part of the quality assurance requirements for the Argonne Contract and as a necessary starting point in the materials availability study, a complete manufacturing flow diagram was constructed. Part of the diagram consists of a numbered sequence of the documents required in the manufacturing process. These documents cover raw material specifications, manufacturing work instructions, test/inspection procedures, and packing/shipping instructions where appropriate.

The Quality Assurance Plan, which forms part of the Quality Assurance Manual for the Argonne Contract, was completed. Also, all the necessary changes were made to the Gould Research-New Business Quality Assurance Manual to personalize it for the Nickel-Zinc/Electric Vehicle Project.

Distribution for ANL/OEPM-78-11

Internal:

J. J. Barghusen
D. Barney
C. Bean
E. C. Berrill
A. Brown
L. Burris
G. Chapman
A. A. Chilenskas
K. Choi
C. C. Christianson
G. Cook
D. Corp
S. A. Davis
W. DeLuca
R. C. Elliott
P. R. Fields
F. Foster
D. Fredrickson
B. R. T. Frost
G. T. Garvey
E. C. Gay
J. Geller
M. Genge
F. Hornstra
C. C. Hsu
J. Klinger
V. Kremesec
A. B. Krisciunas
M. L. Kyle
W. W. Lark
T. Lee
M. Liu
R. Loutfy
W. Massey
J. Miller
W. Miller
P. A. Nelson
M. V. Nevitt
E. G. Pewitt
D. Poa
J. Rajan
J. J. Roberts
M. F. Roche
H. Shimotake
R. K. Steunenberg
C. A. Swoboda
Z. Tomczuk
R. Varma
P. D. Vashishta
D. R. Vissers
D. S. Webster
N. P. Yao (64)
ANL Contract File
ANL Libraries (5)
TIS Files (6)

External:

DOE-TIC, for distribution per UC-94ca (315)
Manager, Chicago Operations and Regional Office, DOE
Chief, Office of Patent Counsel, DOE-CORO
V. Hummel, DOE-CORO
President, Argonne Universities Association
Chemical Engineering Division Review Committee:
C. B. Alcock, U. Toronto
R. C. Axtmann, Princeton University
R. E. Balzhiser, Electric Power Research Institute
J. T. Banchero, Univ. of Notre Dame
T. Cole, Ford Motor Corp.
P. W. Gilles, Univ. of Kansas
R. I. Newman, Allied Chemical Corp.
G. M. Rosenblatt, Pennsylvania State University
E. T. Ames, TRW Systems, Redondo Beach, CA
S. J. Angelovich, Mallory Battery Co., Tarrytown, NY
C. M. Arcand, Idaho State University, Pocatello, ID
R. Aronson, Electric Field Propulsion Corp., Troy, MI
Atomics International, Attn: Library, Canoga Park, CA
G. N. Ault, NASA-Lewis Research Center, Cleveland, OH
A. Backerby, Powertrain, Inc., Salt Lake City, UT
J. D. Baker, Stewart Warner Corp., Chicago, IL
W. Bales, Jet Industries, Inc., Austin, TX
K. F. Barber, DOE, Office of Transportation Programs, Washington, DC
T. Barber, Jet Propulsion Laboratory, Pasadena, CA
R. J. Barkley, Compass Industries, Inc., Hermosa Beach, CA
J. W. Barlass, Westinghouse Electric Corp., Skokie, IL
T. M. Barlow, Lawrence Livermore Laboratory, Livermore, CA

D. Barron, Delco-Remy Div. GMC, Anderson, IN
R. Bassett, Sandia Labs, Albuquerque, NM
E. Baumann, LILCO, Mineola, NY
J. A. Belding, DOE, Office of Transportation Programs, Washington, DC
L. Belove, Marathon Battery Corp., Waco, TX
C. Berlsterling, C. Franklin Institute, Philadelphia, PA
D. N. Bennion, Brigham Young University, Provo, UT
C. Berger, Electrochemical & Water Desa. Tech., Santa Anna, CA
L. Berkowitz, Esso Research & Engineering Co., Linden, NJ
E. Berman, TRW Systems Group., McLean, VA
W. S. Bishop, Air Force Aero Propulsion Lab, Wright-Patterson AFB, OH
K. Blurton, Institute of Gas Technology, Chicago, IL
D. P. Boden, C&D Batteries, Plymouth Meeting, PA
R. L. Boeger, Lectran, Huntington, PA
J. Bolger, University of California, Berkeley, CA
L. M. Bonneford, Battelle Memorial Institute, Washington, DC
Borden Chemical Corp., Central Research Lab., Philadelphia, PA
D. Borello, Die Mesh Corp., Pelham, NY
Borisoff Engineering Co., Van Nuys, CA
Boston Edison Co., Att: Director of Research, Boston, MA
T. Boswell, Elgin National Watch Co., Elgin, IL
P. Bowen, C & D Batteries, Plymouth Meeting, PA
D. Bowman, United States Postal Service, Washington, DC
J. C. Boylan, Electric Dynamics Corp., Plainwell, MI
J. Brennand, General Research Corp., Santa Barbara, CA
A. F. Brewer, Malibu, CA
D. C. Briggs, Philco-Ford Corp., Palo Alto, CA
P. Bro, J. R. Mallory & Co., Inc., Burlington, MA
R. Brodd, Union Carbide Corp., Cleveland, OH
E. P. Broglio, Eagle-Picher Industries, Joplin, MO
A. D. Brown, EVE Electric Motor Car, Inc., East Lansing, MI
P. J. Brown, DOE, Office of Transportation Programs, Washington, DC
R. Buchholz, Honeywell Corp., Minneapolis, MN
T. Burgess, Lucas Industries, N. A. Inc., Troy, MI
H. Burghart, Cleveland State University, Cleveland, OH
D. Burns, Onan Corporation, Minneapolis, MN
B. W. Burrows, Gould Inc., Rolling Meadows, IL
J. D. Busi, USA Foreign Science & Tech. Center, Charlottesville, VA
E. Buzzelli, Westinghouse Electric Corp., Pittsburgh, PA
W. P. Cadogan, Emhart Corp., Hartford, CT
E. Cairns, Lawrence Berkeley Lab., Univ. of Cal., Berkeley, CA
E. Campbell, Electric Vehicle Consultants, Inc., New York, NY
P. Campbell, University of Southern California, Los Angeles, CA
J. Campbell, DOT/UMTA, Washington, DC
R. T. Carpenter, Kimberly Clark Corp. Neenah, WI
T. V. Carvey, Hughes Aircraft Corp., Culver City, CA
R. Childs, Energy Research & Development Corp., Olmsted Falls, OH
L. D. Christian, General Electric, Gainesville, FL
R. C. Chudecek, McGraw Edison Co., Bloomfield, NH
R. Clark, Sandia Labs Org. 2523, Albuquerque, NM
J. E. Clifford, Battelle Memorial Institute, Columbus, OH
P. D. Cole, Naval Ordinance Laboratory, Silver Springs, MD

J. G. Colin, Englehard Industries Inc., Edison, NJ
W. B. Collins, Martin Marietta Corp., Denver, CO
J. E. Cooper, Aero Propulsion Laboratory, Wright-Patterson AFB, OH
R. E. Corbett, Lockhead Missiles & Space Co., Sunnyvale, CA
J. F. Corcoran, Wolverine Diesel Power Co., Traverse City, MI
K. E. Cox, University of New Mexico, Albuquerque, NM
W. W. Craig, Edward Harding and Co., Chicago, IL
D. Crane, United States Postal Service, Washington, DC
R. A. Crawford, PPG Industries, Barberton, OH
H. H. Crist, AM General Corp., Wayne, MI
D. Davis, Lawrence Livermore Laboratory, Livermore, CA
P. Davis, DOE, Office of Transportation Programs, Washington, DC
R. J. Dawson, ESB Inc., Madison, WI
N. A. Demerdash, Virginia Polytechnic Institute, Blacksburg, VA
G. A. DiBari, INCO, Sterling Forest Suffern, NY
W. J. Dippold, DOE, Office of Transportation Programs, Washington, DC
T. P. Dirske, Calvin College, Grand Rapids, MI
D. Douglas, EPRI, Palo Alto, CA
D. Dow, Consulting Engineer, Detroit, MI
E. F. Echolds, AiResearch Manufacturing Co., Torrance, CA
D. B. Eisenhaure, Charles Stark Draper Lab Inc., Cambridge, MA
M. W. Ellison, Hughes Aircraft Corp., El Segundo, CA
B. Enserik, Dynamic Science, Phoenix, AZ
Environmental Protection Agency, Att: Div. of Policy Plng., Washington, DC
R. E. Evans, John Hopkins University, Silver Springs, MD
A. Ewing, DOE, Office of Transportation Programs, Washington, DC
Exchange & Gift Div., Library of Congress, Washington, DC
F. Fedor, Bell Laboratories, Murray Hill, NJ
W. H. Fengler, Meteor Research Limited, Roseville, MI
R. Ferraro, Electric Power Research Institute, Palo Alto, CA
A. Fleischer, Orange, NJ
R. F. Fogle, North American Rockwell, Anaheim, CA
R. T. Foley, American University, Washington, DC
J. S. Fordyce, NASA-Lewis Research Center, Cleveland, OH
Franklin Institute, Philadelphia, PA
D. Friedman, Minicars, Inc., Goleta, CA
Garrett Corp., Att: Dir. ADV Program, Los Angeles, CA
G. Gelb, Advanced Ground Systems, Long Beach, CA
General Electric Co. R & D Ctr., Att: Whitney Library, Schenectady, NY
S. Geppert, Eaton Corporation, Southfield, MI
L. J. Gerlach, United States Postal Service, Rockville, MD
J. A. Gilchrist, Chloride America, Tampa, FL
W. Gillespie, Structural Plastics Inc., Tulsa, OK
C. Glassman, Transportation Research Center, East Liberty, OH
M. Globerman, GSA, Washington, DC
W. Goldman, Electric Vehicle Engineering, Lexington, MA
G. Goodman, Globe-Union Inc., Milwaukee, WI
R. E. Goodson, Purdue University, W. Lafayette, IN
J. Gould, Unique Mobility Inc., Englewood, CO
C. B. Graff, NASA-George C. Marshall Space Flight Center, Huntsville, AL
H. Grepke, TurElec Inc., Bradenton, FL
R. Guess, General Electric Research Lab, Schenectady, NY
R. G. Gunther, General Motors Research Labs, Warren, MI

M. Hadden, Billings Energy Corp. Provo, UT
G. Hagey, DOE, Division of Technology Overview, Washington, DC
N. Halterm, Chrysler Corporation, Detroit, MI
G. Halpert, NASA-Goddard Space Flight Center, Greenbelt, MD
H. Hamilton, University of Pittsburgh, Pittsburgh, PA
R. Hamilton, Institute for Defense Analysis, Arlington, VA
B. Hamling, Zircar, Florida, NY
D. Hanify, Fiat, Chicago, IL
K. L. Hanson, General Electric Co., Philadelphia, PA
W. Harhay, Electric Vehicle Associates, Cleveland, OH
J. H. Harrison, Naval Ship R&D Center, Anapolis, MD
G. Hartman, ESB Incorporated, Yardley, PA
J. Hartman, General Motors Research Labs, Warren, MI
E. A. Heintz, Airco Speer Carbon Graphite, Niagara Falls, NY
R. Heppenstall, Penn Jersey Suburu Inc., Pennsauken, NJ
V. Hlavin, NASA-Lewis Research Center, Cleveland, OH
G. Hobbib, ESB Inc., Cleveland, OH
R. Hoenburg, Mechanical Technology Inc., Latham, NY
N. W. Hop, AiResearch Mfg. Co., Phoenix, AZ
R. Hudson, Eagle-Picher Industries, Joplin, MO
H. L. Hughes, Oklahoma State University, Stillwater, OK
J. R. Hunt, International Nickel Co., Washington, DC
H. R. Ivey, Wood-Ivey Systems Corp., Winterpark, FL
G. H. Jantz, Rensselaer Polytechnic Institute, Troy, NY
J. T. Jackson, Georgia Institute of Technology, Schl. of Mech. Engr., Atlanta GA
J. Jacus, Moorehaven, FL
A. W. Johnson, General Electric Co., Philadelphia, PA
F. Johnson, Department of Industry, Trade and Commerce, Ottawa, Canada
L. Jokl, MERADCOM, Fort Belvoir, VA
W. J. Jones, Westinghouse Electric Corp., Pittstburgh, PA
D. Kane, National Motors Corp., Lancaster, PA
E. Kanter, Gulton Battery Corp., Metuchen, NJ
N. Kaplan, Harry Diamond Laboratories, Washington, DC
R. Kaylor, Kaylor Energy Products, Menlo Park, CA
H. C. Kelly, OTA U.S. Congress, Washington, DC
J. A. Kerrella, Delco-Remy Division/GMC, Anderson, IN
R. A. Keyes, Robert A. Keyes Associates, Martinsville, IN
R. A. Kingery, Oconomowoc, WI
R. S. Kirk, DOE, Office of Transportation Programs, Washington, DC
G. B. Kliman, General Electric Co., Schenectady, NY
G. B. Klinean, General Electric Co., Schenectady, NY
R. A. Knight, AMF Inc., Stanford, CT
J. G. Krisilas, Aerospace Corporation, El Segundo, CA
R. R. Kubalek, St. Joe Lead Co., Clayton, MD
L. Kulin, Whirlpool Corp. Benton Harbor, MI
H. Lauve, Electric Auto Corporation, Troy, MI
Lawrence Berkeley Lab., Univ. of Cal., Att: Library, Berkeley, CA
I. J. Levine, Con Edison, New York, NY
C. Liang, P.R. Mallory and Co., Burlington, MA
H. Lim, Hughes Research Lab., Malibu, CA
A. Long, Zeonics Corp., Fairfax, VA
M. Lugash, Maxon Industries, Huntington Park, CA
T. Lynch, Fiber Materials, Inc., Biddeford, MI

E. N. Mabuce, Union Electric Co., St. Louis, MO
J. MacDougall, AT&T, Basking Ridge, NJ
J. Mader, Electric Power Research Institute, Palo Alto, CA
J. Maisel, Cleveland State University, Cleveland, OH
V. Manson, National Aeronautics and Space Adm., Washington, DC
T. W. Martin, United State Postal Service, San Bruno, CA
A. Masters, Packaged Promotions Inc., Chicago, IL
C. E. May, NASA-Lewis Research Center, Cleveland, OH
E. Meeks, Derl Manufacturing Co., Compton, CA
J. D. Meiggs, Kaman Sciences Corp., Colorado Springs, CO
N. Merriman, Army Picatinny Arsenal Engr. Science Div., Dover, NJ
Midwest Research Institute, Att: Physical Science Lab., Kansas City, MO
P. Mighdoll, Booz-Allen & Hamilton, Cleveland, OH
R. P. Mikkelson, General Dynamics, San Diego, CA
D. G. Miley, U.S. Naval Ammunition Depot, Crane, IN
H. Miller, Department of Transportation, Cambridge, MA
D. K. Miner, Copper Development Associates, Birmingham, MI
L. J. Minnich, G&W H. Corson, Inc., Plymouth Meeting, PA
F. J. Mollura, Rome Air Development Center, Griffiss AFB, NY
F. Moore, DOE, Energy Storage Systems, Washington, DC
F. Morse, Univ. of Md., Dept. of Mech. Engr., College Park, MD
A. Moss, Leesona Moos Laboratories, Warwick, RI
R. Mueller, University of California, Berkeley, CA
J. H. Muir, Dimension V Inc., Indialantic, FL
J. P. Mulling, National Aeronautics and Space Adm., Washington, DC
G. Murphy, Northwestern University, Evanston, IL
N. T. Musial, NASA-Lewis Research Center, Cleveland, OH
J. McCallum, Invention Talents, Inc., Columbus, OH
B. McCormick, Los Alamos Scientific Labs, Los Alamos, NM
R. McCoy, B&Z Electric Car, Long Beach, CA
McDonnell Douglas Astro Co., Att: Library, Huntington Beach, CA
R. McKee, McKee Engineering Corp., Palatine, IL
J. McKeown, DOE, Office of Program Administration, Washington, DC
P. McRay, ILC Technology, Sunnyvale, CA
W. J. Nagle, NASA-Lewis Research Center, Cleveland, OH
NASA-Lewis Research Ctr., Att: Tech. Utility Off. MS 7-3, Cleveland, OH
NASA-Lewis Research Ctr., Att: Library MS 60-3, Cleveland, OH
NASA-Lewis Research Ctr., Att: Report Control MS 5-5, Cleveland, OH
H. V. Nadham, Bogue Batteries, El Segundo, CA
L. Nalley, Creative Research Co., Roebuck, SC
Nat'l. Aeronautics & Space Adm., Att: Section Hd. Code 711, Greenbelt, MD
Nat'l. Aeronautics & Space Adm., Att: KT/Tech. Util Off., Washington, DC
Nelpar-Technical Information Center, Falls Church, VA
J. S. Newton, Newton Engineering Co., Glen Ellyn, IL
M. M. Nickolson, Atomics International Division, Canoga Park, CA
J. Norberg, ESB Inc., Philadelphia, PA
North American Rockwell Corp., Att: Library, Canoga Park, CA
NASA-Scientific & Tech. Info. Ctr., Att: Accessioning Dept., Baltimore/
Washington Int. Airport, MD
J. Newman, Univ. of California, Berkeley, CA
NASA-Goddard Space Flight Ctr., Att: G. Halpert (Code 711.2), Greenbelt, MD
Office of Naval Research, Att: Dir. Power Programs, Arlington, VA
R. Oglesby, GM Transportation Systems Ctr., Warren, MI
L. Omohundro, Kingery Research & Development, Wake Forest, MC

J. Orsino, San Clemente, CA
R. Osteryound, Colorado State University, Fort Collins, CO
B. N. Otzinger, North American Aviation, Downey, CA
J. E. Oxley, Gould Inc., Rolling Meadows, IL
E. Papandreas, REI, Lake Worth, FL
J. S. Parkinson, Johns-Manville R&D Center, Manville, NJ
E. Patagalia, GSA, Washington, DC
S. Pauling, Naperville, IL
J. E. Pavolsky, NASA/Lyndon B. Johnson Space Ctr., Houston, TX
C. Pax, DOE, Office of Transportation Programs, Washington, DC
G. F. Pezdirtz, DOE, Energy Storage Systems, Washington, DC
A. G. Plunckett, General Electric R&D Center, Schenectady, NY
M. Pocabello, Triad Services, Dearborn, MI
Power Information Ctr., University City Science Ctr., Philadelphia, PA
RAI Research Corp., Hauppauge, L.I., NY
V. J. Puglisi, Yardney Electric Corp., Pawcatuck, CT
J. Purcell, Chicago Operations Office, Argonne, IL
E. Ramirez, Amectran, Dallas, TX
E. Raskin, USAF Cambridge Research Laboratory, Bedford, MA
A. D. Raynard, AiResearch Manufacturing Co., Torrance, CA
E. C. Read, Exxon Enterprises, Linden, NJ
H. L. Recht, Atomics Internations Division, Canoga Park, CA
C. Ridgway, Walt Disney World Co., Lake Buena Vista, FL
E. Rizkalla, DOE, Washington, DC
S. J. Romer, Solargen Electronics Ltd., New York, NY
L. Rosenblum, NASA-Lewis Research Center, Cleveland, OH
N. Rosenburg, Department of Transportation, Cambridge, MA
R. Rosey, Westinghouse Electric Corp., Pittsburgh, PA
J. W. Ross, Texas Instruments Inc., Attleboro, MA
J. Rossmon, Cornell University, Ithaca, NY
G. Rowland, General Electric, Schenectady, NY
J. Rubenzer, NASA-Ames Research Center, Moffett Field, CA
P. H. Rubie, Electric Passenger Cars Inc., San Diego, CA
G. Rowland, General Electric, Schenectady, NY
SAMSO/DYAE, Worldway Postal Center, Los Angeles, CA
J. Salihi, Otis Elevator, Co., Parsipanny, NJ
A. J. Salkind, ESB Technology Center, Yardley, PA
I. O. Salyer, Monsanto Research Corp., Dayton, OH
G. Scharback, American Motors Corp., Wayne, MI
D. F. Schmidt, General Electric Co., Washington, DC
R. Schmidt, Volkswagon of America Inc., Englewood Cliffs, NJ
L. W. Schopen, NASA-Lewis Research Center, Cleveland, OH
S. Schuldiner, Naval Research Laboratory, Washington, DC
R. Schwartz, ASL Enginering, Goleta, CA
R. Schwarz, South Coast Technology, Inc., Santa Barbara, CA
W. R. Scott, TRW Systems Inc., Redondo Beach, CA
H. Seigel, South Coast Technology Inc., Santa Barbara, CA
H. Seiger, Waterford, CT
J. Seliber, Fluid Drive Engineering Co., Wilmette, IL
E. Seo, Gates Energy Products, Denver, CO
L. Shahnasarian, Elcar Corp., Elkhart, IN
R. C. Shair, Hollywood, FL
H. Shalit, ARCO Chemical Corp., Glendoden, PA
D. W. Sheibley, NASA-Lewis Research Center, Cleveland, OH

H. P. Silverman, TRW Systems, Redondo Beach, CA
E. Small, Amectran Corporation, Washington, DC
J. Smits, Nevada Operations Office, Las Vegas, NV
I. J. Soloman, IIT Research Institute, Chicago, IL
Southwest Research Institute, Att: Library, San Antonio, TX
Stanford Research Institute, Att: Librarian, Menlo Park, CA
J. S. Stanley, Dept. of the Army, U.S. Army Foreign Sci. & Tech. Center, Charlottesville, VA
R. Strauss, Communications Satellite Corp., Clarksburg, MD
R. L. Strombotne, Transportation Systems Center, Cambridge, MA
F. Tepper, Catalyst Research Corp., Baltimore, MD
C. E. Thomas, Chrysler Corp., New Orleans, LA
F. Thomas, Grumman Aerospace Corp., Bethpage, NY
G. M. Thur, DOE, Office of Transportation Programs, Washington, DC
C. W. Tobias, University of California, Berkeley, CA
P. C. Symons, Energy Development Associates, Madison Heights, MI
TRW, Incorporated, Att: Library, Redondo Beach, CA
F. Tepper, Catalyst Research Corp., Baltimore, MD
A. Topouzian, Ford, Dearborn, MI
L. Topper, National Science Foundation, Washington, DC
W. Toth, Society of Automotive Engineers, Inc., Warrendale, PA
H. Toulmin, Bloomfield, MI
I. Trachtenberg, Texas Instruments, Dallas, TX
G. H. Turney, Western Research Industries, Las Vegas, NV
E. A. Ulrich, Creative Automotive Research, Whittier, CA
R. L. Ulrich, GSA, Washington, DC
T. Ulrich, McGraw-Edison Co., Bloomfield, NJ
G. Underhill, A. D. Little, Cambridge, MA
Union Carbide, Dev. Lab. Library, Cleveland, OH
Union Carbide Corp., Parma Lab. Library, Parma, OH
University of Pennsylvania, Nat. Ctr. for Energy Mgmt. & Power, Philadelphia, PA
U.S. DOE, Dir. Program Mgmt. Space & Nonnuclear Energy Programs, Oakland, CA
U.S. DOE, Pittsburgh Energy Research Ctr., Pittsburgh, PA
U.S. DOE, Dir. Off. of Trans. Programs, Washington, DC
U.S. DOE, Denver Office, Lakewood, CO
U.S. DOE, Albuquerque Operations Office, Albuquerque, NM
U.S. DOE, Asst. Gen. Counsel for Patents, Washington, DC
U.S. San Francisco Oper. Off., Att: PMIC-SD, San Diego, CA
C. J. Venuto, C&D Batteries, Plymouth Meeting, PA
E. H. Wakefield, Linear Alpha Inc., Evanston, IL
C. H. Waterman, C. H. Waterman Industries, Althol, MA
G. Way, Troy, MI
W. Webster, DOE, Div. of Energy Storage Systems, Washington, DC
E. Y. Weissman, GASF Wynadotte Corp., Wynadotte, MI
R. Walker, University of Florida, Gainesville, FL
I. Wender, Bureau of Mines, Pittsburgh, PA
R. L. Wentworth, Dynatech Corp., Cambridge, MA
Western Environmental Testing Lab., Colorado Springs, CO
Westinghouse Hanford Co., Att: Doc. Control, Richland, WA
R. D. Wherle, Sandia Labs., Albuquerque, NM
M. E. Wilke, Burgess Battery Company., Freeport, IL
R. Wilks, Lavelle Aircraft Co., Newton, PA
C. F. Williams, Teledyne Isotopes, Timonium, MD

J. M. Williams, E. I. DuPont DeNemours & Co., Wilmington, DE
E. Willhnganz, C&D Batteries, Plymouth Meeting, PA
J. F. Wing, Booz-Allen & Hamilton Inc., Bethesda, MD
K. Winters, Chrysler Corp., New Orleans, LA
T. J. Wissing, Eaton Corp., Southfield, MI
J. Wooldrige, Boeing Corp., Seattle, WA
V. Wouk, Petro-Electric Motor Ltd., New York, NY
R. A. Wynveen, Life Systems Inc., Cleveland, OH
L. Yanni, Booz-Allen & Hamilton Inc., Bethesda, MD
L. S. Yao, University of Illinois, Urbana, IL
Yardney Electric Corp. , Att: V. P. Engr., Pawcatuck, CT
H. Yoder, Battronic Truck Corp., Boyertown, PA
J. E. Zanks, NASA - Langley Research Center, Hampton, VA
P. Zanoi, Boulder, CO
M. Zlotnick, DOE, Conservation Research & Technology, Washington, DC